Mechanisms of Metabolic Disorders and Memory/Learning Dysfunction Induced by Vitamin B_{12} Deficiency and Production of the Vitamin-Enriched Food for Preventing the Deficiency

（ビタミン B_{12} 欠乏症による代謝異常症と記憶・学習障害の発症メカニズムの

解明および欠乏症予防のためのビタミン B_{12} 強化食品の開発）

Tomohiro Bito

2015

Contents

Chapter I **Introduction** 1

Chapter II **Preparation of vitamin B_{12}-deficient *Caenorhabditis elegans* as a model animal** 8

Section 1 Vitamin B_{12}-deficient *Caenorhabditis elegans* prepared by the feeding of vitamin B_{12}-limited *Esherichia coli* OP-50 as a diet 10

Section 2 Vitamin B_{12}-deficient *Caenorhabditis elegans* prepared by the treatment of vitamin B_{12} dodecylamine derivative 22

Section 3 Effects of hydroxocobalamin dodecylamine derivatives on the activities of vitamin B_{12}-dependent enzymes in cultured COS-7 cells 42

Chapter III **Mechanisms of metabolic disorders and memory/learning dysfunction induced by vitamin B_{12} deficiency in *Caenorhabditis elegans*** 52

Section 1 Vitamin B_{12} deficiency in *Caenorhabditis elegans* results in sever oxidative stress, leading to memory/learning dysfunction 54

Section 2 Vitamin B_{12} deficiency in *Caenorhabditis elegans* results in metabolic disorders of polyamines, modulators of synaptic transmission 75

Chapter IV Production of vitamin B_{12}-enriched food for preventing the deficiency among vegetarians and elderly subjects 91

Section 1 Miniaturized high performance thin-layer chromatography of vitamin B_{12} compounds in foods 93

Section 2 Characterization of vitamin B_{12} compounds in the fruiting bodies of shiitake mushroom (*Lentinula edodes*) 101

Section 3 Characterization of vitamin B_{12} compounds in organic fertilizers containing purple photosynthetic bacteria 116

Section 4 Production and characterization of vitamin B_{12}-enriched lettuce (*Lactuca sativa* L.) grown using hydroponics 123

Chapter V Conclusion 139

References 157

Acknowledgements 175

Abbreviations

$AdoB_{12}$; 5'-Deoxyadenosylcobalamin

B_{12}; Vitamin B_{12} (cobalamin)

Cat; Catalase

CBS; Cystathionine-β-synthase

CH_3-B_{12}; Methylcobalamin

C.I.; Chemotaxis index

CN-B_{12}; Cyanocobalamin

DNPH; 2,4-Dinitrophenylhydrazine

ESI-MS/MS; Electro spray ionization tandem mass spectrometer

GPx, Glutathione peroxidase

GSH, Glutathione or reduced glutathione

GSSH; Glutathione disulfide or oxidized glutathione

GSR; Glutathione reductase

GST; Glutathione *S*-transferase

Hcy; Homocysteine

HPLC; High performance liquid chromatography

IF; Intrinsic factor

KCN; Potassium cysnide

KPB; Potassium phosphate buffer

MCM; Methylmalonyl-CoA mutase

MMA; Methylmalonic acid

MS; Methionine synthase

NADPH; Nicotinamide adenine dinucleotide phosphate

NGM; Nematode growth medium

NMDA; *N*-methyl-*D*-aspartate

NOS; Nitric oxide synthase

OH-B_{12}; Hydroxycobalamin

qPCR; Quantitative polymerase chain reaction

RNS; Reactive nitrogen species

ROS; Reactive oxygen species

SAH; *S*-Adenosylhomocysteine

SAM; *S*-Adenosylmethionine

SOD; Superoxide dismutase

TBA; Thiobarbituric acid

TCA; Trichloroacetic acid

TLC; Thin-layer chromatography

RDA; Recommended dietary allowance

Chapter I

Introduction

Vitamin B_{12} or cobalamin (B_{12}) is exclusively synthesized by some anaerobic bacteria and then concentrated in the bodies of higher predatory organisms in the natural food chain [1]. B_{12} has the highest molecular weight (1355.4) among vitamins and a complicated structure with a cobalt complex ion (**Fig. 1**). B_{12} compounds contain a corrin ring with a cobalt atom coordinated by the lower axial ligand (base-on conformation), which is an unusual ribonucleoside with dimethylbenzimidazole as a base moiety. Although B_{12} is officially defined as cyanocobalamin, the upper axial ligand of B_{12} can be substituted by several functional groups (hydroxo, methyl, or 5'-deoxyadenosyl). The coordinated dimetnylbenzimidazole of the lower ligand can be dissociated from cobalt atom (base-off conformation). The base-on and base-off conformations appear to play a role in the stability of different forms of B_{12} as well as their ability to bind to proteins [2].

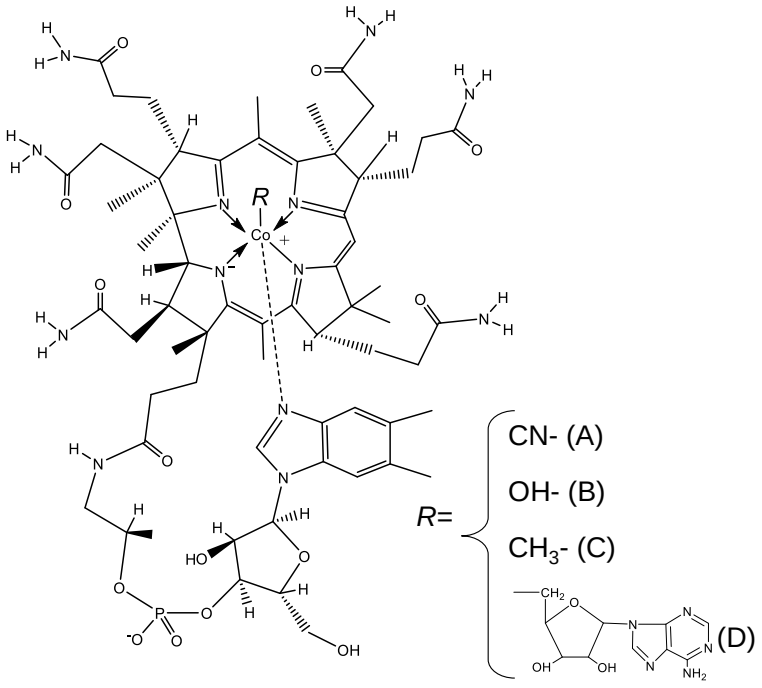

Fig.1. Structures of vitamin B_{12}. (A) CN-B_{12}, cyanocobalamin; (B) OH-B_{12}, hydroxocobalamin; (C) CH_3-B_{12}, methylcobalamin; (D) AdoB_{12}, adenosylcobalamin.

B_{12} has a complex process for gastrointestinal absorption of dietary B_{12}, which is normally bound to proteins in food [3, 4] (**Fig. 2**). B_{12} is released from the proteins by the action of HCl present in the stomach and the formed free B_{12} is immediately bound by haptocorrin (HC, a B_{12}-binding protein produced by the salivary grands) [5]. Subsequently, B_{12} is released from HC by the action of pancreatic proteases (e.g. trypsin) and the formed free B_{12} is bound by intrinsic factor (IF, a B_{12}-binding protein produced by the stomach cells). The IF-B_{12} complex is absorbed by enterocytes of the ileum; the IF-B_{12} complex is specifically bound by the receptor (such as cubilin and megalin) involved in gastrointestinal absorption of B_{12} and then internalized into the enterocytes by the receptor-mediated endocytosis [6, 7]. The IF-B_{12} complex liberated from the receptor is transferred to lysosomes of enterocytes. In lysosomes, proteases are responsible for digestion of the protein component of the complex, and subsequent lysosomal exit of B_{12} involves LMBD1 transporter [8, 9]. Free B_{12} is transported cellularly and/or processed as coenzyme forms and then exported into the portal circulation. The exported B_{12} is normally bound to transcobalamin-II (TC-II, a B_{12}-binding protein).

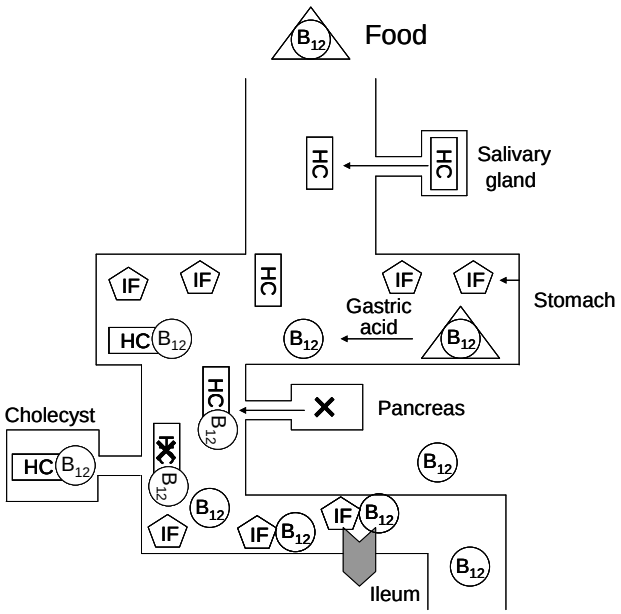

Fig.2. Gastrointestinal absorption mechanism of vitamin B_{12}

On the target cell surface, the TC-II-B_{12} complex is specifically recognized by TC receptor CD 320 [10]. The TC-II-B_{12} complex is transported inside the cells by the receptor-mediated endocytosis. **Fig. 3** shows the summary of transport and processing of B_{12} in the mammalian cells. The endocytic vesicle containing the TC-II-B_{12} complex is transferred to lysosomes, in which proteases are responsible for digestion of the protein component of the complex [11]. Subsequently, the export of B_{12} from lysosomes to cytosol involves LMBD1 (*cblF*) [8, 9]. Cytosolic B_{12} [cob(III)alamin] is bound to the tracking protein methylmalonic aciduria CblC type (MMACHC) and then reduced to cob(II)alamin (one electron-reduced form of cobalt atom) by the action of methylmalonic aciduria CblD type (MMADHC) protein. Cob(II)alamin is further processed and then converted into two coenzyme forms, 5'-deoxyadenosylcobalamin ($AdoB_{12}$) and methylcobalamin (CH_3-B_{12}) (**Fig. 1**), which function as the coenzymes for mitochondrial methylmalonyl-CoA mutase (MCM; EC 5.4.99.2) [12] and cytosolic methionine synthase (MS; EC 2.1.1.13) [13], respectively. MS catalyzes the methylation of homocysteine (Hcy) to form methionine (Met) using 5-methyltetrahydrofolate as methyl donor. The prosthetic B_{12} functions as transient acceptor of the methyl group, with cycling of B_{12} between cob(I)alamin (two electron-reduced cobalt atom) and CH_3-B_{12}. Whereas, cytosolic cob(II)almamin is transported into the mitochondria by the mediation of an unknown system and then reduced to cob(I)alamin and synthesized to $AdoB_{12}$ by cob(I)alamin adenosyltransferase (MMAB; EC 2.5.1.17) [14, 15]. Methylmalonic aciduria CblA type (MMAA) protein functions as an escort protein that transfers the synthesized $AdoB_{12}$ directly to MCM [16, 17].

MCM catalyzes the coversion of (*R*)-methylmalonyl-CoA to succinyl-CoA, an intermediate of TCA cycle, and plays important roles in catabolic pathways of branched chain-amino acids (valine, leucine, isoleucine, and threonine), odd-numbered fatty acids, cholesterol, and thymine (**Fig. 4**) [18].

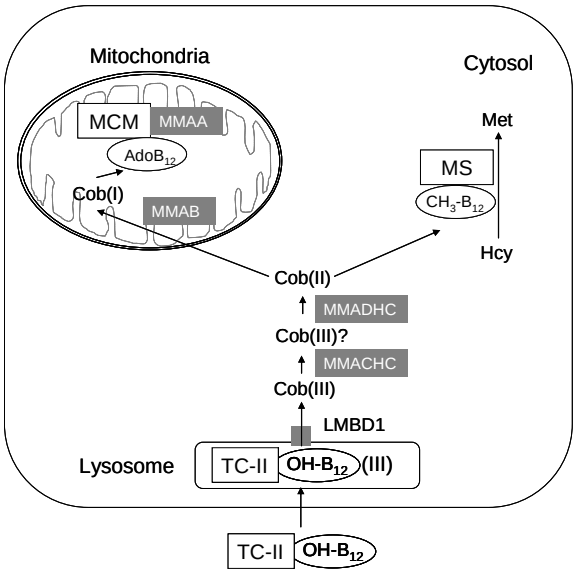

Fig. 3. Transport and cellular processing of vitamin B_{12}. Abbreviation: LMBD1; the limb region 1, MCM; methylmalonyl-CoA mutase, MMAA; methylmalonic aciduria CblA type, MMAB; methylmalonic aciduria CblB type, MMACHC; methylmalonic aciduria CblC type, MMADHC; methylmalonic aciduria CblD type, MS; methionine synthase, TC- II; transcobalamin II.

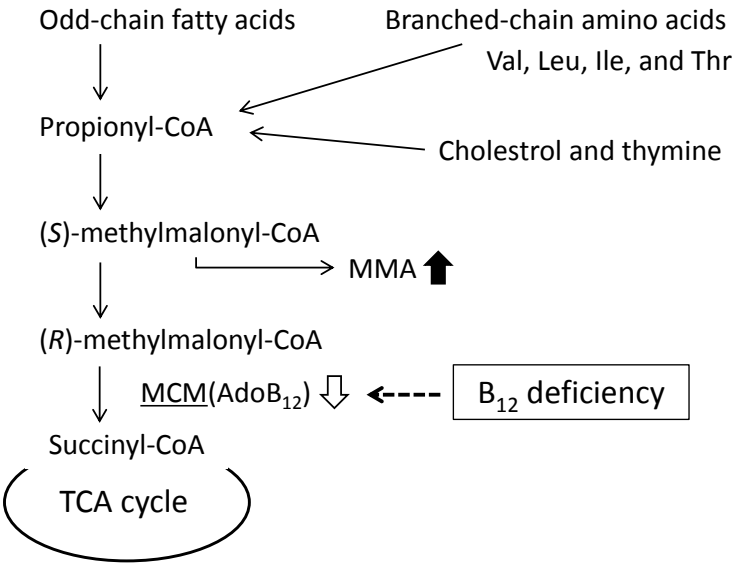

Fig. 4. Vitamin B_{12}-dependent methylmalonyl-CoA metabolic pathway.

MS catalyzes the synthesis of Met from Hcy with 5'-methyltetrahydrofolate (CH_3-THF) (**Fig. 5**) and plays important roles in sulfur amino acid, folate, polyamine, and

S-adenosylmethionine (SAM) metabolisms; in particular SAM involves various cellular methylation reactions such as DNA, RNA, proteins, and lipids [19, 20]. Urinary excretion of methylmalonic acid (MMA) and/or increased serum (or plasma) Hcy are clinically used as indexes of B_{12} deficiency [21, 22].

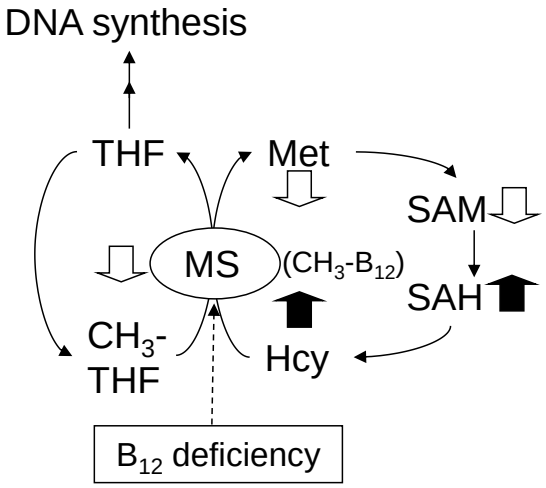

Fig. 5. Vitamin B_{12}-dependent methionine metabolic pathway.

Several studies have suggested that B_{12} deficiency is linked to serious health complications such as growth retardation, megaloblastic anemia, metabolic disorders, and neuropathy [23], although the underlying disease mechanisms are poorly understood [24]; in particular, further research is required to elucidate the precise mechanisms of B_{12}-deficient neuropathy in elderly people and vegetarians, high risk populations. As described above, B_{12} deficiency causes peripheral neuropathy, spinal cord disorders, and cognitive dysfunction. Hyperhomocysteinemia (HHcy) is reportedly associated with vascular dementia and Alzheimer Disease (AD) [25-27]. Moreover, significant accumulation of Hcy potentiates oxidative injury in vascular disease and AD [28, 29]. McCaddon *et al*. [30] proposed that biological consequence of oxidative stress caused by HHcy induced AD. However, the precise mechanism of B_{12}-deficient neuropathy is not clear.

Ebara *et al*. [22] demonstrated that B_{12} deficiency in rats caused serine and threonine metabolic disorders, which are attributable to impairment of the adenylyl

cyclase system. The *N*-methyl-*D*-aspartate (NMDA) receptor involving in the long-term memory preservation is significantly modulated by Hcy and/or polyamines [31]. However, there is no information on whether B_{12} deficiency induces the metabolic disorders of polyamines. In addition, the precise mechanism of the cognitive dysfunction caused B_{12} deficiency in humans [32] is poorly understood.

Developing animal models of B_{12} deficiency is essential for investigating the molecular mechanisms that are defective in this metabolic disorder. However, such animal models have proven difficult to generate because animals must be fed with a B_{12}-deficient diet for long periods to achieve B_{12} deficiency [33]. The lack of robust B_{12}-deficient animal models has limited investigations to the biochemical mechanisms induced by B_{12} deficiency.

Caenorhabditis elegans offers several advantages for genetic and biochemical studies, including a short lifespan, a 3 day life cycle, a completely sequenced genome, <1000 somatic cells, and the ability to change reproductive rates, life cycle, and locomotive behavior [34]. In addition, many molecular and cellular processes are conserved between nematodes and mammals. Most human disease genes and pathways are present in the worm [35]. Thus, this animal has been widely used as a model organism for studying a variety of biological processes. However, whether B_{12} is an absolute requirement for normal growth and physiological function in *C. elegans* is unknown. If a method for creating viable B_{12}-deficient worms can be found, *C. elegans* could serve as a suitable model organism for studying the effects of B_{12} deficiency.

In the present thesis, I describe the preparation and characterization of B_{12}-deficient *C. elegans* grown under B_{12}-deficient conditions (**Chapter II, Section 1**). Furthermore, I characterized various B_{12} dodecylamine derivatives as potent inhibitors of B_{12}-dependent MS and MCM in worms and mammalian cells (**Chapter II, Section 2 and 3**), indicating that B_{12}-deficient *C. elegans* is readily prepared using the dodecylamine derivatives. **In Chapter III**, I describe the molecular mechanisms of metabolic disorders and memory/learning dysfunction induced by B_{12} deficiency in *C. elegans*.

Strict vegetarians and/or elderly people are at a high risk of developing B_{12} deficiency [36]. A large number of people have low serum B_{12} levels that result more commonly from malabsorption of protein-bound B_{12} (food-bound B_{12} malabsorption) rather than pernicious anemia [37]. Food-bound B_{12} malabsorption is found in people with certain gastric dysfunctions, particularly atrophic gastritis with low stomach acid secretion, which prevails in elderly people [38, 39]. It is therefore necessary to identify plant foods containing high free B_{12} to prevent vegetarians or elderly people from developing B_{12} deficiency. Thus, I developed a simple method for analyzing B_{12} compounds in various food samples using miniaturized high-performance TLC (**Chapter IV, Section 1**). In **Chapter IV, Section 2**, I characterized B_{12} compounds in the fruiting bodies of Shiitake mushroom as a plant-derived food. Finally, I describe production and characterization of a B_{12}-enriched vegetable to prevent vegetarians or elderly people from developing B_{12} deficiency. (**Chapter IV, Section 3 and 4**).

Chapter II

Preparation of Vitamin B_{12}-deficient *Caenorhabditis elegans* as a model animal

The major signs of B_{12} deficiency are megaloblastic anemia and neuropathy [23]. The underlying cause(s) of various symptoms (growth retardation, metabolic disorders, and neuropathy) caused by B_{12} deficiency are not still understood [24, 40]. Developing animal models of B_{12} deficiency is essential for investigating the molecular mechanisms that are defective in the metabolic disorders linked to such diseases. However, they cannot be readily prepared because animals (e.g. rats) must be fed with a B_{12}-deficient diet for long periods to achieve B_{12} deficiency [33]. *C. elegans* has been widely used as a model organism for studying a variety of biological processes [34]. In addition, the enzymes involved in human methylmalonic aciduria caused by B_{12} deficiency have been studied in *C. elegans* [41, 42]. However, whether B_{12} is an absolute requirement for normal growth and physiological function in *C. elegans* is unknown. If a method for creating viable B_{12}-deficient worms can be found, *C. elegans* could serve as a suitable model organism for studying the effects of B_{12} deficiency.

The B_{12} analogue with a modification of side chain of C-ring, B_{12}[*c*-lactam], has been reported to antagonize B_{12} in the cultured HL 60 cells [43]. Subcutaneous administration of OH-B_{12}[*c*-lactam] to rats has indicated that the analogue has the ability to act as a potent inhibitor of the mammalian B_{12}-dependent enzymes to make the rats B_{12} deficiency [44]. However, considerably high concentration of OH-B_{12}[*c*-lactam] must be administered for several weeks with osmotic mini pumps in order to prepare B_{12}-deficient rats because IF hardly binds OH-B_{12}[*c*-lactam] [44]. Although McEwan *et al*. [45] demonstrated high affinity binding of IF to a B_{12} dodecylamine derivative, our preliminary experiments indicated that this derivative was inactive in B_{12}-dependent microorganisms typically employed in B_{12} the bioassay. If the B_{12} alkylamine derivatives act as potent inhibitors of mammalian B_{12}-dependent enzymes *in vivo*, B_{12}-deficient animals would be readily prepared by oral administration

of the derivative.

In Chapter II, I describe the preparation and characterization of B_{12}-deficient *C. elegans* grown under B_{12}-deficient conditions (**Section 1**). Furthermore, I characterized various B_{12} dodecylamine derivatives as potent inhibitors of B_{12}-dependent MS and MCM in worms and mammalian cells (**Section 2** and **3**), indicating that B_{12}-deficient *C. elegans* is readily prepared using the dodecylamine derivatives.

Section 1 Vitamin B_{12}-deficient *Caenorhabditis elegans* prepared by the feeding of vitamin B_{12}-limited *Escherichia coli* OP-50 as a diet

Introduction

B_{12} deficiency results in growth retardation, metabolic disorders, and neuropathy [24, 40]. However, the underlying disease mechanisms are poorly understood. To investigate the precise mechanisms of these B_{12}-deficient symptoms, B_{12}-deficient rat have been used as a human model animal. However, they require for long periods to make them B_{12} deficiency [33]. Therefore, the lack of robust B_{12}-deficient animal models such rats has limited investigations to the biochemical mechanisms induced by B_{12} deficiency. Recently, the new model animal turning into rats is demanded.

C. elegans has been widely used as a model organism for studying a variety of biological processes [24]. Many molecular and cellular processes are conserved between nematodes and mammals. Most human disease genes and pathways are present in the worm [35]. However, whether B_{12} is an absolute requirement for normal growth and physiological function in *C. elegans* is unknown.

In this section, I describe a novel method for inducing B_{12} deficiency in *C. elegans* and the effects of B_{12} deficiency on various biomarkers, and characterize the physiological roles of B_{12} in this model organism.

Materials and Methods

Organisms and growth conditions

The N2 Bristol wild-type *C. elegans* strain was maintained at 20°C on nematode growth medium (NGM) plates using the *Escherichia coli* OP50 strain as the food source [46]. To induce B_{12} deficiency, worms were grown on 1.7% (w/v) agar plates containing M9 medium (3 g/L KH_2PO_4, 6 g/L Na_2HPO_4, 0.5 g/L NaCl, 1 g/L NH_4Cl, 1 mmol/L

$MgSO_4$, 50 μmol/L $CaCl_2$, 2 g/L glucose, 4 mg/L thiamine hydrochloride, and 5 mg/L cholesterol) in l L H_2O. Plates containing B_{12}-supplemented (100 μg/L cyanocobalamin) M9-medium each received one egg obtained from worms grown on NGM plates with B_{12}-deficient OP50 *E. coli* (described below). Eggs were allowed to hatch and develop into egg-laying adult worms. The adult worms were then removed from each plate, eggs were collected, and each egg was transferred onto a new control plate. After this procedure was repeated at least 10 times, the resultant worms were used as experimental controls.

Preparation of B_{12}-deficient E. coli cells

E. coli OP50 was grown in M9 medium (3 g/L KH_2PO_4, 6 g/L Na_2HPO_4, 0.5 g/L NaCl, 1 g/L NH_4Cl, 1 mmol/L $MgSO_4$, 50 μmol/L $CaCl_2$, 2 g/L glucose, and 4 mg/L thiamine hydrochloride) at 37°C for three days. Cells were inoculated every three days into fresh M9 medium and used as a food source for *C. elegans*. The B_{12} content (0.2 μg/g wet weight) of *E. coli* cells grown in the M9 medium was significantly reduced compared with cells grown in the standard Luria-Bertani medium (11.1 μg/g wet weight).

Preparation of B_{12}-deficient C. elegans

C. elegans were grown at 20°C on B_{12} (100 μg/L)-supplemented medium using B_{12}-deficient *E. coli* OP50 as a food source. An individual worm egg was transferred onto each plate, which contained fresh B_{12}-deficient medium seeded with the B_{12}-deficient *E. coli* OP50. After the eggs hatched, worms were allowed to grow until they became adults and had laid eggs (yielding the F1 generation). Individual eggs were removed from the plate and each was transferred onto a fresh plate containing B_{12}-deficient medium and grown to maturity under the same conditions (yielding the F2

generation). This process was repeated for five generations. After three days, adult worms of each generation (F1-F5) were used for experiments. **Fig. 6** shows the preparative procedure of B_{12}-deficient worms.

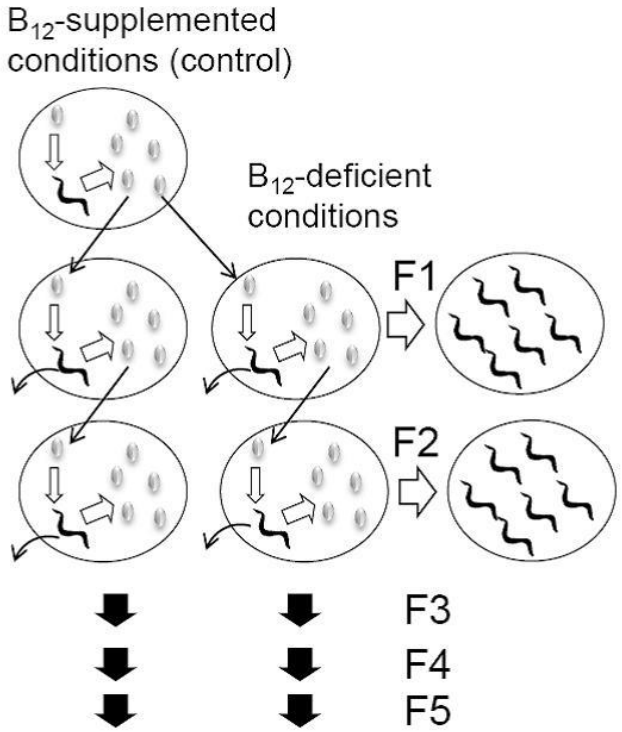

Fig. 6. Preparation of B_{12}-deficient *C. elegans*. Single eggs from *C. elegans* adults grown on NGM plate were transferred onto individual plates containing B_{12}-supplemented M9 seeded with B_{12}-deficient *E. coli* OP50 (control) and grown for three days. The eggs hatched and developed into adult worms, which then laid eggs. The adult worm was removed from each plate and individual eggs were transferred individually onto fresh identical plates. This procedure was repeated at least 10 times. These worms were used as experimental control worms. To prepare B_{12}-deficient worms, single eggs from the control worm were transferred onto individual plates containing B_{12}-deficient M9 medium seeded with B_{12}-deficient *E. coli* and allowed to reach maturity and lay eggs (F1 generation). F1 worms obtained from these eggs were used to generate F2 worms following the same procedures. This process was repeated to prepare F5 B_{12}-deficient worms.

Vitamin B_{12} assay

F1-F5 worms grown under B_{12}-supplemented or B_{12}-deficient conditions were harvested and incubated for 1 h at 20°C in fresh M9 medium to remove any residual *E.*

coli cells. Worms (2 g wet weight) were then disrupted using a hand homogenizer (AS ONE Corp., Osaka, Japan) and sonicated (6 kHz for 60 s) three times. The worm homogenate was resuspended in 100 mL of 57 mmol/L sodium acetate buffer (pH 4.8) containing 0.05% (w/v) KCN and boiled for 30 min. The extract was centrifuged at 15,000 × *g* for 15 min at 4°C and the supernatant was used for assaying B_{12} concentrations by standard microbiological methods utilizing *Lactobacillus delbrueckii* subsp. *lactis* ATCC 7830, as described previously [40].

B_{12}-related biomarker assays

F1-F5 worms grown under B_{12}-supplemented or B_{12}-deficient conditions were collected and washed in M9 medium as described above. The harvested worms were resuspended in 0.5 mL of 100 mmol/L potassium phosphate buffer (pH 7.0) at 2°C and homogenized using a hand homogenizer. The cell homogenate was centrifuged at 15,000 × *g* for 15 min at 4°C and the supernatant was used as a crude homogenate for subsequent biomarker assays.

MMA and Hcy, two indices of B_{12} deficiency, were assayed using the high performance liquid chromatography (HPLC) methods of Al-Dirbashi *et al*. [47] and Febriani *et al*. [48], respectively. MCM-[49] and MS-[50, 51] activities were assayed at 37°C as previously described. Total- and holo-enzyme activities were determined in the presence or absence of each B_{12} coenzyme (Ado-B_{12} for MCM and CH_3-B_{12} for MS).

Analysis of egg-laying capacity, life cycle, and lifespan

Measurement of egg-laying capacity was based on the method of Byerly *et al*. [52]. Individual L4-stage worms grown under B_{12}-supplemented or B_{12}-deficient conditions were selected, transferred onto the fresh plates containing the same culture medium, and incubated for one day at 20°C. After laying eggs, each worm was removed from the plate, and the eggs were counted. Egg counting was performed in triplicate.

The life cycle and lifespan of B_{12}-deficient F5 worms were determined at 20°C using the synchronization method of Johnson and Wood [53]. Worms were scored as dead when they no longer responded to prodding with a pick. In each survival experiment, 100 worms were used.

Protein quantitation

Proteins were assayed by the method of Bradford [54] using ovalbumin as a standard.

Statistical analysis

The effects of B_{12} deficiency on various *C. elegans* biomarkers were evaluated by one-way ANOVA, and a post-hoc analysis was performed using Tukey's multiple comparison tests. Analyses were performed with GraphPad Prism 3 for Windows version 2.01 (GraphPad software Inc., La Jolla, CA, USA). All data are presented as the mean ± SD. Differences were considered statistically significant when $p < 0.01$.

Results and Discussion

Effects of B_{12}-deficient growth conditions on various B_{12}-related biomarkers in C. elegans

Nematodes grown on B_{12}-supplemented M9 medium with B_{12}-deficient *E. coli* OP50 as a food source (control) showed identical growth rates that were identical to that of worms grown under normal conditions, indicating that the experimental control conditions were adequate for the normal growth of *C. elegans*. The control worms were able to ingest both B_{12}-enriched agar medium and B_{12}-deficient *E. coli* cells. Therefore, they would mainly absorb sufficient amount of free B_{12} from the agar medium because

of low B_{12} content in *E. coli*.

Under B_{12}-deficient conditions, the B_{12} content of the worms decreased gradually over four generations (**Fig. 7**). The B_{12} concentration in F5 generation worms was only 4% compared with that in the control worms. These results indicate that dietary B_{12} deprivation over five generations leads to a significantly decreased B_{12} status in *C. elegans*.

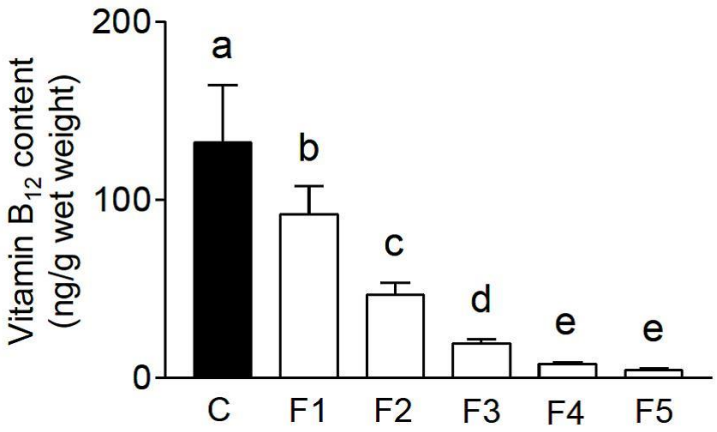

Fig. 7. B_{12} content is reduced in worms grown under B_{12}-supplemented and -deficient conditions. The B_{12} content of F1-F5 worms grown under control (black bar) and B_{12}-deficient (white bars) conditions was assayed using microbiological methods. Data represent the mean ± SD of ten independent experiments. Different letters (a-e) indicate values that are significantly different ($p < 0.01$); identical letters indicate values that are not significantly different.

The MMA and Hcy indices of B_{12} deficiency were assayed in *C. elegans* grown under both control and B_{12}-deficient conditions. There was a significant increase in the levels of both compounds between F3 and F5 generation worms (**Fig. 8A** and **B**). Hcy and MMA levels were approximately four and five times greater, respectively, in F5 worms grown under B_{12}-deficient conditions than in the control worms. Although holo-MCM activity significantly decreased in F4 and F5 worms grown under B_{12}-deficient conditions (**Fig. 8E**), the total MCM activity (holo- and apo-enzymes) increased (**Fig. 8C**). The result indicates that apo-MCM activity is significantly increased by B_{12} deficiency.

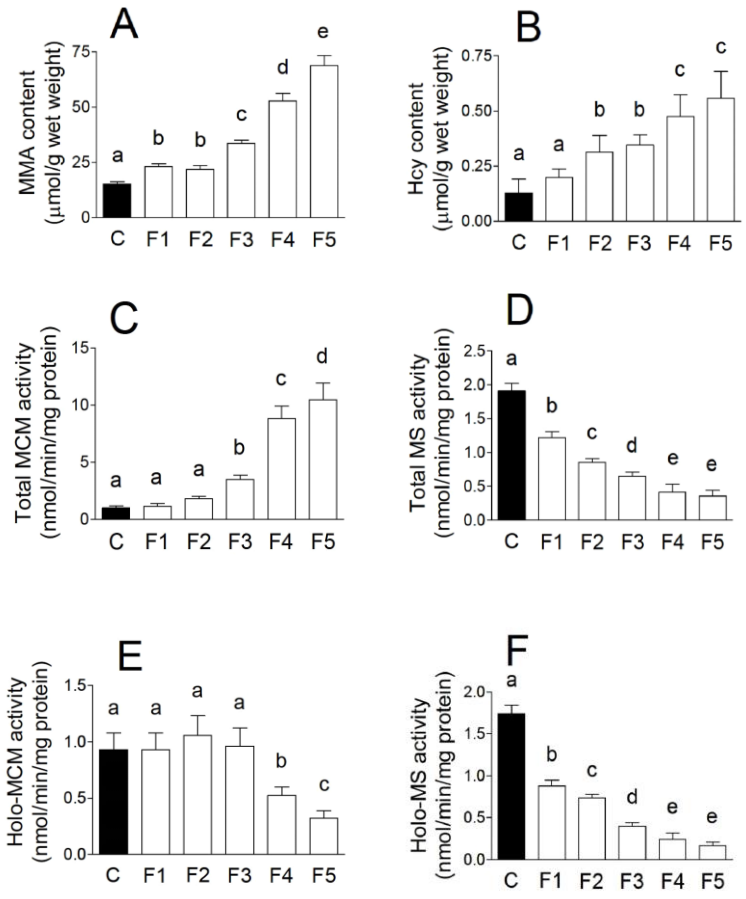

Fig. 8. Vitamin B_{12} deficiency changes the concentration of various B_{12}-related biomarkers. (A) Methylmalonic acid (MMA) and (B) homocysteine (Hcy) content, (C) total- and (E) holo-methylmalonyl-CoA mutase (MCM) activity, and (D) total- and (F) holo-methionine synthase (MS) activity were measured in extracts of worms grown under B_{12}-supplemented (black bar) and B_{12}-deficient conditions (white bars) for up to 5 generations. For (E) holo-MCM and (F) holo-MS activities, measurements were made in the absence of specific coenzymes. Data represent mean ± SD of ten independent experiments; a-e indicate values that are significantly different, $p < 0.01$.

Both total- and holo-MS activities significantly decreased with each generation until the F4 generation and were maintained at a constant level thereafter (**Fig. 8D** and **F**). These results indicate that F5 generation worms grown under B_{12}-deficient conditions develop severe B_{12} deficiency. However, one day after transfer of B_{12}-deficient worms onto the B_{12}-supplemented medium, the level of these B_{12}-related biomarkers recovered considerably (unpublished data). These results indicate that B_{12} functions as a cofactor for both MCM and MS in *C. elegans* and that B_{12}-dependent changes in both MCM and

MS enzyme activities occur in *C. elegans* and mammals [55, 56]. However, using the nematode model, the time needed to produce a severely B_{12}-deficient animal is only 15 days (i.e. five generations).

Holo-MS activity was rapidly decreased by F1 generation under B_{12}-deficient conditions (**Fig. 8F**), but holo-MCM activity was not changed until the F4 generation (**Fig. 8E**). These results indicated that MS is more sensitive to cellular B_{12} concentrations than MCM. Yamada *et al*. have demonstrated that most MS activity is derived from holo-enzyme in B_{12}-sufficient or -deficient mammals because the apo-enzyme is very unstable [55]. In contrast, Nakao *et al*. have indicated that holo-MCM activity was less than 5% of the total enzyme activity in B_{12}-sufficient rats and that a marked increase in the apo-enzyme activity occurred under B_{12}-deficient conditions [56]. In this *C. elegans* study, holo-MCM activity was 97% of the total enzyme activity in the control worms and holo-enzyme activity gradually decreased in the F1 (92%), F2 (50%), and F3 (24%) generations, under B_{12}-deficient conditions. However, the specific activity of holo-MCM did not change until the F4 generation even if the B_{12} content of the worms significantly decreased along with increased MMA content. The details of the occurrence of this MCM-independent increase in MMA concentration soon after the onset of B_{12} deficiency remain to be elucidated.

B_{12} deficiency affects C. elegans egg-laying capacity, life cycle and lifespan

Egg-laying rates significantly decreased in B_{12}-deficient worms (**Fig. 9A**), which also showed a significantly prolonged life cycle compared with the control worms (**Fig. 9B**). Similarly, B_{12}-deficient rats have been reported to show severe growth retardation [21] and infertility [57].

The lifespan of B_{12}-deficient F5 worms were significantly decreased by B_{12} deficiency (**Fig. 9C**). The maximal lifespan of B_{12}-deficient worms was reduced to 18 days, compared with a lifespan of 24 days in the control worms (**Fig. 9C**). These data demonstrate for the first time that B_{12} deficiency significantly reduces the lifespan of

animals.

B_{12} deficiency causes severe growth retardation and various metabolic disorders in mammals [21]. The B_{12} coenzyme $AdoB_{12}$ functions as a coenzyme of MCM, catalyzing the isomerization of (*R*)-methylmalonyl-CoA to succinyl-CoA in the mitochondria. Odd-numbered fatty acids, branched chain amino acids, and cholesterols are metabolized by methylmalonyl-CoA to the tricarboxylic acid (TCA) cycle intermediate succinyl-CoA *via* MCM [12]. When MCM activity was significantly decreased by B_{12} deficiency, MMA abnormally accumulated in the cells [21].

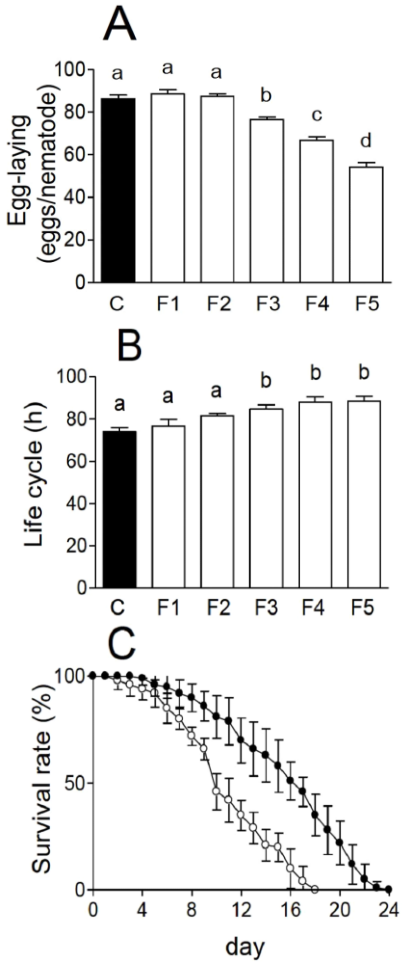

Fig. 9. Vitamin B_{12} deficiency reduces egg-laying capacity and lifespan, and increases the length of the life cycle in *C. elegans*. (A) Total number of eggs per worm, (B) the length of the life cycle (h), and (C) the lifespan were determined in the control (black bar) and B_{12}-deficient (white bars) F5 worms. Data represent mean ± SD of ten independent experiments; a-d indicate values that are significantly different, $p < 0.01$.

The elevated concentration of MMA mainly inhibits mitochondrial respiration because of competitive inhibition of succinate dehydrogenase (EC 1.3.99.1) by MMA [57]. TCA cycle inhibition by MMA accumulation contributes to various metabolic disorders associated with B_{12} deficiency [21], including severe growth retardation (prolonged life cycle) in the B_{12}-deficient worms.

Many studies have demonstrated that there is a relationship between B_{12} deficiency and infertility in males and females [58, 59]. However, the mechanism whereby B_{12} deficiency causes infertility is poorly elucidated. CH_3-B_{12} functions as a coenzyme of MS, which catalyzes the methyl transfer from CH_3-THF to Hcy, resulting in the donation of a methyl group to Hcy, forming Met [13]. MS is important to re-synthesize Met and to metabolize CH_3-THF. THF is the precursor for the methylene derivative of folate, which is essential for thymidine supply and normal DNA replication in cells [60]. Furthermore, Met is one of the amino acid building blocks of protein and acts as the universal methyl group donor (SAM) for a large number of methylation reactions. Yamada *et al*. [61] reported that reduced testicular MS activity is the primary cause of pathological impairment of spermatogenesis owing to B_{12} deficiency and that methionine supplementation to the diet can reduce this impairment. Bennet [62] has reported that B_{12} deficiency may lead to recurrent fetal death owing to the elevated Hcy levels. The epigenetic regulation of gene expression involves remodeling of chromatin by either the addition of methyl group to DNA and/or the post-translational modification of histone amino acid residues. SAM is a critical substrate for histone methyltransferases, whereas *S*-adenosylhomocysteine (SAH) is a potent inhibitor of the enzymatic reaction [63]. It has been observed that the concentration of SAM is reduced, with a concomitant increase in SAH concentration, in B_{12}-deficient animal models or humans [64]. Our experiments indicated that SAM/SAH ratios significantly decrease in B_{12}-deficient *C. elegans* relative to control worms (Details see in **Chapter III**, **Section 2**). The decreased SAM/SAH ratios may lead to abnormal epigenetic regulation of gene expression, including gene relevant to fertility.

These observations suggest that decreased egg-laying and prolonged life cycle

found in B_{12}-deficient worms are because of various B_{12}-associated metabolic disorders, which results in abnormal epigenetic regulation of the expression of certain genes.

Approximately 1 % of B_{12}-deficient worms showed a specific morphological abnormality (**Fig. 10**), similar to the short and plump "dumpy" mutant phenotype that is formed because of disordered cuticle collagen biosynthesis [65, 66]. However, there is no information available on the relationship between B_{12} deficiency and collagen biosynthesis. Hcy, which is significantly increased by B_{12} deficiency, has been shown to interfere with post-translational modifications of collagen directly by inhibiting lysyl oxidase (EC 1.4.3.13), which is involved in collagen cross-linking [67]. This observation and our data indicate a possible link between B_{12} deficiency and collagen biosynthesis including post-translational modifications of collagen cross-linking.

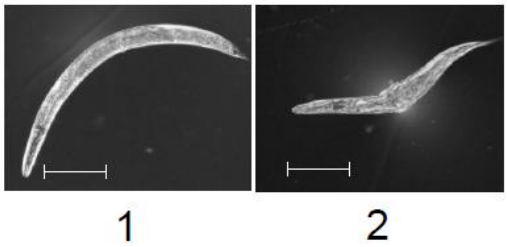

Fig. 10. B_{12}-deficient *C. elegans* show morphological changes. Differential interference microscopy images of the (1) control and (2) B_{12}-deficient worms were obtained using an IX71 microscope (OLYMPUS Corp., Tokyo, Japan). The length of individual worms was measured using Image J software, bar = 200 μm.

Above results indicate that B_{12} is essential for *C. elegans* growth and that prolonged B_{12} deficiency induces a number of phenotypes, including decreased egg-laying capacity (infertility), prolonged life cycle (growth retardation), and a reduced lifespan. Therefore, I propose that *C. elegans* is an ideal model organism for investigating the mechanisms driving such B_{12}-deficient phenotypes, as B_{12} deficiency can be induced in this animal in only 15 days. However, there are some limitations to this animal model; for example, *C. elegans* does not have any blood corpuscle systems. Moreover, bioinformatic analyses indicate that *C. elegans* also does not have any orthologs of three

B_{12}-transport proteins (HC, IF, and TC-II) involved in human gastrointestinal absorption and subsequent blood circulation of B_{12}. Thus, *C. elegans* is not suitable for use as a model organism to study the mechanisms of some human B_{12}-deficient disease phenotypes, such as megaloblastic anemia and dysfunctions of intestinal absorption and transport of B_{12}. However, this animal is widely used as a model organism for studying the mechanisms of fertilization [68] and embryonic cell division [69]. Moreover, *C. elegans* is often used for understanding human brain and neuronal disorders [70] in addition to the effects of certain molecules on learning and memory [71]. *C. elegans* may become a suitable organism and a powerful new tool for the study of B_{12}-deficient human diseases such as infertility [58, 59, 61], fetal death [62, 72], neuropathy [73], and cognitive impairment [74].

Summary

B_{12} deficiency has been linked to developmental disorders, metabolic abnormalities, and neuropathy; however, the mechanisms involved remain poorly understood. *C. elegans* grown under B_{12}-deficient conditions for five generations develop severe B_{12} deficiency associated with various phenotypes that include decreased egg-laying capacity (infertility), prolonged life cycle (growth retardation), and reduced lifespan. These phenotypes resemble the consequences of B_{12} deficiency in mammals, and can be induced in *C. elegans* in only 15 days. Thus, *C. elegans* is a suitable animal model for studying the biological processes induced by vitamin deficiency.

Section 2 Vitamin B_{12}-deficient *Caenorhabditis elegans* prepared by the treatment of vitamin B_{12} dodecylamine derivative

Introduction

When *C. elegans* was grown under B_{12}-deficient conditions for five generations (approximately 15 days), worm developed severe B_{12} deficiency (**Chapter II**, **Section 1**). The B_{12}-deficient worms showed various phenotypes including decreased egg-laying capacity (infertility), prolonged life cycle (growth retardation), and reduced life span. These phenotypes resemble those of B_{12}-deficient mammals. If development of animal models of B_{12} deficiency is facilitated by the use of a potent inhibitor of B_{12}-dependent enzymes, B_{12}-deficient animals would be prepared in a short time. McEwan *et al*. [45] synthesized ribose-5'-carbamate derivatives of B_{12} and demonstrated high-affinity binding of IF to certain alkylamine derivatives. My preliminary experiments indicate that these alkylamine derivatives lack detectable biological activity in certain microorganisms that require B_{12} for growth, such as *Escherichia coli* 215, *L. delbrueckii* ATCC 7830, and *Euglena gracilis* Z. In this section, I show that CN-B_{12} dodecylamine derivative potently inhibited the B_{12}-dependent enzymes MCM and MS of *C. elegans*.

Materials and Methods

Chemicals

CN-B_{12}, 1, 1'-carbonyldiimidazole, and dodecylamine were purchased from Wako Pure Chemical Industries (Osaka, Japan). Phenyl-Toyopearl 650M was purchased from Tosoh Corporation (Tokyo, Japan).

Organisms and culture conditions

The maintenance of worms and preparation of control or B_{12}-deficient worms was

performed as described in **Chapter II, Section 1**.

Preparation of the CN-B_{12} dodecylamine derivative

The CN-B_{12} dodecylamine derivative (**Fig. 11**) was prepared according to the method by McEwan *et al*. [45]. In brief, solid 1, 1'-carbonyldiimidazole (26 mg) was added to CN-B_{12} (0.1 g) dissolved in dimethyl sulfoxide (1.2 mL) at 30°C, and the mixture was stirred for 25 min. Dodecylamine (0.27 mmol) was added to the mixture and then stirred for 24 h at 25°C. The B_{12} compound was extracted twice from the mixture with 2 mL of phenol/dichloromethane (1:2, v/v) and then re-extracted twice from the combined phenol fractions with 2 mL of distilled water. The water-soluble fractions were combined and chromatographed using a TSK gel-Toyopearl 650M column (2.4 × 24 cm) equilibrated with 250 mL of 25% (v/v) ethanol. Unreacted and modified CN-B_{12} compounds were eluted with 250 mL of 25% (v/v) and 60% (v/v) ethanol. The fractions containing products were combined, the solvent was evaporated under reduced pressure, and the residue was dissolved in 5 mL of 80% (v/v) ethanol. The product was further purified using silica-gel 60 TLC with the solvent 1-butanol:2-propanol:water (10:7:10, v/v/v). After drying the TLC sheet, the CN-B_{12} derivative was collected, extracted with 80% (v/v) methanol, and the solvent was evaporated under reduced pressure. The residue was dissolved in a small amount of 18% (v/v) acetonitrile and then purified using a reversed-phase HPLC column (Wakosil-II 5C18RS, φ 4.6 × 150 mm) and a Shimadzu HPLC system (SCL-10A VP System controller, DGU-20A 3R Degassing unit, LC-20AB Liquid chromatograph, SPD-20A UV/VIS detector, and CTO-20AC Column oven). The CN-B_{12} derivative was eluted with a linear gradient of acetonitrile (18%－28% for 8.5 min and 28%－100% for 13 min, 1.0 mL/min) at 40°C and monitored by measuring absorbance at 254 nm. The peak fraction was collected, the solvent was evaporated under reduced pressure, and the residue was used for the following experiments. The purified dodecylamine

derivative of CN-B_{12} (approximately 94% purity) was dissolved in distilled water, and its concentration was determined at λ_{361} (ε =13,000) as described previously [45].

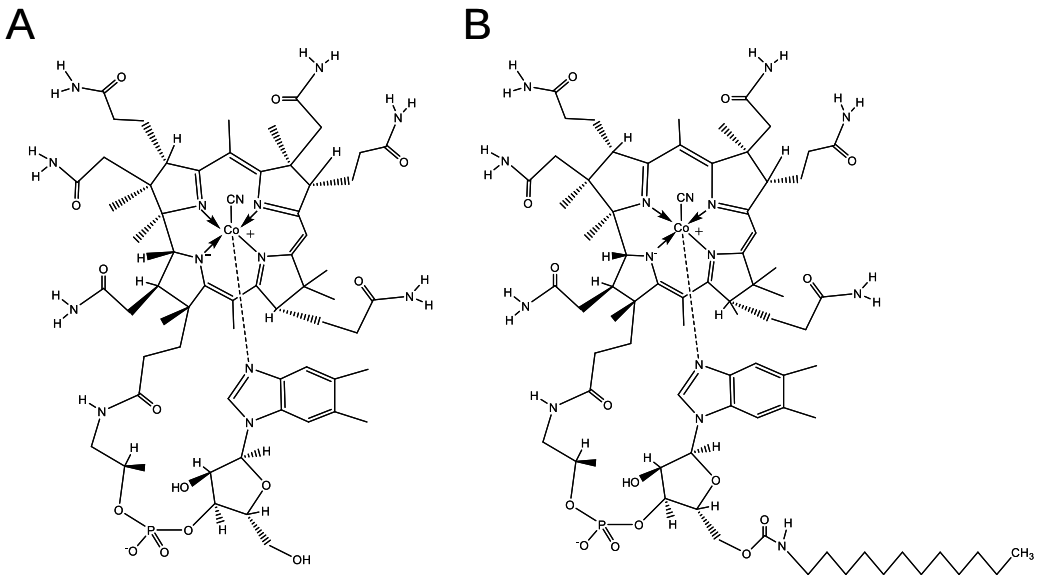

Fig. 11. Structures of CN-B_{12} and its dodecylamine derivative. (A) CN-B_{12} (B) CN-Cbl dodecylamine derivative.

Preparation of C. elegans treated with CN-B_{12} dodecylamine derivative

Control worm eggs were transferred to and hatched on an M9 plate containing the CN- B_{12} derivative (100 μg/L) and *E. coli* OP50 and grown to maturity.

Determination of the levels of CN-B_{12} and its derivative in C. elegans

Worms grown in the absence or presence of CN-B_{12} or its dodecylamine derivative were harvested and incubated for 1 h at 20°C in fresh M9 medium to remove any residual *E. coli*. The washed worms (1.0 g wet weight) were homogenized in 0.5 mL of 100 mmol/L potassium phosphate buffer (pH 7.0) at 4°C using a manual homogenizer (AS ONE Corp., Osaka, Japan) and sonicated (6 kHz for 60 s) three times on ice. The

worm homogenate was resuspended in 25 mL of 57 mmol/L sodium acetate buffer (pH 4.8) containing 0.05% (w/v) KCN, boiled for 30 min, and centrifuged at 15,000 ×*g* for 15 min at 4°C. The B_{12} content of the supernatant fraction was determined using a microbiological assay as described previously [75].

CN-B_{12} and the B_{12} derivative were extracted from treated worms using the same conditions as described above. The supernatant fraction (20 mL) that was chromatographed using a Sep-Pak Plus C18 cartridge (Waters Corp., Milford, MA, USA) to separate the CN-B_{12} derivative from CN-B_{12}. After the cartridge was washed with 10 mL of distilled water, CN-B_{12} and the CN-B_{12} derivative were eluted sequentially with 10 mL of 20% (v/v) ethanol solution and 60% (v/v) ethanol, respectively. The solvent of each fraction was evaporated under reduced pressure and then dissolved in 100 μL of distilled water. CN-B_{12} was determined using the microbiological B_{12} assay method described above, and the CN-B_{12} derivative was assayed using a Shimadzu HPLC system (SCL-10A VP System controller, DGU-20A 3R Degassing unit, LC-20AB Liquid chromatograph, SPD-20A UV/VIS detector, and CTO-20AC column oven) with a CDS ver. 5 chromato-data processing system (LAsoft, Ltd., Chiba, Japan). Samples (20 μL) were chromatographed using a reversed-phase HPLC column (Wakosil-II 5C18RS, φ 4.6 × 150 mm) and eluted (1.0 mL/min) with a linear gradient of methanol (20%－90% for 30 min) containing 1% (v/v) acetic acid at 40°C. The B_{12} derivative was monitored by its absorbance at 254 nm, and its retention time was 30.3 min.

Determination of coenzyme forms of the B_{12}-dodecylamine derivative

All procedures were performed in the dark. Hydroxo (OH)- and adenosyl (Ado)-forms of the B_{12}-dodecylamine derivative were prepared from the CN-B_{12} derivative. In brief, the CN-B_{12} dodecylamine derivative was dissolved in distilled water, bubbled with nitrogen gas for 30 min, reduced with sodium tetrahydroborate until the solution turned dark brown, and neutralized with 1.0 mol/L HCl. Most of the CN-B_{12}

derivative was converted to the OH-B_{12} dodecylamine derivative. To prepare AdoB_{12} dodecylamine derivative, a small amount of 5'-iodo-5'-deoxyadenosine was added to the reduced form of the B_{12} dodecylamine derivative, and this solution was neutralized as described above. The neutralized preparations were desalted using a Sep-pak Vac 20 cc (5 g) C18 cartridge (Waters corp.), and the desalted and concentrated solutions were treated with silica-gel 60 TLC as described above to separate the OH- or Ado-form of the dodecylamine derivative and unmodified CN-B_{12} dodecylamine derivative. After drying the TLC sheet, the OH- or Ado-form of the dodecylamine derivative was collected, extracted with 80% (v/v) ethanol, and the solvent was evaporated to dryness under reduced pressure. Each residue was dissolved in a small amount of distilled water and used as the authentic OH-B_{12} dodecylamine or AdoB_{12} dodecylamine derivatives. I was unable to prepare a CH_3-B_{12} dodecylamine derivative with high purity.

To extract B_{12} derivatives, including its coenzyme forms from worms, 100 mL of 80% (v/v) ethanol was added to lyophilized samples of worms treated with the CN-B_{12} dodecylamine derivative. The samples were heated at 98°C for 30 min under reflux and cooled to room temperature [76], centrifuged at 10,000 × *g* for 10 min, and the supernatant was evaporated under reduced pressure. The residue was dissolved in 5 mL of distilled water and centrifuged at 10,000 × *g* for 10 min to remove insoluble material. The supernatant fraction was chromatographed a Sep-Pak Plus C18 cartridge, which was washed with 10 mL of distilled water and eluted with 2 mL of ethanol. The ethanol elute was evaporated under reduced pressure and the residue was dissolved in 100 μL of distilled water. The levels of coenzyme forms of the B_{12} dodecylamine derivative in worms treated with the CN-B_{12} dodecylamine derivative were determined using HPLC as described above. The retention times of OH-, CN-, and Ado-forms of B_{12} dodecylamine derivatives were 22.0, 30.6, and 36.2 min, respectively.

Assays for B_{12}-related biomarkers

The worms (1.0 g wet weight) grown each condition were assayed B_{12}-related biomarkers described in **Chapter II, Section 1**.

Inhibition of MCM and MS activities by the CN-B_{12} dodecylamine derivative

My previous study showed that the levels of apo-MCM are increased up to approximately 97% of the total MCM (holo- and apo-MCMs) in B_{12}-deficient worms. Thus, a cell homogenate of B_{12}-deficient worms was used as an apo-MCM preparation in the following experiments (**Chapter II**, **Section 1**). Lineweaver-Burk analysis was used to determine the K_m value of worm MCM for $AdoB_{12}$ in reaction mixtures containing 0, 2.5, 5, and 10 μmol/L of $AdoB_{12}$. Dixon plots [77] were used to determine the apparent K_i value of MCM in reaction mixtures containing 0, 1, 3, 5, and 10 μmol/L of CN-B_{12} or its dodecylamine derivative.

A cell homogenate of B_{12}-supplemented (control) worms was used as a holo-MS enzyme preparation, because most MS activity is derived from the holoenzyme in B_{12}-supplemented or -deficient worms. Holo-MS activity was determined in reactions containing 0, 1, 3, 5, and 10 μmol/L of CN-B_{12} or its dodecylamine derivative.

Western blotting

Worms grown in the absence of CN-B_{12} or in the presence of CN-B_{12} or the CN-B_{12} dodecylamine derivative were homogenized in 100 mmol/L potassium phosphate buffer (pH 7.0) at 4°C. Each homogenate was centrifuged at 15,000 ×g for 10 min and the supernatant fraction was analyzed. We used a precast slab gel (PAGEL, type NPG-520L, ATTO Corporation, Tokyo, Japan) for electrophoresis of samples through a 5%－20% (w/w) linear gradient of polyacrylamide in the presence of SDS. After electrophoresis, proteins were transferred to a PVDF membrane (Immuno-Blot PVDF, Bio-Rad Laboratories, Inc. Hercules, CA, USA) in a Trans-Blot SD semi-dry electrophoretic

transfer cell (Bio-Rad). The PVDF membrane was probed with an anti-MS antibody (ab66039, abcam®, Cambridge, MA, USA). We performed the immunodetection reactions using an anti-mouse IgG antibody secondary antibody (Promega KK, Tokyo, Japan) coupled to horseradish peroxidase and an immunoblot-staining kit for peroxidase (EzWestBlue, ATTO), according to the manufacturer's instructions. A Protein Ladder One Triple-color kit (Nacalai Tesque Inc., Kyoto, Japan) was used to determine molecular mass. After the treated PVDF membrane was photographed using a digital camera (Coolpix 4300, Nikon, Japan), the intensities of the protein bands were calculated of Image J software [78].

Quantitative PCR analysis (qPCR)

Total RNA was prepared from worms using Sephasol®-RNA1 (Nacalai Tesque). Poly(A)$^+$ mRNA prepared from total RNA using the Poly (A)$^+$ Isolation kit from Total RNA (Nippon Gene, Tokyo, Japan) was used to synthesize cDNA using PrimeScript™ Ⅱ 1st Strand cDNA Synthesis kit (Takara Bio, Otsu, Japan). Primer pairs used for qPCR analysis were designed using GENETYX software (GENETYX Corporation, Tokyo, Japan) (**Table 1**). Gene-specific primers were selected such that the resulting PCR products were approximately 100 bp. A CFX Connect™ Real-Time System (Bio-Rad) with SYBR Premix Ex Taq (Takara Bio) was used to perform qPCR. The level of the mRNA encoding β-actin was used as an internal standard. The qPCR experiments were repeated at least three times for each cDNA prepared from three preparations of worms.

Analysis of egg-laying capacity and life cycle

Measurements of egg-laying capacity and life cycle were performed according to the method described in **Chapter II**, **Section 1**. Individual worms grown in the presence of CN-B_{12}, its dodecylamine derivative or in the absence of B_{12} were transferred to fresh plates containing the respective culture media and incubated for 1 day at 20°C. After

laying eggs, each worm was removed from the plate, and the eggs were counted in triplicate.

Table 1. Primer pairs used for the qPCR analysis

Gene name	Primer sequences (5' to 3')
mmcm-1	ATTAAAGCAGGGCAGCAAGGAC and
	GGCACGGATATGGTTCAACTTGG
metr-1	AAAGACCACGACAAGCCACTGA and
	CGCTTGATGATTCGAGCACGTT
mmaa-1	TTGGAAAGAAGGCGACAGGA and
	TTGTTTCTGCAGCCAGACCA
mmab-1	GCTCTTCTGATTTGGGAAGAGG and
	CGACGCTCATTGTTGTACAGAG
cblc-1	ATGTTGCTGGAGCAGCTTTC and
	AGTGTCCACCGTAGATTGGATG
mtrr-1	AAGACCGCTGATTCGTGTACTC and
	GCATGTCAGCCAATGACAATCC
act-1	TCCAAGAGAGGTATCCTTACCC and
	CTCCATATCATCCCAGTTGGTG

Primer pairs for the qPCR were designed using GENETYX software. Each gene is involved in the metabolisms of B_{12}, including MCM (*mmcm-1*), MS (*metr-1*), methylmalonic acidemia cobalamin A complementation group (*mmaa-1*), cob(I)alamin adenosyltransferase (*mmab-1*), methylmalonic aciduria B_{12} C type (*cblc-1*), and MS reductase (*mtrr-1*). For normalization, β-actin (*act-1*) mRNA levels served as the internal standard.

Protein quantitation

Protein concentrations were determined using the Bradford method [54] with ovalbumin as a standard.

Statistical analysis

The effects of the CN-B_{12} dodecylamine derivative on *C. elegans* phenotypes were evaluated using one-way ANOVA with Tukey's multiple comparison test (GraphPad Prism 3 for Windows version 2.01; GraphPad Software Inc., La Jolla, CA, USA). All data are presented as the mean ± standard deviation (SD). Significant differences were defined as $p < 0.05$.

Results and Discussion

Effects of the CN-B_{12} dodecylamine derivative on B_{12}-related biomarkers of C. elegans

Although McEwan *et al*. [45] demonstrated high affinity binding of the gastric B_{12}-binding protein IF to the CN-B_{12} dodecylamine derivative, my preliminary experiments indicated that this derivative was inactive in B_{12}-dependent microorganisms typically employed in B_{12} the bioassay. Therefore, I evaluated effects of the CN-B_{12} dodecylamine derivative on B_{12}-related phenotypes using *C. elegans* as a model. **Table 2** shows the concentrations of B_{12} and its dodecylamine derivative in homogenate prepared from adult worms grown in the presence of the CN-B_{12} derivative for 3 days. Remarkably, the B_{12} concentration of worms grown in the presence of the CN-B_{12} derivative was only 35% compared with that of control worms and was similar to that of worms grown for two generations (6 days) in the absence of B_{12} (**Chapter II**, **Section 1**). In contrast, the CN-B_{12} dodecylamine derivative was absorbed and accumulated by worms grown in the presence of the CN-B_{12} derivative (approximately 110 ng/g wet weight). These results suggest that the CN-B_{12} dodecylamine derivative did not inhibit the uptake of B_{12} in the intestine, but it was readily accumulated in worms and significantly decreased their B_{12} concentrations.

To determine whether the dodecylamine derivative detected in the treated worms was converted into other forms of B_{12}, corrinoid compounds were extracted using 80%

(v/v) ethanol from worms grown in the presence of the dodecylamine derivative and analyzed using reversed-phase HPLC.

Table 2. Contents of CN-B_{12} and the CN-B_{12} dodecylamine derivative in worms

	CN-B_{12}	CN-B_{12} dodecylamin derivative (ng/g wet weight)
Control worms	132.2 ± 26.7	-
Treated worms	46.5 ± 7.8	110.0 ± 17.2

Control and treated worms were grown on plates containing CN-B_{12}- and CN-B_{12} dodecylamine derivative-supplemented (each at 100 μg/L) M9 media for 3 days, respectively. Corrinoids were extracted from the treated worms by boiling with KCN at acidic pH. CN-B_{12} and the CN-B_{12} dodecylamine derivative were separated each other using a Sep-Pak Plus C18 cartridge and their levels were determined using the microbiological assay and HPLC, respectively. Data represent the mean ± SD of five independent experiments.

The retention times of authentic OH-B_{12}, CN-B_{12}, AdoB_{12}, CH_3-B_{12}, OH-B_{12} dodecylamine, CN-B_{12} dodecylamine, and AdoB_{12} dodecylamine were 3.5, 8.1, 9.5, 12.8, 22.0, 30.6, and 36.2 min, respectively (**Fig. 12A-D**). The compounds extracted from worms exposed to the derivative eluted with retention times of 3.8－30.3 min (**Fig. 12E**). A major peak with the retention time of 30.3 min was identical to that of authentic CN-B_{12} dodecylamine, and peaks were not detected with retention times of CN-B_{12} (8.1 min), OH-B_{12} dodecylamine (22.0 min), or AdoB_{12} dodecylamine (36.2 min). These results indicate that the CN-B_{12} dodecylamine derivative accumulated by worms was not converted to any other B_{12}-related compound, including its coenzyme forms.

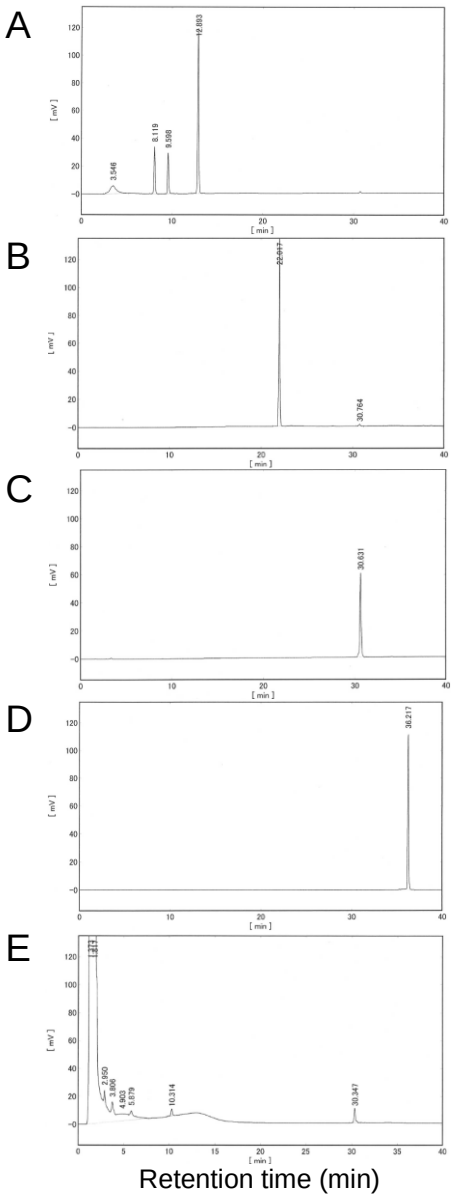

Fig. 12. HPLC analysis of B_{12} compounds detected in worms treated with the CN-B_{12} dodecylamine derivative. B_{12} analogs were analyzed using HPLC as described in Materials and Methods. (A) Authentic B_{12} compounds. Retention times of OH-B_{12}, CN-B_{12}, AdoB_{12}, and CH_3-B_{12} were 3.5, 8.1, 9.5, 12.8 min, respectively. (B) OH-B_{12} dodecylamine derivative. The retention time of the OH-B_{12} derivative was 22.0 min. (C) CN-B_{12} dodecylamine derivative. The retention time of the CN-B_{12} dodecylamine derivative was 30.6 min. (D) AdoB_{12} dodecylamine derivative. The retention time of the AdoB_{12} derivative was 36.2 min. (E) Corrinoid compounds detected in the worms grown in the presence of the CN-B_{12} dodecylamine derivative.

The levels of MMA and Hcy were assayed in *C. elegans* grown for 3 days in the presence of the CN-B_{12} dodecylamine derivative (**Fig. 13A and B**). The levels of both indicators were significantly increased in worms exposed to the dodecylamine derivative compared with those of the control worms. The increased MMA and Hcy levels were identical to those of B_{12}-deficient worms. These results show that the worms developed severe B_{12} deficiency when they were treated with the CN-B_{12} dodecylamine derivative for only 3 days.

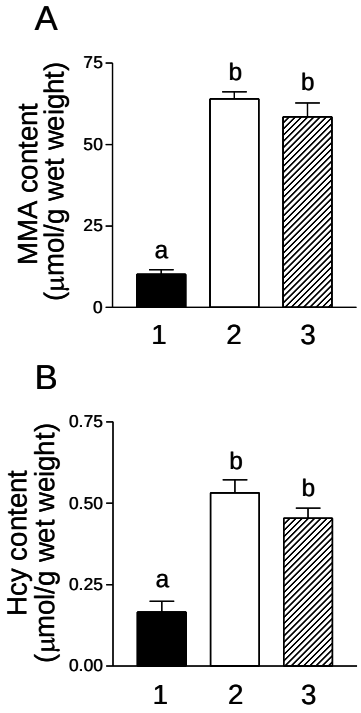

Fig. 13. Methylmalonic acid and homocysteine contents of worms treated with the CN-B_{12} dodecylamine derivative. (A) Methylmalonic acid (MMA) and (B) homocysteine (Hcy) were measured in cell homogenates of worms grown in the presence of CN-B_{12} (control; 1, black bar), the CN-B_{12} dodecylamine derivative (2, white bar), or B_{12}-deficient worms (3, shaded bar). Data represent the mean ± SD of five independent experiments. The different letters indicate values that are significantly different, $p < 0.05$.

Effects of the CN-B_{12} dodecylamine derivative on B_{12}-dependent enzymes in C. elegans

The increased levels of MMA and Hcy in worms exposed to the CN-B_{12}

dodecylamine derivative indicate that the activities of MCM and MS were significantly inhibited by the accumulation of the CN-B_{12} derivative. To determine whether the dodecylamine derivative inhibited these B_{12}-dependent enzyme activities, homogenates of worms grown in the presence (control) or absence of B_{12} or in the presence of the derivative were assayed for MCM and MS activities. The holo-MCM and MS activities of the worms treated with the dodecylamine derivative decreased to approximately 8% (**Fig. 14A**) and 18% (**Fig. 14B**), respectively, compared with those of control worms.

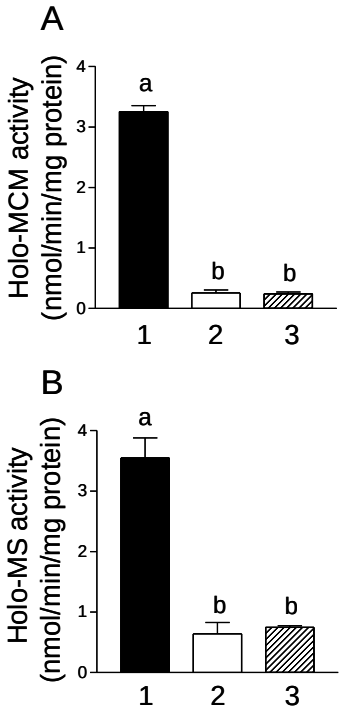

Fig. 14. B_{12}-dependent enzyme (methylmalonyl-CoA mutase and methionine synthase) activities in worms treated with the CN-B_{12} dodecylamine derivative. Holo-methylmalonyl-CoA mutase (MCM) (A) and holo-methionine synthase (MS) activities were measured in cell homogenates prepared from worms grown in the presence of CN-B_{12} (control; 1, black bar), the CN-B_{12} dodecylamine derivative (2, white bar), or B_{12}-deficient worms (3, shaded bar). Data represent the mean ± SD of five independent experiments; the different letters indicate values that are significantly different, $p < 0.05$.

To define the mechanism of inhibition of MCM by the CN-B_{12} derivative, I determined the effects of the CN-B_{12} derivative on apo-MCM activity of worms in the presence or absence of AdoB_{12} (**Fig. 15**). The apparent K_m value of the worm

apoenzyme was 4.7 μmol/L for $AdoB_{12}$. The CN-B_{12} dodecylamine derivative competitively inhibited the apoenzyme. The K_i value of the worm apoenzyme was 1.5 μmol/L for CN-B_{12} dodecylamine derivative, which has increased affinity for the apoenzyme relative to that of $AdoB_{12}$. CN-B_{12} did not reduce the apo-MCM activity in the presence of $AdoB_{12}$.

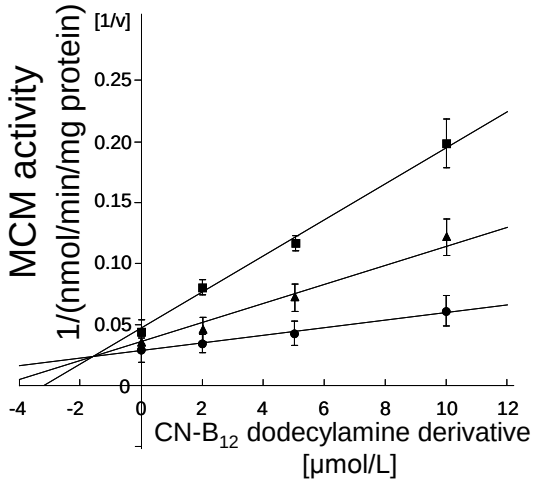

Fig. 15. Effects of the CN-B_{12} dodecylamine derivative on the enzyme activity of *C. elegans* apo-MCM in the presence of $AdoB_{12}$. A cell homogenate of worms grown under conditions of B_{12} deficiency was used as an apo-MCM preparation. MCM activity was assayed in the reaction mixture containing various concentrations (0, 2, 5, 10 μmol/L) of the CN-B_{12} dodecylamine derivative in the presence of ■ 2.5 μmol/L, ▲ 5.0 μmol/L, or ● 10.0 μmol/L of $AdoB_{12}$. MCM activity data were analyzed using the Dixon plot. Data represent the mean ± SD of three independent experiments.

Fig. 8 (**Section 1**) shows that the holo-MS present in B_{12}-supplemented or -deficient worms accounts for most MS activity. To determine whether holo-MS activity was inhibited by the addition of CN-B_{12} dodecylamine derivative, MS activity was assayed in a homogenate of the control worms in the presence of the dodecylamine derivative (**Fig. 16**). CN-B_{12} did not inhibit holo-MS activity. In contrast, the dodecylamine derivative significantly inhibited enzyme activity in a dose-dependent manner, and enzyme activity was completely inhibited in the presence of 10 μmol/L dodecylamine. These results suggest that the CN-B_{12} derivative is exchanged for CH_3-B_{12} bound to MS, inhibiting enzyme activity.

These results indicate that the affinity of CN-B_{12} dodecylamine derivative is higher for MCM compared with that of AdoB_{12} and that the inhibitions of MCM and MS activities are attributable to the formation of inactive CN-B_{12} derivative-enzyme complexes.

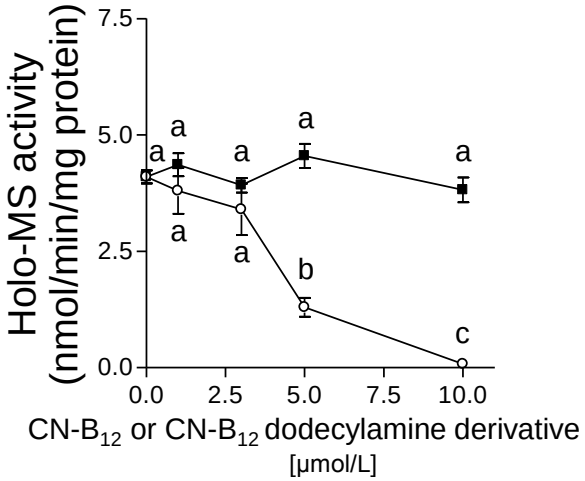

Fig. 16. Effects of the CN-B_{12} dodecylamine derivative on the activity of the *C. elegans* holo-MS. A cell homogenate of worms grown in the presence of CN-B_{12} (control) was used as a holo-MS preparation. MS activity was assayed in the presence of various concentrations (0, 1, 3, 5, and 10 μmol/L) of CN-B_{12} (■) or the CN-B_{12} dodecylamine derivative (○). Data represent the mean ± SD of three independent experiments; the different letters indicate values that are significantly different, $p < 0.05$.

Yamada *et al*. demonstrated that most MS activity is derived from the holo-enzyme in normal or B_{12}-deficient rats because the apo-enzyme is very unstable [55]. Although MS protein levels in liver extracts of B_{12}-deficient rats are significantly decreased compared with those of control rats, the level of the mRNA encoding MS is not affected by the B_{12} concentration of rat livers [55]. To determine the changes in MS protein and mRNA levels (*metr-1*) of worms treated with the CN-B_{12} derivative, I conducted western blot and qPCR analyses and found that the level of mRNA was unchanged (**Fig. 17A**), whereas the level of MS protein in B_{12}-deficient worms was reduced to approximately 32% compared with that of controls. This result differs from the detection of an extremely faint band of MS in the livers of B_{12}-deficient rats, suggesting that the worm apo-enzyme is not very unstable. The intensity of the MS protein band in

extracts prepared from worms treated with the CN-B_{12} derivative was identical to that of the controls (**Fig. 17B**). These results suggest that the binding of the CN-B_{12} derivative to MS completely inhibited MS activity and did not affect the level of MS protein. **Fig. 18** showed the predicted mechanism of inhibition of CN-B_{12} dodecylamine derivative for B_{12}-dependent enzymes.

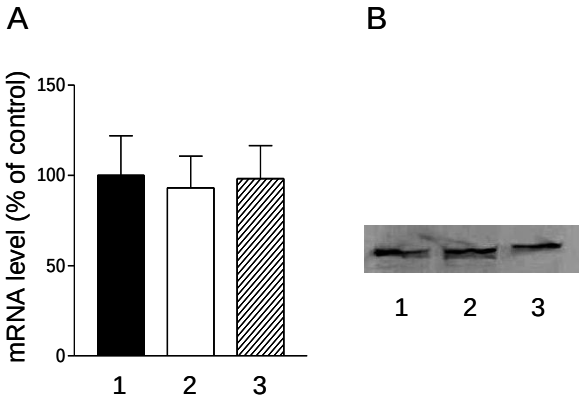

Fig. 17. Levels of mRNA and protein of MS in worms treated with the CN-B_{12} dodecylamine derivative. (A) qPCR analysis of the mRNA levels of MS in homogenates of worms exposed to CN-B_{12} (control; 1, black bar), the CN-B_{12} dodecylamine derivative (2, white bar) or B_{12}-deficient worms (3, shaded bar). (B) Western blot analysis using an anti-MS antibody of homogenates (100 μg of protein) prepared from worms exposed to CN-B_{12} (control; 1), the CN-B_{12} dodecylamine derivative (2), or B_{12}-deficient worms (3) was treated by SDS-polyacrylamide slab gel electrophoresis followed by immunoblotting with an anti-MS antibody. Immunoreactive components were visualized using an immunoblot-staining kit for peroxidase.

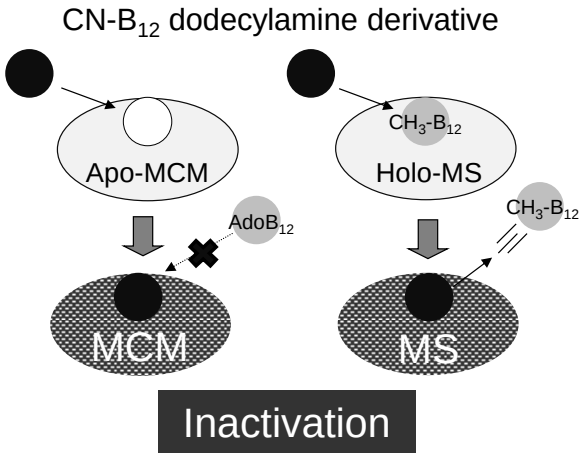

Fig. 18. Predicted mechanism of inhibition of CN-B_{12} dodecylamine derivative for B_{12}-dependent enzymes in *C. elegans*.

Effects of the CN-B_{12} dodecylamine derivative on the levels of mRNAs encoding proteins involved in B_{12} metabolism in C. elegans

To evaluate the effects of the CN-B_{12} derivative on the levels of mRNAs encoding proteins involved in B_{12} metabolism, we performed qPCR analyses to detect mRNAs encoding MCM (*mmcm-1*), methylmalonic acidemia Cbl A complementation group; MMAA (*mmaa-1*), cob(I)alamin adenosyltransferase; MMAB (*mmab-1*), methylmalonic aciduria cblC type; MMACHC (*cblc-1*), and methionine synthase reductase; MSR (*mtrr-1*). The mRNA levels of *mmaa-1*, *cblc-1*, and *mtrr-1* did not differ significantly among three experimental conditions (**Fig. 19A**, **B**, **D**, and **E**). However, the levels of *mmab-1* mRNA of worms treated with the CN-B_{12} derivative was significantly increased compared with that of the control worms, and the increased level was identical to that of B_{12}-deficient worms (**Fig. 19C**).

Effects of the CN-B_{12} dodecylamine derivative on the C. elegans egg-laying capacity and life cycle

My study demonstrates that B_{12} deficiency decreases the egg-laying rates and prolongs the life cycle of *C. elegans* (**Chapter II**, **Section 1)**. In the present study, the egg-laying rates of worms exposed to the CN-B_{12} dodecylamine derivative were significantly decreased (**Fig. 20A**), and the life cycle was increased, but the difference was not statistically significant (**Fig. 20B**). These results suggest that increased B_{12} deficiency, long exposure to B_{12}-deficient conditions, or both are necessary to significantly prolong life cycle.

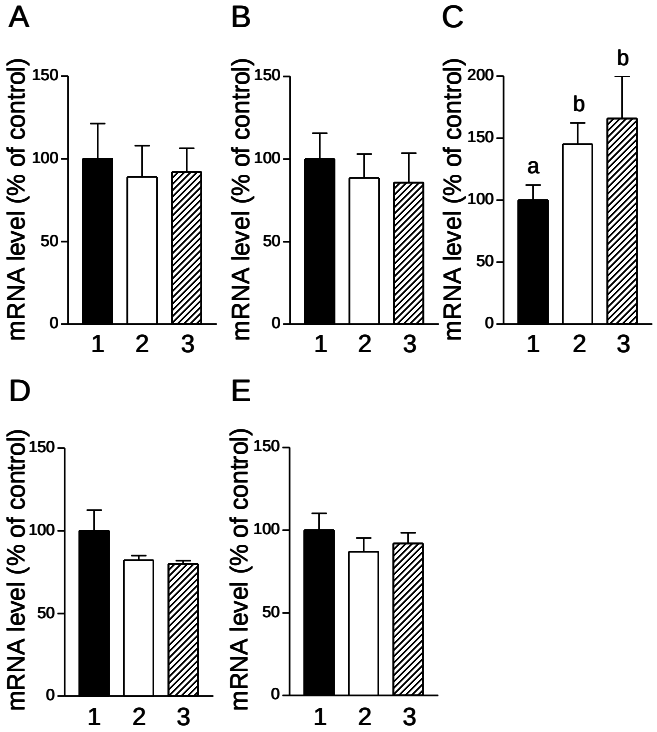

Fig. 19. Levels of mRNAs encoding proteins involved in B_{12} metabolism in worms treated with the CN-B_{12} dodecylamine derivative. Using qPCR, we determined the levels of mRNAs encoding (A) methylmalonyl-CoA mutase, MCM; (B) methylmalonic aciduria type A protein, MMAA; (C) methylmalonic aciduria type B,MMAB (mmab-1 encodes an orthlog of human cob(I)alamin adenosyltransferase in *C. elegans*); (D) B_{12} deficiency C complementation group (human) homolog, MMACHC; and (E) methionine synthase reductase, MSR in worms treated with CN-B_{12} (control; 1, black bar), the CN-B_{12} dodecylamine derivative (2; white bar), and B_{12}-deficient worms (3; shaded bar). Data represent the mean ± SD of three independent experiments. The letters indicate values that are significantly different, $p < 0.05$.

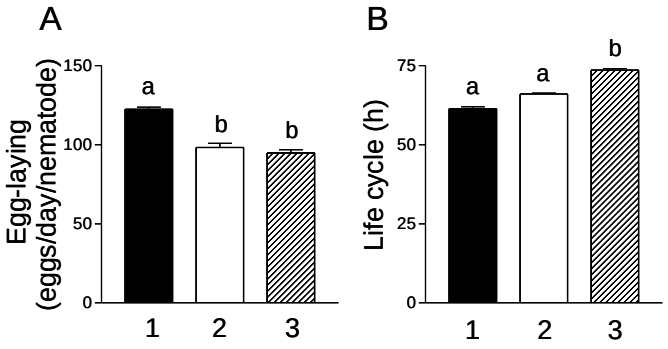

Fig. 20. Egg-laying capacity and the length of the life cycle of worms treated with the CN-B_{12} dodecylamine derivative. Egg numbers per day per worm (A) and length (h) of the life cycle (B) of worms treated with CN-B_{12} (control; 1, black bar), CN-B_{12} dodecylamine derivative (2, white bar), and B_{12}-deficient worms (3, shaded bar). Data represent the mean ± SD of five independent experiments. The letters indicate values that are significantly different, $p < 0.05$.

These results indicate that the CN-B_{12} dodecylamine derivative acts a potent inhibitor of B_{12}-dependent MCM and MS activity, which leads to metabolic disorders caused by B_{12} deficiency.

Chandler *et al*. [42] described that MMA level was approximately three times greater in *C. elegans* treated with RNA interference against *mmcm-1*, *mmaa-1*, and *mmab-1* than in the wild-type worms and that the *mmcm-1*deletion mutant accumulated 17 times more MMA than the wild-type worms after propionic acid loading. In this study, MMA level was approximately four times greater in B_{12}-deficient and CN-B_{12} derivative-treated worms than in the control worms (**Fig. 13A and B**); the magnitude of MMA elevation was similar to that of the worms treated with RNA interference against *mmcm-1*.

Chapter II, **Section 1** indicated that MS is more sensitive to cellular B_{12} concentrations of *C. elegans* than MCM, suggesting that the phenotype observed in this and previous studies would rather be attributable to the results of impaired remethylation *via* the MS reaction than those of perturbed propionyl-CoA oxidation in the MCM pathway.

CN-B_{12}[*c*-lactam], a CN-B_{12} analog with a modified C-ring side chain inhibits the MS activity of cultured HL-60 cells to induce cell death but does not affect MCM activity [43]. However, Sponne *et al*. [79] indicated that when 10 mg/L OH-B_{12}[*c*-lactam] was added to a culture medium of rat oligodendrocytes and incubated for 25 days, MMA and Hcy were approximately 200 times and twice greater, respectively, in OH- B_{12}[*c*-lactam]-treated cells than in the control cells.

Subcutaneous administration of OH-B_{12}[*c*-lactam] to rats causes B_{12} deficiency because plasma MMA was approximately 331 times and twice greater in the treated rats than in the control and B_{12}-deficient rats, respectively [80]. Hepatic holo-MCM and MS activities of OH-B_{12}[*c*-lactam]-treated rats decreased to approximately 65% and 43% of the control activities, respectively, indicating that OH-B_{12}[*c*-lactam] potently inhibits mammalian B_{12}-dependent enzymes [44].

However, high concentrations of OH-B_{12}[*c*-lactam] must be administered for

several weeks using osmotic mini-pumps to produce B_{12}-deficient rats [45] because of poor binding to IF [44]. Compared with OH-B_{12}[*c*-lactam], the CN-B_{12} dodecylamine derivative is easy to prepare and acts a potent inhibitor of both MCM and MS. Moreover, this compound shows high affinity binding of IF [45]. These properties of the CN-B_{12} dodecylamine derivative suggest that B_{12} deficiency in mammals may be readily induced by oral or intravenous administration of this compound.

Summary

In this study, I showed that CN-B_{12} dodecylamine derivative was absorbed and accumulated to significant levels by *C. elegans* and was not further metabolized. The levels of MMA and Hcy, which serve as indicators of B_{12} deficiency, were significantly increased in *C. elegans* treated with the dodecylamine derivative, indicating severe B_{12} deficiency. Kinetic studies show that the affinity of the CN-B_{12} dodecylamine derivative was greater for two B_{12}-dependent enzymes, MCM and MS, compared with their respective coenzymes, suggesting that the dodecylamine derivative inactivated these enzymes. The dodecylamine derivative did not affect the levels of mRNAs encoding these enzymes or those of other proteins involved in intercellular B_{12} metabolism, including MCM (*mmcm-1*), methylmalonic acidemia cobalamin A complementation group (*mmaa-1*), methylmalonic aciduria cblC type (*cblc-1*), and MS reductase (*mtrr-1*). In contrast, the level of the mRNAs encoding cob(I)alamin adenosyltransferase (*mmab-1*) was increased significantly and identical to that of B_{12}-deficient *C. elegans*. These results indicate that the CN-B_{12} dodecylamine derivative acts as a potent inhibitor of B_{12}-dependent enzymes and induces severe B_{12} deficiency in *C. elegans*.

Section 3 Effects of hydroxocobalamin dodecylamine derivatives on the activities of vitamin B_{12}-dependent enzymes in cultured COS-7 cells

Introduction

B_{12}[*c*-lactam], a B_{12} analogue with a modification of side chain of C-ring, has been reported to antagonize B_{12} in the cultured HL 60 cells [43]. Subcutaneous administration of OH-B_{12}[*c*-lactam] to rats has indicated that the analogue has the ability to act as a potent inhibitor of the mammalian B_{12}-dependent enzymes to achieve B_{12} deficiency [44]. However, considerably high concentration of OH-B_{12}[*c*-lactam] must be administrated for several weeks with osmotic mini pumps in order to prepare B_{12}-deficient rats because IF hardly binds OH-B_{12}[*c*-lactam]. As shown in **Chapter II**, **Section II**, CN-B_{12} dodecylamime derivative exerted inhibitory effects against both B_{12}-dependent enzymes in *C. elegans*. The dodecylamine derivative-treated worms developed severe B_{12} deficiency in approximately 3 days. If the B_{12} alkylamine derivatives act as potent inhibitors of mammalian B_{12}-dependent enzymes *in vivo*, B_{12}-deficient animals would be readily prepared by oral administration of the derivative. Here I describe characterization of the OH-B_{12} alkylamine derivatives as potent inhibitors of the B_{12}-dependent enzymes in the mammalian cultured cells.

Materials and Methods

Materials

CN-B_{12}, 1,1'-carbonyldiimidazole, hexylamine, dodecylamine, and dexadecylamine were purchased from Wako Pure Chemical Industries (Osaka, Japan). OH-B_{12} was obtained from Sigma (St. Louis, USA). Phenyl-Toyopearl 650M was purchased from

TOSHO Corporation (Tokyo, Japan). An antibody for human MS (anti-MTR antibody) was obtained from Abcam® Japan (Tokyo, Japan).

Preparation of alkylamine derivatives of CN-B_{12}

Alkylamine derivatives of CN-B_{12} were prepared according to the method of McEwan *et al*. [45]. In briefly, solid 1,1'-carbonyldiimidazole (26 mg) was added to CN-B_{12} (0.1 g) which had been dissolved in dimethyl sulfoxide (1.2 mL) at 30˚C and the mixture was stirred at 300 rpm for 25 min. Hexylamine, dodecylamine, or hexadecylamine (each at 0.27 mmol) was added to the mixture and then stirred at 300 rpm for 24 h at 25˚C (**Fig. 21**). B_{12} compounds were extracted and purified as described in **Chapter II**, **Section 2**. Hexylamine, dodecylamine, and hexadecylamine derivatives of CN-B_{12} were dissolved in distilled water and their concentrations were determined with λ_{361} = (ε = 10,500, 16,900 and 20,000, respectively) as described in the cited reference [45].

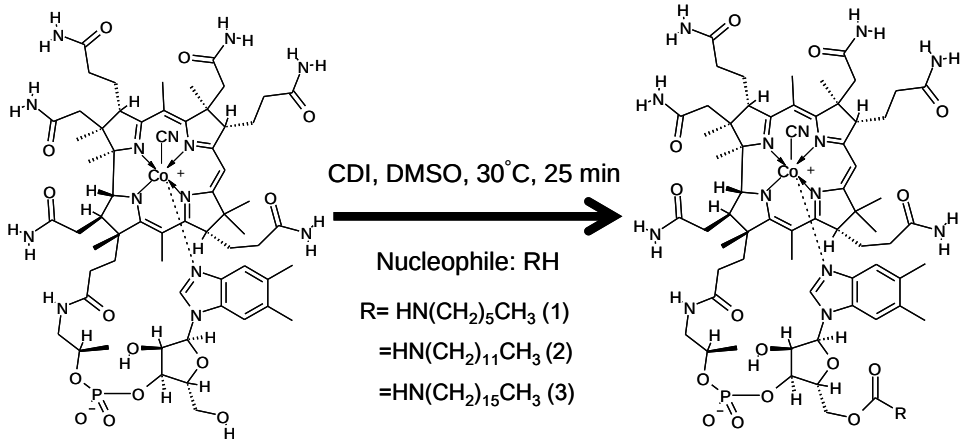

Fig. 21. Summary of preparation of CN-B_{12} alkylamine derivatives. CDI, 1,1'-carbonyldiimidazole; DMSO, dimethyl sulfoxide; and RH, hexylamine (1), dodecylamine (2), and hexadecylamine (3).

Preparation of CN-B_{12}[c-lactam]

CN-B_{12}[*c*-lactam] was prepared from CN-B_{12} by the method as described previously [81] .

Preparation of alkylamine and c-lactam derivatives of OH-B_{12}

The above alkylamine and *c*-lactam derivatives of CN-B_{12} were dissolved in 5.0 mL of distilled water and bubbled with N_2 gas for 20 min and reduced with NaH_4. Each treated solution was neutralized with 1.0 mol/L HCl. Most of the CN-B_{12} derivatives were converted to the respective OH-B_{12} derivatives. After the formed OH-B_{12} derivatives were desalted with a Sep-pak Vac 20 cc (5 g) C18 cartridge (Waters Corp.), they were separated from the remaining CN-B_{12} derivatives with silica gel 60 TLC under the same conditions as described above. After the TLC sheet had been dried, each OH-B_{12} derivative was collected, extracted with 80% (v/v) methanol solution, and evaporated to dryness under the reduced pressure.

Cell culture

COS-7 (African green monkey kidney) cells were cultured in 10 mL Dulbecco's modified Eagle's medium, containing 10% (v/v) fetal bovine serum, penicillin (100 units/mL) and streptomycin (100 μg/mL), on a 100 mm dish at 37˚C in a humidified 5% CO_2 - 95% air (v/v) atmosphere. Authentic OH-B_{12} was added into the medium at a varied concentration (0, 0.1, and 1.0 μmol/L) in the presence or absence of 1.0 μmol/L alkylamine and *c*-lactam derivatives of OH-B_{12}. After reaching confluence, the cells were harvested and homogenised in 100 mmol/L KPB (pH 7.0), containing leupeptin (1 mg/mL), aprotinin (10 mg/mL) and 0.1 mmol/L 4-(2-aminoethyl)-benzenesulfonyl fluoride, with a Teflon homogenizer at 4˚C. The homogenate was centrifuged at 10,000 × *g* for 10 min at 4˚C, and the supernatant fraction obtained was used as a crude enzyme solution for the enzyme assay.

Enzyme assay

MCM and MS activities were assayed by HPLC methods described previously [49, 50].

Western blotting

The cell homogenate described above was subjected to SDS-PAGE. Proteins in the gel were electroblotted to a polyvinylidene difluoride membrane. The membrane was treated with an anti-MS antibody, and immunoreactive proteins on the membrane were detected by a chemiluminescent method using a commercial kit (Super Signal West Pico Chemiluminescent substrate system; Pierce, Rockford, IL, USA) with horseradish peroxidase-conjugated goat anti-rabbit IgG antibodies. Digital images were obtained with a luminescent image analyzer (LAS-1000 Plus; Fuji Film, Tokyo, Japan).

Statistical analyses

Total and holo-MCM and MS activities of the COS-7 cells treated with or without the alkylamine derivatives of OH-B_{12} and OH-B_{12}[*c*-lactam] were statistically analyzed by one-way ANOVA, and post hoc analyses were done by the Tukey's multi-comparison test. These analyses were performed with GraphPad Prism® for windows version 5.03 (GraphPad Software Inc., La Jolla, CA 92037 USA). All data are expressed as means and standard deviations, and statistical significance is defined as $p < 0.05$.

Results and Discussion

Effects of three alkylamine derivatives of OH-B_{12} on MCM and MS activities of COS-7 cells

The prepared alkylamine [hexylamine (1), dodecylamine (2), and hexadecylamine (3) in **Fig. 22**] derivatives of OH-B_{12} (1.0 μmol/L) were evaluated as B_{12}-dependent enzyme inhibitors in total and holo-MCM and MS activities of the COS-7 cells grown in 0.1 mmol/L OH-B_{12}-supplemented medium (**Fig. 23**).

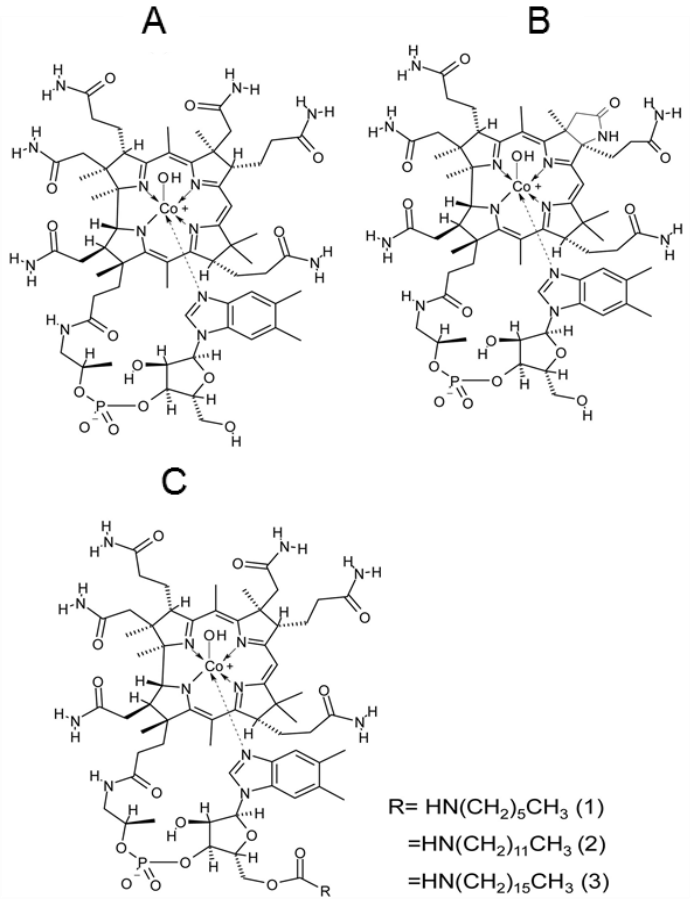

Fig. 22. Structural formula of alkylamine and c-lactam derivatives of OH-B_{12} used in this study. (A) OH-B_{12}; (B) OH-B_{12}[*c*-lactam]; and (C) Hexylamine (1), dodecylamine (2), and hexadecylamine (3) derivatives of OH-B_{12}.

All alkylamine derivatives did not affect the enzyme activity of total MCM (holo and apo-enzymes), but significantly inhibited the enzyme activity of the holo-MCM. While the addition of each alkylamine derivative showed the same degrees of inhibition in the enzyme activities of both total and holo-MS. The dodecylamine and hexadecylamine derivatives are stronger inhibitors in both holo-enzymes (about 30% and 45% activities of MCM and MS of the control cells, respectively) than the hexylamine derivative. All alkylamine derivatives used did not show any cytotoxicity in the cultured COS-7 under the experimental conditions. McEwan *et al*. [45] have demonstrated that the dodecylamine derivative of B_{12} can bind IF considerably (36% of intact B_{12}), but hexadecylamine derivative cannot. Therefore, OH-B_{12} dodecylamine derivative was selected for further experiments.

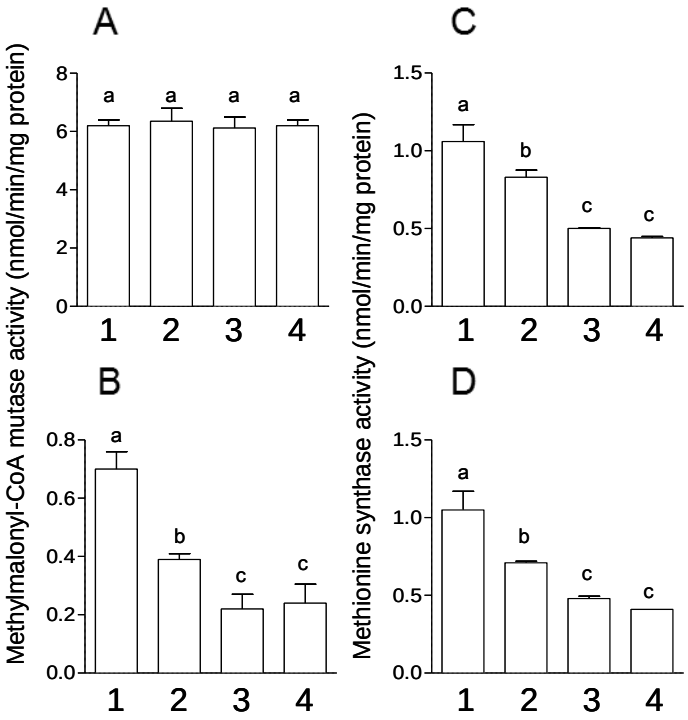

Fig. 23. Effects of the addition of three alkylamine derivatives of OH-B_{12} on MCM and MS activities of COS-7 cells. (A) Total MCM activity; (B) Holo-MCM activity; (C) Total MS activity, and (D) Holo-MS activity. These enzyme activities were assayed in the cell homogenates of COS-7 treated with none (1) and hexylamine (2), dodecylamine (3), and hexadecylamine (4) derivatives of OH-B_{12} (1.0 μmol/L) in the presence of authentic OH-B_{12} (0.1 μmol/L). Values are the means of three dishes, with standard deviations represented by vertical bars. [abc]Values with unlike letters were significantly different ($p < 0.05$).

Effect of the OH-B_{12} dodecylamine derivative and OH-B_{12}[c-lactam] on MCM activity of COS-7 cells

I evaluated effects of the dodecylamine derivative of OH-B_{12} (1.0 μmol/L) on total and holo-MCM activities of the cells grown in OH-B_{12} (at 0, 0.1, and 1.0 μmol/L)-supplemented medium, compared with the OH-B_{12}[*c*-lactam] that is known as the B_{12}-dependent enzyme inhibitor [43, 44]. When total MCM activity was significantly decreased with increase in concentration of the added OH-B_{12}, 1.0 μmol/L dodecylamine and *c*-lactam derivatives did not affect the total enzyme activity at each concentration of authentic OH-B_{12} (**Fig. 24**).

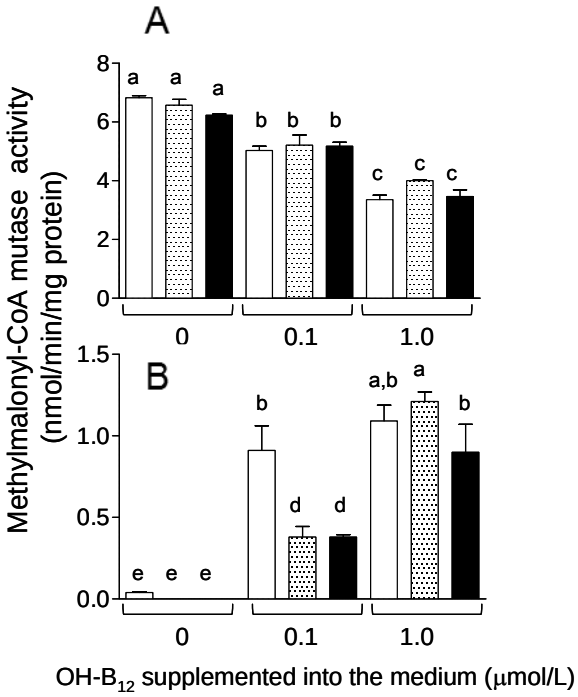

Fig. 24. Effects of the addition of dodecylamine and *c*-lactam derivatives of OH-B_{12} on MCM activity of COS-7 cells. Total (A) and holo- (B) MCM activities were assayed in the cell homogenates of COS-7 treated with none (□), 1.0 μmol/L OH-B_{12} dodecylamine derivative(▨), and OH-B_{12}[*c*-lactam] (■) in the presence of the indicated authentic OH-B_{12}. Values are the means of three dishes, with standard deviations represented by vertical bars. [abcde]Values with unlike letters were significantly different ($p < 0.05$).

The dodecylamine and *c*-lactam derivatives of OH-B_{12}, however, inhibited significantly the holo-MCM activity (about 60% activity of the control) in the presence of 0.1

μmmol/L authentic OH-B_{12}. Although the dodecylamine derivative did not affect any holo-MCM activity in the presence of 1.0 μmmol/L authentic OH-B_{12}, OH-B_{12}[*c*-lactam] could inhibit about 17% of the holo-enzyme activity.

Effect of the OH-B_{12} dodecylamine derivative and OH-B_{12}[c-lactam] on MS activity of COS-7 cells

One μmol/L dodecylamine derivative could inhibit significantly both total and holo-MS enzyme activities (about 47% and 45% activity of the control, respectively, in the presence of 1.0 μmol/L OH-B_{12}), while OH-B_{12}[*c*-lactam] did not inhibit both total and holo-enzyme activities of the cells grown in the presence of 1.0 μmol/L OH-B_{12}. Most MS has been reported to exist as the holo-enzyme in mammalian cells [82] (**Fig. 25**). Although I have no information available on the mechanism of inhibition of MS by the OH-B_{12} dodecylamine derivative, it is possible that the OH-B_{12} derivative competitively inhibits MS. For further elucidation of the decrease in the MS activity in the dodecylamine derivative-treated cells, MS protein expression was examined by SDS-PAGE followed by immunobloting with an antibody of human MS. As shown in **Fig. 26**, the expression level of MS protein was significantly increased with dose-dependent manner by the addition of authentic OH-B_{12}. The dodecylamine derivative could hardly affect the MS protein levels at each OH-B_{12} concentration, indicating that the dodecylamine derivative could not inhibit the MS protein level, but inhibit MS enzyme activity. These results indicate that the dodecylamine derivative of OH-B_{12} acts as a potent inhibitor of the B_{12}-dependent MS, the key enzyme involved in various methylation reaction (DNA, phospholipids, and so on) *via* SAM [83]. Since the OH-B_{12} dodecylamine derivative is simply prepared over considerably high yield (~50%) relative to OH-B_{12}[*c*-lactam], the dodecylamine derivative would be a useful tool to prepare B_{12}-deficient mammalian cells and to elucidate the metabolic disorders caused by the reduced enzyme activity of MS which exerts an important influence on the cellular metabolisms.

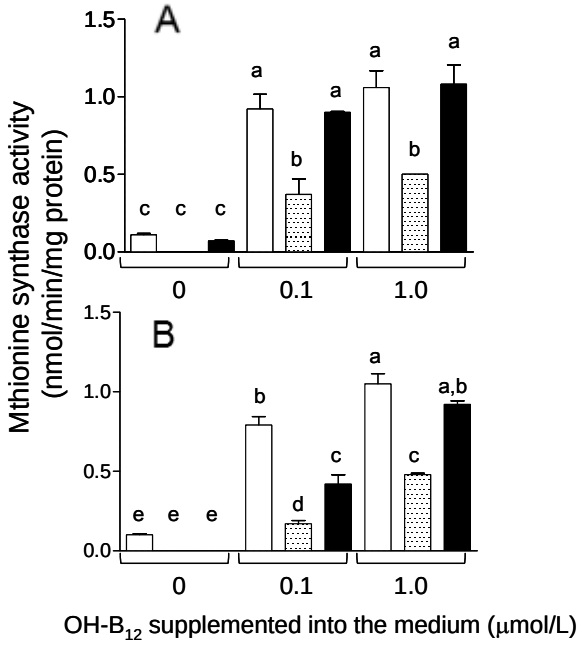

Fig. 25. Effects of the addition of dodecylamine and *c*-lactam derivatives of OH-B_{12} on MS activity of COS-7 cells. Total (A) and holo- (B) MS activities were assayed in the cell homogenates of COS-7 treated with none (□), 1.0 μmol/L OH-B_{12} dodecylamine derivative (▒), and OH-B_{12}[*c*-lactam] (■) in the presence of the indicated concentrations of authentic OH-B_{12}. Values are the means of three dishes, with standard deviations represented by vertical bars. [abcde]Values with unlike letters were significantly different ($p < 0.05$).

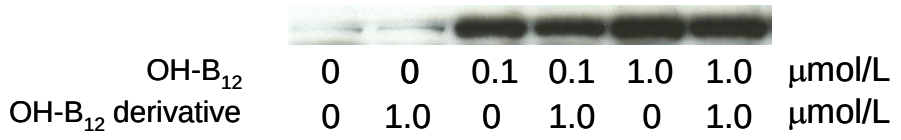

Fig. 26. Western blot analysis of MS protein in the cell homogenates of COS-7 treated with or without 1.0 μmol/L OH-B_{12} dodecylamine derivative in the presence of the indicated concentrations of authentic OH-B_{12}. Data are typical immunoreactive patterns of the MS protein from three independent western blot analyses of the treated COS-7 cells.

Moreover, B_{12} dodecylamine derivative shows high affinity binding of IF [45], suggesting that B_{12} deficiency in mammals may be readily induced by oral or intravenous administration of this compound. **Table 3** summarized the results of **Chapter II**.

Table 3. Summary of Chapter II in this study.

	B_{12} deficiency		$CN\text{-}B_{12}$ dodecylamine derivative	$OH\text{-}B_{12}$ dodecylamine derivative
	Mammals	*C. elegans*	*C. elegans*	COS-7
MMA	↑	↑	↑	-
Hcy	↑	↑	↑	-
MCM				
activity	↓	↓	↓	→
mRNA expression	↓	→	→	-
protein expression	↑	-	-	-
MS				
activity	↓	↓	↓	↓
mRNA expression	↓	→	→	→
protein expression	↓	↘	→	→

Summary

I evaluated whether the dodecylamine derivative of $OH\text{-}B_{12}$ acts as a potent inhibitor of B_{12}-dependent enzymes in an African green monkey kidney cell, COS-7. When the dodecylamine derivative (1.0 μmol/L) did not show any cytotoxicity in the cultured cells, the derivative could not affect MCM (holo-enzyme) activity, but significantly inhibit MS (holo-enzyme) activity in the cell homogenates of COS-7 grown in 1.0 μmol/L $OH\text{-}B_{12}$-supplemented medium. An immunoblot analysis indicated that the dodecylamine derivative could not decrease the protein level of MS, but significantly inhibit the enzyme activity.

Chapter III

Mechanisms of metabolic disorders and memory/learning dysfunction induced by vitamin B_{12} deficiency in *Caenorhabditis elegans*

Vitamin deficiency, in particular B_{12}, folate, B_6, significantly increases blood Hcy, which appears to develop advanced atherosclerosis as the manifestations of aging [84].

"Why is Hcy so toxic?" The proposed answers are as follows; 1) superoxide anion radical (O_2^-) is significantly formed during self-oxidation of Hcy since Hcy has pro-oxidant activity [85]. 2) Hcy can activate NADPH oxidase to generate O_2^-. The formed O_2^- is immediately converted to hydrogen peroxide (H_2O_2) by the action of superoxide dismutase. Subsequently, H_2O_2 is readily converted to hydroxyl radical (HO^-) in the presence of metal ions. When these reactive oxygen species (ROS) are produced significantly, an imbalance between ROS production and anti-oxidant abilities occurs as oxidative stress [86]. Disturbance in normal redox state of the living cells leads to sever damages of various cellular components such as proteins, lipids, and DNA.

B_{12} deficiency stimulates accumulation of Hcy, which induces oxidative stress. However, there is little information on the direct relationship between B_{12} deficiency and oxidative stress (or disturbance in normal redox state). Some researchers proposed that oxidation stress is one of the causes of cognitive dysfunction but the underlying mechanism of B_{12}-deficient neuropathy is poorly understood.

As described in **Chapter II**, B_{12}-deficient worms showed significant accumulation of MMA and Hcy. In **Chapter III**, **Section 1**, using this B_{12}-deficinent model animal, I evaluate how much oxidative stress is induced during B_{12} deficiency and then whether such oxidative stress leads to oxidative damages of cellular components. Furthermore, I demonstrated that B_{12}-deficiency induced severe memory/learning impairment, which was partially attributable to oxidative stress.

B_{12}-dependent MCM and MS function in catabolism of branched chain-amino

acids and synthesis of methionine, respectively, in mammalian cells [64]. Leucine 2,3-aminomutase catalyzing the conversion of leucine to β-leucine, appears to require $AdoB_{12}$ as a cofactor [87]. Ebara *et al*. [22] demonstrated that B_{12} deficiency results in metabolic disorders of various amino acids in rats, in particular, serine and threonine metabolic disorders, which are attributable to impairment of the adenylyl cyclase system. Kenyon *et al*. [19] proposed that B_{12}-dependent MS activity was regulated by polyamines, which are synthesized from ornithine. Furthermore, NMDA receptor involving in the long-term memory preservation is significantly modulated by Hcy and/or polyamines [31]. However, there is no information on whether B_{12} deficiency induces the metabolic disorders of polyamines. Thus, I describe the effects of B_{12} deficiency on amino acid and polyamine metabolisms in *C. elegans* (**Chapter III**, **Section 2**).

Section 1 Vitamin B_{12} deficiency in *Caenorhabditis elegans* results in sever oxidative stress, leading to memory/learning dysfunction

Introduction

During B_{12} deficiency, the failure of the B_{12}-dependent methionine biosynthesis leads to accumulation of Hcy [84], which has pro-oxidant activity [84] and can activate NADPH oxidase to generate reactive oxygen species (ROS) [85]. NADPH oxidase is simultaneously stimulated by *S*-adenosylhomocyteine (SAH) accumulated by B_{12} deficiency [88]. On the other hand, one of reactive nitrogen species (RNS), nitric oxide (NO), can inhibit both MCM and MS activities [89, 90]. These observations suggest that B_{12} deficiency disrupts cellular redox homeostasis to induce oxidative stress, which is implicated in various human diseases [88] including atherosclerosis and neurodegenerative diseases. Such diseases are major symptoms of B_{12} deficiency, although the underlying disease mechanisms are poorly understood.

In humans, insulin appears to regulate learning and memory in the central nervous system as well as energy metabolism in the peripheral tissues [91]. Insulin is synthesized in the brain [92] and its receptors are localized to synapses [93]. Insulin/phosphoinositide 3-kinase (PI 3-kinase) pathway in neural and behavioral plasticity is highly conserved in mammals [94] and it regulates various neurological processes. Inhibition of this insulin signaling pathway in the central nervous system causes learning and memory impairment [95].

The nervous system of *C. elegans* is composed of 302 neurons, and their neural connections are studied extensively [96]. Worms sense various chemicals by sensory neurons and show several forms of plasticity. Worms subjected to prolonged exposure to attractive salt (NaCl) under starvation conditions show a dramatic reduction of chemotaxis to NaCl and eventually show a negative chemotaxis. Exposure to NaCl in the presence of food does not lead to a reduction of chemotaxis, suggesting that worms

change their behavior by integrating two stimuli, NaCl and starvation [97]. Tomioka *et al*. [94] demonstrated that the insulin/PI 3-kinase pathway regulates this NaCl chmotaxis memory/learning in worms.

As shown in **Chapter II**, *C. elegans* is a suitable model animal for studying the biological processes induced by B_{12} deficiency. Thus, I used this model animal to clarify how much oxidative stress is induced during B_{12} deficiency and then whether such oxidative stress leads to oxidative damages of cellular components. Furthermore, I demonstrated that B_{12} deficiency induced severe memory/learning impairment, which was partially attributable to oxidative stress.

Materials and Methods

Organisms and preoaration of B_{12}-deficient C. elegans

The N2 Bristol wild-type *C. elegans* strain was maintained at 20°C on NGM plates using the *E. coli* OP50 strain as the food source [46]. The B_{12}-sufficient (control) and -deficient worms were prepared and used as described previously.

Preparation of a cell homogenate of worm

Control and B_{12}-deficient worms (0.1 g wet weight) were homogenized in 500 μL of 100 mmol/L KPB (pH 7.0) on the ice using a hand homogenizer (AS ONE corp.). The homogenates were centrifuged at 15,000 × *g* for 10 min at 4°C and these supernatant were used as crude enzymes or crude homogenates.

Enzyme activity assays

NADPH oxidase activity was determined using the luminescence assay method with lucigenin (Tokyo chemical industry co., LTD, Tokyo, Japan) as the electron acceptor

[98]. The reaction was started by the addition of the crude enzyme and luminescence was monitored using Luminescencer-Octa AB-2270 (ATTO corp, Tokyo, Japan).

Total nitric oxide synthase (NOS) activity was assayed using an ultrasensitive colorimetiric NOS assay kit (Oxford Biomedical Research, Ink., MI, USA). NOS activity was calculated based on the amount of nitrite that was converted from NO formed in the enzymatic reaction.

Total superoxide dismutase (SOD) was assayed using SOD assay kit-WST (Dojindo Molecular Technologies, Inc., Kumamoto, Japan). Mn-SOD activity was determined in the reaction mixture containing 1 mmol/L KCN, which inhibits both Cu/Zn-SOD and extracellular SOD, resulting in the detection of only Mn-SOD activity [99, 100].

Catalase (Cat) activity was determined using a catalase activity assay kit NWLSS^{TM} (Northwest Life Science Specialties, LLC WA, USA). Catalase activity was calculated on the base of the amount of H_2O_2 decreased in the enzymatic reaction mixture, which was monitored by measuring absorbance at 240 nm using a Shimadzu spectrophotometer (UV-2550).

Glutathione peroxidase (GPx) activity was assayed using a glutathione peroxidase assay kit (Noryhwest Life Science Specialties, LLC, WA, USA). The crude enzyme was diluted to 10 times by 100 mmol/L KPB (pH 7.0) and used. After preincubation of the reaction mixture for 1 min, changes in absorbance at 340 nm were monitored for 5 min using the Shimadzu spectrophotometer (UV-2550).

NOS, SOD, Cat, and GPx activities were assayed according to the respective manufacturer's instructions.

Assays of oxidative stress markers

H_2O_2 concentration was determined using a H_2O_2 assay kit (BioVision, Inc., CA, USA). OxiRed probe reacts with H_2O_2 to produce a product with color (570 nm) in the presence of horseradish peroxidase. The reaction product was determined by measuring absorbance at 570 nm using a microplate reader (Tecan Group Ltd., Männedorf,

switzerland).

NO was assayed using a nitric oxide (NO_2/NO_3) assay kit (Dojindo NO_2/NO_3 assay kit-C II, colorimetric). The crude homogenate described above was heat-treated to remove proteins and then used. NO was calculated based on the amount of NO_2/NO_3 by measuring absorbance at 540 nm using a microplate reader (Tecan).

Malondialdehyde (MDA) was determined using a TBARS assay kit (ZeptoMetrix Crop., NY, USA). MDA-thiobarbituric acid adduct formed from the reaction of MDA in the sample was determined by measuring absorbance at 540 nm using a microplate reader (Tecan).

Glutathionine (GSH) or reduced GSH and GSH disulfide or oxidized GSH (GSSG) were determined using a GSH/GSSG assay kit (OXIS International Inc., OR, USA). 5,5'-Dithiobis(2-nitrobenzoic acid) was monitored by measuring at absorbance at 412 nm using a Shimadzu spectrophotometer (UV-2550).

All oxidative stress markers were assayed according to the respective manufacturer's instructions.

Fluorescent staining of H_2O_2 in the living worms

To detect cellular H_2O_2 in control and B_{12}-deficient worm bodies, a fluorescent probe BES-H_2O_2-Ac (Wako pure chemical industry co., LTD, Tokyo, Japan) was used. BES-H_2O_2-Ac was dissolved in a small amount of dimethyl sulfoxide, diluted to a final concentration of 200 μmol/L by a sterilized M9 medium, and used as a staining solution. Control and B_{12}-deficient worms (approximately 12 worms each) were treated with 150 μL of the staining solution for 1 h under aseptic conditions. To remove the remaining stain solution on the worm body surface, each worm was transferred to a B_{12}-dificient medium without *E. coli* and incubated at 20°C for 1 h. The washed worms were treated with 20 μL of 1 mmol/L sodium azide solution on a slide glass and observed with fluorescence microscope (λex: 485 nm, λem: 530 nm)

Assay of protein carbonyls in the worms

The crude homogenates of worms grown under various conditions as described in **Chapter II**, **Section 1** were treated with by SDS-polyacrylamide slab gel electrophoresis. I used a precast gel (PAGEL, type NPG-520L, ATTO) for electrophoresis of samples through a 5%-20% (w/w) linear gradient of polyacrylamide in the presence of SDS. After electrophoresis on the slab gel was complete, proteins in the gels were transferred to a polyvinylidene fluoride (PVDF) membrane (Immuno-Blot PVDF, Bio-Rad Laboratories, Inc. Hercules, CA, USA) in a Trans-Blot SD semi-dry electrophoretic transfer cell (Bio-Rad). The PVDF membrane was treated with a 2,4-dinitrophenylhydrazine (DNPH) solution and an anti-rabbit DNP antibody using a protein carbonyls western blot detection kit (Shima Laboratories Co., Ltd., Tokyo, Japan), according to the manufacurer's instructions. I performed the immunoreactions with a secondary antibody (anti-rabbit IgG antibody) coupled to horseradish peroxidase (Epitomics, Burlingame, CA, USA) and an immunoblot staining kit for peroxidase (SuperSignal West Pico, Thermo Fisher Scientific K. K., kanagawa, Japan), according to the manufacturer's instructions. A protein ladder on triple-color kit (Nacalai Tesque Inc., Kyoto, Japan) was used as the prestained standard proteins. The immunoreactive proteins on the PVDF membrane were captured using chemiluminescence imager ImageQuant LAS 4000 (GE Healthcare Japan, Tokyo, Japan).

Carbonyl content in proteins of control and B_{12}-deficient worms was determined by a modified DNPH method of the cited reference [101]. Each worm homogenate described above was treated with 20 % (w/v) trichloroacetic acid (TCA) on ice and the precipitate proteins were treated with 2 mol/L HCl in the presence or absence of 10 mmol/L DNPH at 25°C for 1 h. The treated mixture was centrifuged at 10,000 × *g* for 10 min at 25°C and the precipitate was washed three times with 20% (w/v) TCA containing ethanol:ethyl acetate (1:1) solution. The washed precipitate was dissolved in 6 mol/L guanidine chloride. Carbonyl content was determined by measuring absorbance at 380 nm and calculated using a molar absorption coefficient of 21,000 $(mol/L)^{-1}cm^{-1}$.

Quantitative PCR analysis (qPCR)

The cDNA of Control and B_{12}-deficient worms was prepared as described in **Chapter II**, **Section 2**. Primer pairs used for qPCR analysis were designed using GENETYX software (GENETYX Corporation, Tokyo, Japan) (**Table 4**). Gene-specific primers were selected such that the resulting PCR products were approximately 100 bp. A CFX Connect™ Real-Time System (Bio-Rad Laboratories, Inc. Hercules, CA, USA) with SYBR Premix Ex Taq (Takara Bio) was used to perform qPCR. The level of the mRNA encoding β-actin was used as an internal standard. The qPCR experiments were repeated at least three times for each cDNA prepared from three preparations of worms.

Table 4. Primer pairs used for the qPCR analysis.

Gene name	Primer sequences (5' to 3')
sod-1	TCTTCTCACTCAGGTCTCCAAC and TCGGACTTCTGTGTGATCCA
sod-2	AAAACACCGTTCGCTGTGTCTC and GTAAATCTGGCAGCGAGTGCTT
sod-3	CTCGCACTGCTTCAAAGCTTGT and TGCATAGTCGAATGGGAGATCTGG
sod-4	ATCGGTTTCCGGATTAGCAG and TCCACCAGCACTTAGACAAC
sod-5	TTGCCAATGCCGTTCTTCCA and TCACCTTCGGCTTTCTGGGTAA
gst-10	CGAGGATTCGGAGAATACATCC and CTTCAAGCATGGCAACTGAC
F26E4.12	TCGCTTCACAGTGTGGACTT and CGATTTCACACGATGGTTCCTG
gsr-1	GAGAACATTGCCACAGTGGT and CTTTTCAACGGCCTCAGCTT
cbs-1	ATTGCGGGATCTTTGGAAGACC and GAATTCTCCCTTTGGTGCGTAGA
cth-1	ATTATGCTCGTGGTGGAAACCC and ACAATGTTTGGCGCCCTCAA
cth-2	TATATCCGCCGTGTTGCTGTTC and CACTGCGGCAATATCAACAACC
cbl-1	GAAGACAATCACGGTGCCAACT and TGCACTAATCGCTGCAAGACC
gcs-1	CGAACAGGACGATGAGAAAACAG and TTCAGTTGGCCGGAATTCGAC
gss-1	GATTGATGGGCGTCAAGTAGCA and TGTAGCCCGATCCATGGAGTT
act-1	TCCAAGAGAGGTATCCTTACCC and CTCCATATCATCCCAGTTGGTG

Primer pairs for the qPCR were designed using GENETYX software. Each gene is involved in oxidative stress pathways, including SOD (*sod-1*; Cu/Zn SOD, *sod-2*; mitochondrial Fe/Mn SOD, *sod-3*; mitochondrial Fe/Mn SOD, *sod-4*; extracellular Cu/Zn SOD, *sod-5*; cytoplasmic Cu/Zn SOD), GST (*gst-10*), GPx (F26E4.12), a protein orthologous to human mitochondrial glutathione reductase (*gsr-1*), an ortholog of the human gene cystathionine-β-synthase (*cbs-1*), a putative cystathionine γ-lyase (*cth-1*, *cth-2*, and *cbl-1*), the *C. elegans* ortholog of γ-glutamine cysteine synthetase (*gcs-1*), and a protein orthologous to the human gene glutathione synthetase (*gss-1*). For revision, β-actin (*act-1*) mRNA levels served as the internal standard.

Assay of memory/learning ability in B_{12}-deficient C. elegans

Memory/learning ability in B_{12}-deficient worms was determined by the modified method of the cited references [97, 102]. The salt chemotaxis assay was performed using a 9 cm assay plate (1 mmol/L KPB, pH 6.0, 1 mmol/L $MgSO_4$, 1 mmol/L $CaCl_2$, 2% (w/v) agar), on which a NaCl (5 mm diameter) close to the edge of the plate. One microliter of 1mM sodium azide was spotted at the NaCl gradient peak and at the opposite ends of the plate, just before placing the worms.

For memory/learning assay, controls and B_{12}-deficient worms were washed with a conditioning buffer (5 mmol/L KPB, pH 6.0, containing 1 mmol/L $MgSO_4$ and 1 mmol/L $CaCl_2$) with 0.06% (w/v) NaCl (NaCl conditioning) or without NaCl (mock conditioning), and incubated at 25°C for 1 h. After the incubation, the treated worms were directly placed at the center of the assay plates, and then incubated at 25°C for 30 min. The assay plate was immediately placed at 4°C to stop the movement of worms, whose numbers in each region were counted. Chemotaxis Index (C.I.) was calculated as (A－B)/(Total－C) where A was the number of worms within 2 cm of the peak spot of NaCl gradient, B was the number of worms within 2 cm of the control spot and C was the number of animals that did not move in the center region (**Fig.27**).

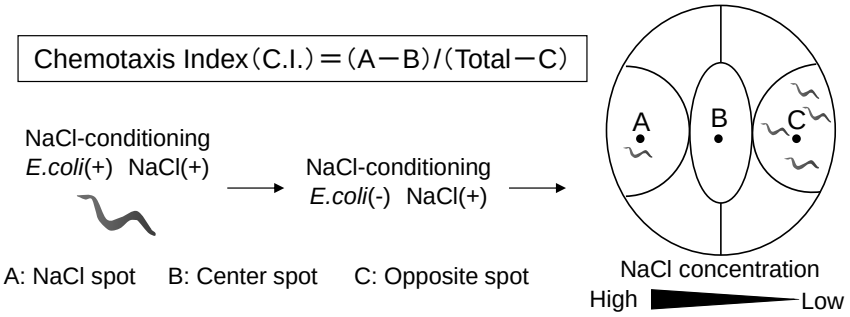

Fig. 27. The method for evaluation of associative learning in *C. elegans*. The procedure for the associative learning assay was as follows. The animals were washed off the plates with conditioning buffer (5mmol/L KPB, pH 6.0, 1mmol/L $MgSO_4$, 1mmol/L $CaCl_2$) and transferred to tube. For the associative learning assay, washed worms were treated with NaCl (0.12 g/100mL)-conditioning buffer for 1 h. After washing, treated worms were put the center of assay plate with the NaCl concentration gradient, and left to move freely on assay plate for 30 min at 25°C. The chemotaxis index (C.I.) was calculated C.I.=(A－B)/(Total－C), where A is the number of worms within the center of the NaCl gradient and C is the number within the control spot.

Effects of antioxidants on memory/learning ability in worms

Worms were grown at 20°C on B_{12} (100 μg/L CN-B_{12})-supplemented M9-medium using B_{12}-deficient *E. coli* OP50 as the food source. Worm egg was transferred onto each plate, which contained fresh B_{12}-deficient medium. After the egg hatched, worms were allowed to grow until they became adults and laid eggs (yielding the F1 generation). Individual eggs were removed from the plate and each was transferred onto a fresh plate containing B_{12}-deficient medium and grown to maturity under the same conditions (yielding the F2 generation). This process was repeated for five generations. After 3 days, adult worms of the F5 generation were used as B_{12}-deficient worms. Antioxidant compound (vitamin E; α-tocopherol or GSH each at final concentration of 1 mM) was added to the B_{12}-deficient medium in each generation to prepare B_{12}-deficient worms treated with each antioxidant compound for the F1-F5 generations. Memory/learning ability was assayed in B_{12}-deficient worms treated with each antioxidant compound for the F1-F5 generations.

Protein assay

Proteins were assayed by the method of Bradford [54] using ovalbumin as a standard.

Statistical analysis

The effects of B_{12} deficiency on various indices of oxidative stress markers and on memory/learning ability in *C. elegans* were evaluated by one-way ANOVA, and a post-hoc analysis was performed using Tukey's multiple comparison tests. Analyses were performed with GraphPad Prism 3 for Windows version 2.01 (GraphPad software Inc., La Jolla, CA, USA). All data are presented as the mean ± SD. Differences were considered statistically significant when $p < 0.05$.

Results

Effects of B_{12} deficiency on the reactive oxygen species (ROS), reactive nitrogen species (RNS), and the related biomarkers in C. elegans

To investigate whether B_{12} deficiency disrupts redox homeostasis to induce oxidative stress, I determined various marker levels of oxidative stress in B_{12}-deficient worms (**Table 5**). H_2O_2 and NO (NO_2^-＋NO_3^-) contents increased approximately twice greater in the B_{12}-deficient worms than in the control worms. The specific activities of NADPH oxidase and NOS in a worm cell homogenate were significantly increased during B_{12} deficiency. Both MDA (as a lipid peroxidation) and protein carbonyl (as a protein modification) levels were approximately twice greater in the B_{12}-deficient worms than in the control worms. The increased levels of H_2O_2, NO, and oxidative damages of cellular components were completely recovered to the control levels when B_{12}-deficient worms were grown in three generations under the B_{12}-supplemented conditions. **Fig. 28** shows mobile patterns of protein carbonyls visualized by an immunological staining by a DNP antibody after SDS-polyacrylamide gel electrophoresis of the crude homogenates of the control and B_{12}-deficient worms. Carbonyl protein level in the B_{12}-deficient worms was significantly increased compared with that in the controls. In particular, proteins with approximately 80 KDa and 60 KDa were significantly accumulated. In the B_{12}-deficient worms grown on B_{12}-supplemented medium for three days, total carbonyl protein levels were recovered to the control levels, but the 80 KDa protein still existed. These results indicate that B_{12} deficiency causes serious oxidative damages in *C. elegans*.

Table 5. Oxidative stress markers

	Control	B_{12} deficiency	Recovery
H_2O_2 (nmol/g wet weight)	14.46 ± 0.67^a	34.17 ± 1.48^b	15.85 ± 0.96^a
$NO_2^- + NO_3^-$ (nmol/g wet weight)	33.74 ± 2.76^a	59.88 ± 5.33^b	39.74 ± 6.31^a
NADPH oxidase (RLU/min/mg protein)	0.70 ± 0.13^a	2.15 ± 0.35^b	0.74 ± 0.05^a
NOS (nmol/hour/mg protein)	2.67 ± 0.69^a	6.41 ± 0.36^b	2.41 ± 0.51^a
MDA (nmol/g wet weight)	23.09 ± 3.83^a	38.89 ± 1.33^b	27.26 ± 3.05^a
Carbonylproteins (nmol/mg protein)	1.86 ± 0.57^a	3.94 ± 0.52^b	2.48 ± 0.23^a

Control or B_{12}-deficient worms were grown on plates containing B_{12} (control) or B_{12}-deficient medium, respectively. To prepare the recovery worms, B_{12}-deficient worms were transferred to B_{12}-supplemented medium for 3 days. Oxidative biomarkers were measured in cell homogenates of each worm. The quantitative determination of H_2O_2 was utilized horse radish peroxidase. Reactive oxygen species (RNS) contents indicates total amount of NO_2^- contents and NO_3^- contents in this study. RNS contents were measured using diazo coupling method. NADPH oxidase activity was assayed by chemiluminescence method using lucigenin. NADPH oxidase activity expressed as Relative Light Unit (RLU)/min/mg protein. Nitric oxide synthase (NOS) activity was assayed with NOS Assay Kit, according to the manufacturer's instructions. Malondialdehyde (MDA) contents as the index of lipid peroxide and carbonyl protein contents were assayed as indices of oxidative stress. Data represent the mean ± SD of three independent experiments. The different letters indicate values that are significantly different, $p<0.05$.

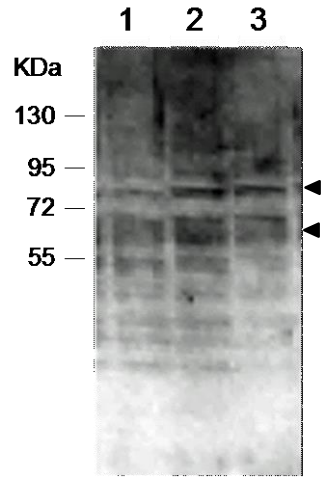

Fig. 28. Carbonyl proteins content in proteins of worms. Carbonyl proteins were detected in worms grown in presence of B_{12} (control, 1), B_{12}-deficient worms (2), or the recovery worms by B_{12} addition (3) using modified DNPH method.

When the control and B_{12}-deficient worms were treated with BES-H_2O_2-Ac as a fluorescent probe for detection of H_2O_2, the intestinal tract and its neighboring regions were stained significantly in the B_{12}-deficient worms, but not in the control worms; the fluorescent intensity in the B_{12}-deficient worms was disappeared by the addition of B_{12} (**Fig. 29**). These results indicated that B_{12} deficiency in worms induced a severe oxidative stress, which leaded to oxidative damages of various cellular components.

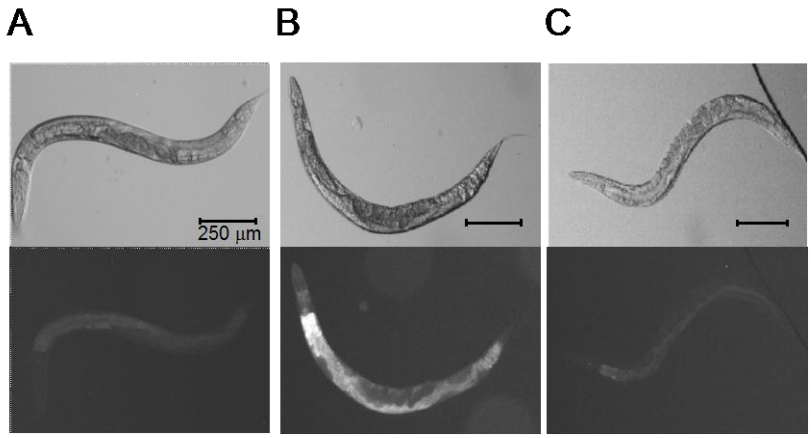

Fig. 29. Accumulation of H_2O_2 in B_{12}-deficient *C. elegans*. (A-C) Representative fluorescent images of worms grown in presence of B_{12} (A), B_{12}-deficient worms (B), or the recovery worms by B_{12} addition (C). Above and below pictures indicate stereoscopic and fluorescent image, respectively. Scale bars are 250 μm.

Effects of B_{12} deficiency on glutathione contents and antioxidative enzyme activities in C. elegans

Table 6 summarizes glutathione contents and antioxidative enzyme activities in the control and B_{12}-deficient worms. Since glutathione is an important antioxidant compound in all living cells, preventing cellular components from ROS, I determined GSH and GSSG in the cell homogenates of the control and B_{12}-deficient worms. Control worms contained approximately 17.5 nmole of GSH per mg of worm proteins and no GSSG was detected. However, the amount of GSH was significantly reduced in the B_{12}-deficient worms, which contained small amount of GSSG (approximately 0.6 nmol/mg protein). The decreased GSH and increased GSSH levels of B_{12}-deficient

worms were recovered to the control levels when B_{12}-deficient worms were grown in three generations under the B_{12}-supplemented conditions. The result indicated that B_{12} deficiency induced significant reduction of GSH in worms.

Although total SOD and Mn-SOD and Cat activities in the B_{12}-deficient worms were decreased to approximately 50%, 60%, and 70% enzyme activities of the control worms, respectively, GPx activity was contrarily increased up to approximately twice activity of the control worms. The decreased SOD and Cat activities were completely recovered when B_{12}-deficient worms were grown under the B_{12}-supplemented conditions. These results indicated that both low molecular and enzymatic defense system against oxidative stress were significantly weakened during B_{12} deficiency.

Table 5. Antioxidants

	Control	B_{12} deficiency	Recovery
GSH (nmol/mg protein)	17.48 ± 1.05^{a}	12.91 ± 0.15^{b}	17.32 ± 1.89^{a}
GSSG (nmol/mg protein)	N.D.	0.61 ± 0.15	N.D.
Total SOD (U/mg protein)	51.56 ± 1.50^{a}	28.46 ± 3.54^{b}	47.61 ± 4.06^{a}
Mn-SOD (U/mg protein)	12.43 ± 1.54^{a}	7.44 ± 0.24^{b}	10.98 ± 1.04^{a}
Cat (U/mg protein)	9.66 ± 0.24^{a}	6.37 ± 0.57^{b}	8.17 ± 0.89^{ab}
GPx (U/mg protein)	2.25 ± 0.14^{a}	4.11 ± 0.32^{b}	2.40 ± 0.35^{a}

Gluthatione (GSH) and Gluthathione peroxidase (GSSG) were assayed as the evaluation of antioxidants. GSH and GSSG were measured by GSH/GSSG Assay Kit and their levels were determined using spectral photometer. Total superoxide dismutase (SOD) activity, Mn-SOD activity, catalase (Cat) activity, and glutathione peroxidase (GPx) activity were assayed in worms grown in presence of B_{12} (control), B_{12}-deficient worms, or the recovery worms. Data represent the mean ± SD of three independent experiments. The different letters indicate values that are significantly different, $p<0.05$. N.D. means not detected.

Effects of B_{12} deficiency on the levels of mRNAs encoding various proteins involved in cellular antioxidative systems

To evaluate the effects of B_{12} deficiency on the levels of mRNAs encoding proteins involved in cellular antioxidative systems, the level of mRNAs encoding SOD (*sod-1*, *sod-2*, *sod-3*, *sod-4*, and *sod-5*), GPx (F26E4.12), GST (*gst-10*), Cat (*ctl-1*, *ctl-2*, and

ctl-3), and orthologous protein to human mitochondrial GSR (*gsr-1*), were measured by qPCR analysis. The mRNA level of GST was significantly decreased in the B_{12}-deficient worms, compared with that of the control worms (**Fig. 30**), but no significant changes in the mRNA levels of the remaining proteins were observed during B_{12} deficiency. These results suggest that B_{12} deficiency did not affect mRNA levels of most proteins involved in cellular antioxidative systems except for GST, which catalyzes the conjugation of GSH to xenobiotic substrates including peroxidized lipids [105].

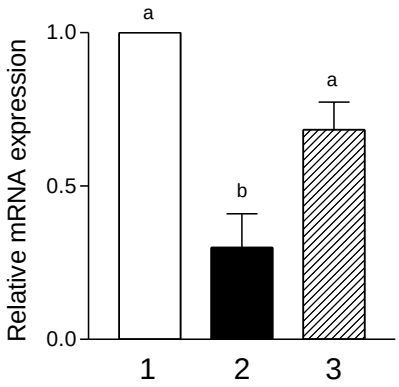

Fig. 30. The expression level of glutathione S-transferase (GST) in B_{12}-deficient *C. elegans*. The mRNA expression of GST; glutathione *S*-transferase (*gst-10*) was determined in the worm grown under B_{12}-supplemented (1; white bar) or B_{12}-deficient (2; black bar) or recovered B_{12}-deficient conditions (3; shaded bar) by real-time PCR method. Data represent mean ± SD of three independent experiments; the different alphabets indicate values that are significantly different, $p < 0.05$.

Effects of B_{12} deficiency on memory/learning ability in C. elegans

Although cognitive impairment caused by B_{12} deficiency has been numerously reported in elderly person [32], the underlying mechanisms for cognitive impairment are poorly understood. To clarify effects of B_{12} deficiency on memory/learning function involved in insulin/PI-3 kinase signaling pathway in central nervous system, the *C. elegans* salt (NaCl) chemotaxis memory/learning assay system was used. Although B_{12} deficiency did not affect *C. elegans* chemotaxis to NaCl (not shown data), the C.I. value

(index of the food-NaCl associative memory/learning) was significant decreased in B_{12}-deficient worms, compared with that of the controls (**Fig. 31**), indicating that B_{12} deficiency leads to sever memory/learning impairment in *C. elegans*. When B_{12}-deficient worms were grown under B_{12}-supplemented conditions during five generations, this memory/learning impairment was gradually improved with increased generations and completely recovered in the B_{12}-deficient worms treated for five generations.

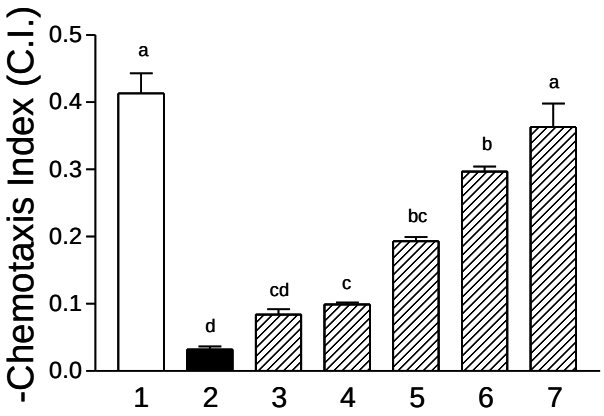

Fig. 31. Effects of vitamin B_{12} deficiency on associative learning in *C. elegans*. Effects of B_{12} deficiency on associative learning in *C. elegans* was evaluated using chemotaxis assay previously. The detailed examination method was described in a text. The associative learning was assayed in worms grown in presence of B_{12} (control; 1, white bar), B_{12}-deficient worms (2, black bar), or the recovery worms by B_{12} supplementation (The shaded bars express the Chemotaxis Index (C.I.) level each recovery period. 3, for 1 generation; 4, for 2 generations; 5, for 3 generations; 6, for 4 generations; 7, for 5 generations.). The graph is shown in - C.I. value to be easy to see. Data represent the mean ± SD of three independent experiments. The different letters indicate values that are significantly different, $p<0.05$.

To investigate the effects of antioxidants on memory/learning ability of the worms during B_{12} deficiency, worms were grown in five generations under the B_{12}-deficient medium with vitamin E (**Fig. 32A**) and GSH (**Fig. 32B**) as fat-soluble and water-soluble antioxidants, respectively. The addition of both antioxidants did not affect the worm chemotaxis to NaCl (not shown data). When worms were grown under the B_{12}-deficient conditions for five generations, vitamin E was added in each generation stage (F1-F5)

of worms. The learning disability caused by B_{12} deficiency was recovered up to approximately 50% of the control worm's ability in the worms treated with vitamin E during three to five generations. Remarkably the learning disability was also recovered up to approximately 50% of the control worm's ability in the worms treated with GSH only during one generation. These results indicated that feeding of vitamin E or GSH for relatively long duration significantly prevented the memory/learning impairment caused by B_{12} deficiency in *C. elegans* and that GSH was more effective in short duration than vitamin E.

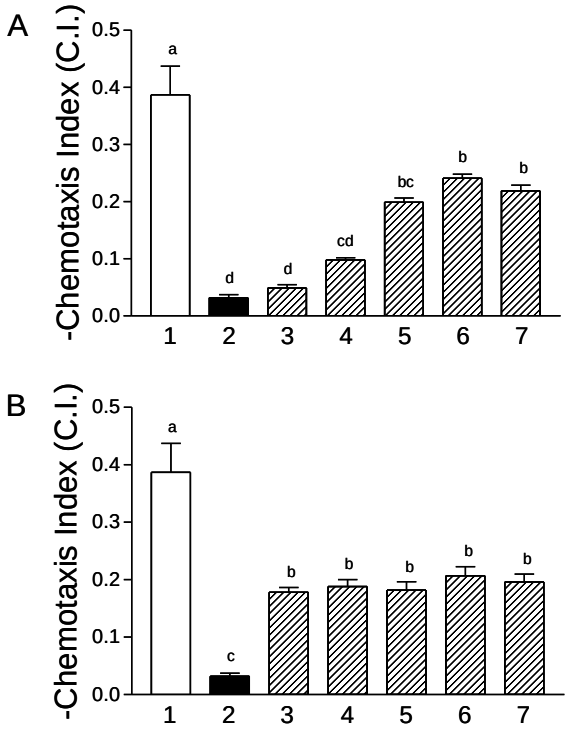

Fig. 32. Effects of oxidative stress on associative learning in *C. elegans*. Effects of (A) vitamin E or (B) glutathione (GSH) as antioxidants on disorders of associative learning in B_{12}-deficient *C. elegans* were evaluated using chemotaxis assay previously. The detailed examination method was described in a text. The associative learning was assayed in worms grown in presence of B_{12} (control; 1, white bar), B_{12}-deficient worms (2, black bar), or the recovery worms by each antioxidant (vitamin E or glutathionne) (The shaded bars express the Chemotaxis Index (C.I.) level each recovery period. 3, for 1 generation; 4, for 2 generations; 5, for 3 generations; 6, for 4 generations; 7, for 5 generations.). The graph is shown in ‐C.I. value to be easy to look. Data represent the mean ± SD of three independent experiments. The different letters indicate values that are significantly different, $p<0.05$.

As shown in **Fig. 33**, MDA level increased by B_{12} deficiency was recovered to that of the control worms by the feeding of vitamin E and GSH during three generations. These results suggest that the memory/learning impairment caused by B_{12} deficiency was partially attributable to oxidative stress in *C. elegans*.

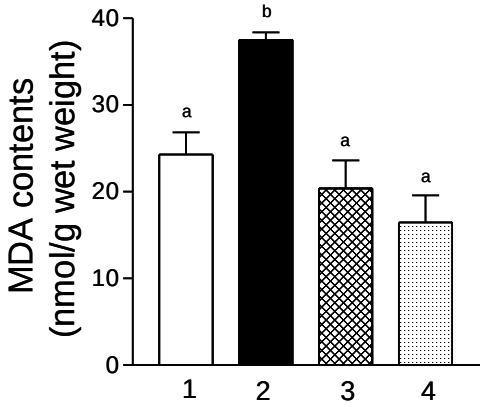

Fig. 33. Effects of antioxidant on oxidation stress in *C. elegans*. To examine the relaxation of oxidation stress by antioxidant supplementation, B_{12}-deficient worms were grown under the vitamin E-supplemented or glutathione-supplemented medium, respectively. As the evaluation of oxidation stress relaxation, we assayed the Malondialdehyde (MDA) content of worms grown in presence of B_{12} (control; 1, white bar), B_{12}-deficient worms (2, black bar), or the prevented worms by vitamin E (3) and glutathione (4). Data represent the mean ± SD of three independent experiments. The different letters indicate values that are significantly different, $p<0.05$.

Discussions

The B_{12} taken up by cells is converted into $AdoB_{12}$ and CH_3-B_{12}, which functions as coenzymes for MCM and MS, respectively. In particular, MS plays important physiological functions in the synthesis of methionine and SAM, which acts as the major methyl donor in living cells. Reduced activity of MS during B_{12} deficiency leads to significant increases in both Hcy and SAH levels and significant decrease in SAM level. Cystathionine β-synthase catalyzing the conversion of Hcy to cystathionine in the transsulfuration pathway is reportedly activated by SAM. Our unpublished study

indicated that mRNA expression level of cystathionine β-synthase was significantly diminished in B_{12}-deficient worms. These suggest that B_{12} deficiency induce unusual accumulation of cellular Hcy.

Hcy is well known to be readily self-oxidized to produce ROS [84]. Moreover, Hcy can activate NADPH oxidase to generate ROS [85]. Yaw *et al*. [85] reported that Hcy stimulates the phosphorylation of NADPH oxidase subunits by protein kinase Cβ in monocytes to enhance the oxidase activity. NADPH oxidase is also stimulated by SAH accumulated by B_{12} deficiency [88].

NO is an important signaling molecule in multicellular organism. Most animals produce NO from *L*-arginine by NOS. However, *C. elegans* lacks NOS because the complete genome of *C. elegans* contains no genes encoding NOS. Recently Gusarov *et al*. [104] demonstrated that NO produced by bacteria (as diets) in the worm gut can diffuse into the worm's tissues and initiate a signaling cascade that results in the extended lifespan. In the present study, significant increases of NO and NOS activity were observed in B_{12}-deficinet *C. elegans* (**Table 5**).

Since NO reportedly has the ability to inhibit the activities of MCM and MS [89, 90], the NO formed excessively by B_{12} deficiency would lead to the further reductions of both B_{12}-dependent enzyme activities; the enzyme inhibition triggered by B_{12} deficiency is significantly enhanced via NO and would result in sever B_{12}-deficient symptoms. Antioxidative enzyme (SOD and Cat) activities were significantly reduced in B_{12}-deficient worms (**Table 6**). Many studies [105-107] have demonstrated that SOD was potently inhibited by H_2O_2, which was accumulated during B_{12} deficiency. Cat as well as SOD is susceptible to oxidative inactivation by singlet oxygen [108]. In human hypocatalasemic patients (inherited catalase deficiency), increased Hcy could promote oxidative stress *via* H_2O_2. B_{12} deficiency did not affect mRNA level of the worm GPx, of which enzyme activity was increased significantly by the deficiency.

GSH is the most abundant low-molecular weight thiol and GSH/GSSH is the major redox couple in the living cells. GSH plays mainly important roles in antioxidant defense; GSH not only effectively scavenges ROS but also substrates for GPx

catalyzing detoxification of H_2O_2 and other peroxides and GST catalyzing the conjugation of GSH to detoxify peroxify peroxidized lipids and various metabolites. As shown in **Table 6**, GSH level was significantly reduced in B_{12}-deficient worms and conversely slight increase of GSSG was found. These observations suggest that B_{12} deficiency disrupts cellular redox homeostasis to induce oxidative stress.

Lipid peroxide, which can work as ROS itself, induces further oxidative modification of cellular components [109]. Lipid peroxidation and protein oxidation were detected in mammalian tissues with Alzheimer disease [105-107], which is classified as a neurodegenerative disorder and and develops various symptoms such as memory loss and cognitive impairments.

B_{12} deficiency in *C. elegans* leads to the defective associative learning, which was attributable to the increased oxidative stress and was recovered up to approximately 50% of the control worm's ability in the worms treated with vitamin E or GSH. INS-1, one of the insulin-like peptides found in *C. elegans*, was secreted from the AIA sensory neuron and then transferred to the ASER sensory neuron, which functions in the associative learning. Tomioka *et al*. [94] demonstrated that certain oxidative modifications of the peptides including INS-1 and lipids by ROS result in defective associative learning in *C.elegans*. Thus, B_{12} deficiency induced at least the significant inhibition of the INS-1 signaling pathway essential for the associative learning by oxidative stress.

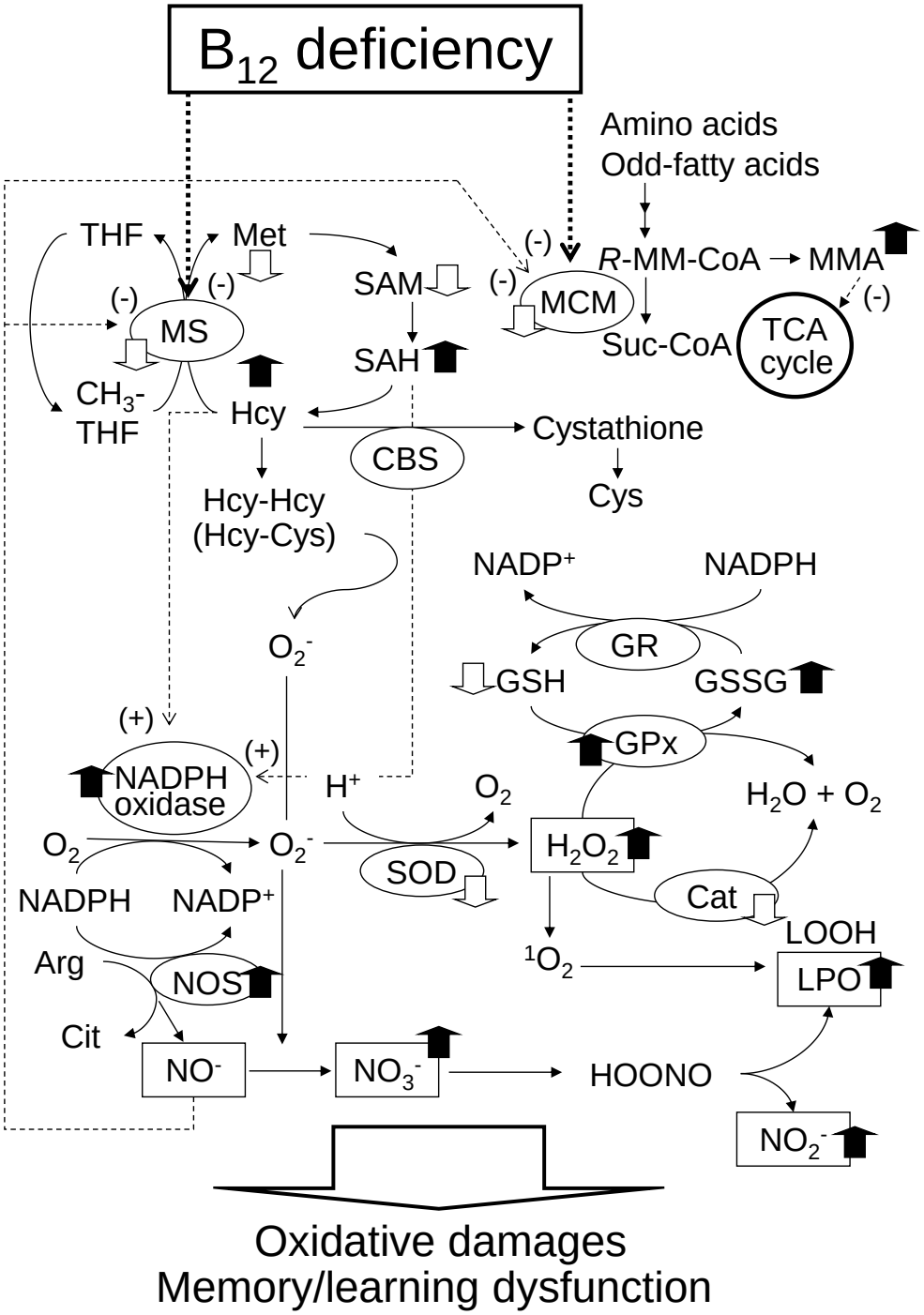

Fig. 34. Chain reaction of the oxidative stress and damages caused by B_{12} deficiency. In this figure, (-) or (+) shows a negative control or a positive control with the certain material, respectively.

Summary

Oxidative stress is implicated in several human diseases including atherosclerosis and neurodegenerative diseases. Such diseases are major symptoms of B_{12} deficiency, although the underlying disease mechanisms are poorly understood. **Chapter II**, **Section 1** indicates that *C. elegans* grown under conditions of B_{12} deficiency develops severe B_{12} deficiency. In this study, I describe the effects of B_{12} deficiency on various oxidative stress markers in worms to elucidate whether the reduced MS reaction is associated with oxidative stress and with neurological dysfunction. NADPH oxidase and NO synthase activities were significantly increased in B_{12} deficient worms. Therefore, H_2O_2 and NO were increased in B_{12}-deficient worms. MDA and carbonyl proteins contents were significantly increased in B_{12}-deficient worms. Whereas, GSH content, SOD and Cat activities were significantly decreased during B_{12} deficiency. These results indicate that B_{12} deficiency causes severe oxidative stress in worms. Moreover, B_{12}-deficient worms showed a significant memory/learning impairment, which could be considerably prevented by the addition of GSH or vitamin E. These results indicated that B_{12} deficiency in *C. elegans* results in severe oxidative stress, which is one of the causes of the memory/learning impairment.

Section 2 Vitamin B_{12} deficiency in *Caenorhabditis elegans* results in metabolic disorders of polyamines, modulators of synaptic transmission

Introduction

After B_{12} is taken up by living cells, it is converted in $AdoB_{12}$ and CH_3-B_{12}, which function as the coenzymes for MCM [12] and MS [13], respectively. MCM catalyses the conversion of *R*-methyl-CoA to succinyl-CoA *via* TCA cycle in the catabolic pathways of amino acids such as valine, leucine and isoleucine, odd-numbered fatty acids, cholesterol, and thymine [18]. B_{12} deficiency causes an unusual accumulation of MMA, which inhibits succinate dehydrogenase, an enzyme involved in the TCA cycle [59], to disrupt normal glucose and glutamic acid metabolisms [57]. MS catalyzing the synthesis of methionine from Hcy and $N^{5'}$-methyltetrahydrofolate plays important functions in folate metabolism as well as sulfur amino acid metabolism, in particular synthesis of *S*-adenosylmethionine (SAM) involved in the methylation reaction of various cellular components such as DNA, RNA, proteins, and lipids [19, 20]. Both MCM and MS function as key-enzymes for the metabolisms of these amino acids, although Ebara *et al*. [22] demonstrated that B_{12} deficiency in rats caused serine and threonine metabolic disorders, which are attributable to impairment of the adenylyl cyclase system. Thus, B_{12} deficiency disrupts directly or indirectly various cellular metabolisms to lead the associated symptoms such as developmental disorders, infertility, and neuropathy.

When I attempted to elucidate effects of B_{12} deficiency on amino acid metabolisms using this model animal, significant change of ornithine other than the above MCM and MS-related amino acids was detected. Ornithine is an amino acid that is produced from arginine by the action of arginase (EC.3.5.3.1) in the urea cycle. On the other hand, ornithine is precursor of polyamines which play multiple roles in cell growth and death including aging and diseases; orinithine decarboxlase (ODC, EC.4.1.1.17) catalyzes the decarboxylation of ornithine to form putrescine and regulates the synthesis of

polyamines (**Fig. 35**).

If B_{12} deficiency disrupt normal polyamine metabolism, the underlying cause(s) of the associated developmental disorders, infertility, and neuropathy would be clarified. Here, I described that B_{12} deficiency causes various amino acid metabolisms, in particular occurrence of unusual accumulation of ornithine and leads to disruption of normal polyamine metabolism.

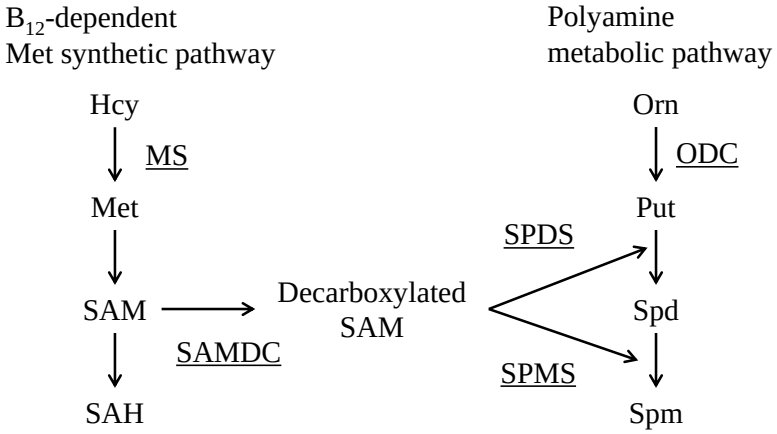

Fig. 35. Polyamine metabolism. Abbreviation: Hcy; homocysteine, Met; methionine, ODC; ornithine decarboxylase, Orn; ornithine, Put; putrescine, SAH; *S*-adenosylhomocysteine, SAM; *S*-adenosylmethionine, SAMDC; *S*-adenosylmethionine decarboxylase, Spd; spermidine, SPDS; spermidine synthase, Spm; spermine and SPMS; spermine synthase.

Materials and Methods

Organisms and preparation of B_{12}-deficient C. elegans

The N2 Bristol wild-type *C. elegans* strain was maintained at 20°C on NGM plates using the *E. coli* OP50 strain as the food source [46]. The B_{12}-sufficient (control) and -deficient worms were prepared and used as described previously.

Determination of free amino acids in worm bodies

Control and B_{12}-deficient worms (0.2 g of wet weight each) were homogenized in 500 μL of 100 mmol/L KPB (pH 7.0) at 4°C using a hand homogenizer (AS ONE Corp., Osaka, Japan). After the homogenates were heated at 80°C for 10 min and then centrifuged at 15,000 × *g* for 10 min at 4°C, the supernatants (200 μL each) were added to 100 μL of 10% (w/v) trichloroacetic acid, mixed vigorously, and centrifuged at 15,000 × *g* for 10 min at 4°C to remove proteins. Each supernatant (250 μL) was diluted with an equal volume of 0.25 mol/L lithium citrate buffer (Wako Pure Chemical Industries, Ltd. Osaka, Japan). The diluted solution, after being filtered with a Millex®-LH membrane filter (Merck Millipore, Billerica, MA, USA), analyzed using an fully-automated amino acid analyzer (JEOL JLC-500/V, Nihon Denshi Datem Co. Ltd. Japan).

SAM and SAH assay

SAM and SAH were assayed by the modified method of the cited reference [110]. Control and B_{12}-deficient worms (0.05 g of wet weight each) were homogenized in 200 μL of 0.4 mol/L $HClO_4$ on ice using a hand homogenizer (AS ONE Corp.), and centrifugation at 15,000 × *g* for 10 min at 4°C. After each supernatant was filtered through a Millex®-LH membrane filter (Merck Millipore), 20 μL of the filtrate was analyzed using a Shimadzu HPLC apparatus (SCL-10A VP system controller, DGU-20A3 degassing unit, LC-10Ai liquid chromatography pumps, SPD-10AV UV/VIS detector, and CTO-6A column oven). The HPLC column was equilibrated with 80% solvent A (50 mmol/L NaH_2PO_4, pH 3.0, containing 8 mmol/L octanesulfonic acid) and 20% solvent B (methanol) for 1 h at 25°C and eluted with a linear gradient of methanol (20% solvent B in 3min, 20% to 40% solvent B in 3 - 9 min, B; 40% solvent B in 9 - 13 min; 40% to 20% solvent B in 13 - 13.5 min, and 20% solvent B in 13.5 - 23 min) as a flow late of 1 mL/min. SAH and SAM were determined by measuring absorbance at 254 nm. The retention times of SAH and SAM were 11.4 min and 14.3

min, respectively.

Determination of polyamines

Polyamines were analyzed by HPLC according to the method of Yamamoto *et al*. [111]. Control and B_{12}-deficient worms (0.05 g of wet weight) were homogenized in 200 μL of 0.3 mol/L $HClO_4$ on ice using a hand homogenizer and centrifuged at 15,000 × *g* for 10 min at 4°C. The supernatants were used as the samples for polyamine analysis. Each sample (100 μL) was added to 1 mL of 2 mol/L NaOH and 10 μL of benzoyl chloride (Tokyo Chemical Industry Co., LTD, Tokyo, Japan) and left for 40 min at 25°C to form benzoyl derivatives of polyamines. The reaction was terminated by the addition of 2 mL of saturated NaCl solution. Cold diethyl ether (2 mL) was added to the reaction mixture and mixed vigorously to extract the formed benzoyl-derivatives of polyamines. After the treated solution was centrifuged at 1,500 × *g* for 5 min at 4°C, an aliquot (1 mL) of the upper diethyl ether layer was sampled, evaporated to dryness under a flow of nitrogen, and dissolved in 200 μL of methanol. The extract was filtered with a membrane filter (Millex®-LH, Merck Millipore) and analyzed with the Shimadzu HPLC apparatus as described above. Putrescine, spermidine, and spermine (Sigma, St. Louis, MO, USA) were used as authentic polyamines and 1,6-hexanediamine was used as an internal standard. The prepared sample and authentic polyamines were injected into a reversed-phase HPLC column (Wakosil-II 5C18HG, φ4.6 × 250 mm) that was equilibrated with solvent A (Milli-Q water) and solvent B (methanol) for 1 h at 35°C. Polyamines were eluted with a linear gradient of methanol (50% to 55% solvent B in 0-5 min, 55% to 60% solvent B in 5-20 min, 60% to 80% solvent B in 20-25 min, 80% solvent B in 30 min, 80% to 50% solvent B in 30-31, and 50% solvent B in 31-45 min) at a flow late of 1 mL/min and determined by measuring absorbance at 254 nm. The retention times of putrescine, spermidine, and spermine were 11.0 min, 19.5 min, and 27.1 min, respectively, and that of 1,6-hexanediamine as a internal standard was 15.9 min.

Ornithine decarboxylase (ODC) activity assay

ODC activity was assayed using HPLC by the modified method of the cited reference [112, 113]. Worms (0.05 g wet weight) were homogenized in 200 mL of 40 mmol/L sodium phosphate buffer (pH 7.5), containing 0.1 mmol/L pyridoxal phosphate and 2 mmol/L dithiothreitol using a hand homogenizer (AS ONE). The cell homogenate was centrifuged at 15,000 × *g* for 15 min at 4°C and the supernatant was used as a crude enzyme. The reaction mixture (200 μL) contained 8 μL of 1mol/L KPB (pH 7.5), 27 μL of Milli-Q water, 5 μL of 6 mmol/L pyridoxal phosphate, 5 μL of 12 mmol/L *L*-ornithine (final concentration; 30 μmol/L), and 100 μL of crude enzyme. The enzymatic reaction was started by the addition of *L*-ornithine, incubated for 1 h at 37°C, and terminated by the addition of 50 μL of 8%(v/v) $HClO_4$. The reaction mixture was 15,000 × *g* for 10 min at 4°C and the supernatant was filtered with a membrane filter (Millex®-LH, Merck Millipore). The filtrate (30 μL) was added to 50 μL of 10 mmol/L borate buffer, pH 9.0, 30 μL phthaldialdehyde reagent (Sigma), and incubated for 4 min at 25°C to form a fluorescent derivative of putrescine according the method of the cited reference [115]. An aliquot (20 μL) of the reaction mixture was analyzed with the Shimadzu HPLC apparatus as described above. The prepared sample was injected into a reversed-phase HPLC column (Wakosil-II 5C18HG, φ4.6 × 250 mm) that was equilibrated with solvent A (Milli-Q water) and solvent B (methanol) for 1 h at 25°C. Putrescine was eluted with a linear gradient of methanol (80% to 100% solvent B in 0-11 min, 100% solvent B in 11-14 min, 100% to 80% solvent B in 14-15 min, and 80% solvent B in 20 min) at a flow late of 1 mL/min at 25°C. The fluorescent derivative of putrescine was determined a fixed excitation (340 nm) and emission (455 nm) wavelengths using a Shimadzu RF-530 fluorescence detector. The retention time of the putrescine derivative was 7.3 min.

Quantitative PCR analysis (qPCR)

The cDNA of Control and B_{12}-deficient worms was prepared as described in

Chapter II, **Section 2**. Primer pairs used for qPCR analysis were designed using GENETYX software (GENETYX Corporation, Tokyo, Japan) (**Table 7**). Gene-specific primers were selected such that the resulting PCR products were approximately 100 bp. A CFX Connect^{TM} Real-Time System (Bio-Rad Laboratories, Inc. Hercules, CA, USA) with SYBR Premix Ex Taq (Takara Bio) was used to perform qPCR. The level of the mRNA encoding β-actin was used as an internal standard. The qPCR experiments were repeated at least three times for each cDNA prepared from three preparations of worms.

Table 7. Primer pairs used for the qPCR analysis

Gene name	Primer sequences (5' to 3')
odc-1	AAGGGCTCGGATTCAAGATGGA and
	TTCAGCAATCAGGCGCTTGT
smd-1	ATGCGAGCCGGTATTGACAAG and
	GGATGGTTGCGTATTGGTCAGT
spds-1	AACGGGATGAGTTCTCCTACCA and
	ACTCGTGCTTCAAGACCTCTCT
act-1	TCCAAGAGAGGTATCCTTACCC and
	CTCCATATCATCCCAGTTGGTG

Protein quantitation

Proteins were assayed by the method of Bradford [54] using ovalbumin as a standard.

Statistical analysis

The effects of B_{12} deficiency on amino acid and polyamine metabolism in C. elegans were evaluated by one-way ANOVA, and a post-hoc analysis was performed using Tukey's multiple comparison tests. Analyses were performed with GraphPad Prism 3 for Windows version 2.01 (GraphPad software Inc., La Jolla, CA, USA). All

data are presented as the mean ± SD. Differences were considered statistically significant when $p < 0.05$.

Results and Discussions

Effects of B_{12} deficiency on amino acid metabolism in C. elegans

The B_{12}-dependent enzyme activities of MCM and MS catalyzing the key enzymatic reactions of the catabolism of branched-chain amino acids (valine, leucine, and isoleucine) and synthesis of methionine, respectively, were significantly decreased in mammals by B_{12} deficiency [18, 21]. To evaluate whether B_{12} deficiency causes the metabolic disorders of these amino acids in *C. elegans*, free amino acid levels were analyzed in B_{12}-deficient worms, compared with those of control worms. As shown in **Table 8**, branched-chain amino acid (valine, leucine, and isoleucine) levels were significantly increased but methionine level was decreased in the B_{12}-deficient C. elegans, indicating that significant changes in these amino acid levels are directly attributable to the decreased MCM and MS activities caused by B_{12} deficiency.

Ebara *et al*. [22, 32] reported that serine, threonine, and lysine levels significantly increased in plasma and urine of the B_{12}-deficient rats and that mRNA and protein levels of serine/threonine dehydratase (EC 4.3.1.19) that catalyzes the conversion of serine and threonine to pyruvate and 2-oxobutyrate, respectively, were significantly lowered by B_{12} deficiency. Similarly, significant increases of threonine and lysine were detected in the B_{12}-deficient worms (**Table 8**).

B_{12} deficiency induced abnormal accumulation of cellular Hcy in *C. elegans* as well as mammals (**Chapter II**, **Section 1**) because of the significant decrease of MS activity. Hcy is usually metabolized to cystathionine by the action of cystathionine β-synthase (EC 4.2.1.22) and subsequently cystathionine is converted into cysteine and 2-oxobutyric acid by the action of cystathionine-γ-lyase (EC 4.2.1.15). The formed

2-oxobutyric acid is metabolized to TCA cycle *via* propionyl-CoA pathway. Kawata *et al*. [114] suggested that hepatic cystathionine β-synthase activity was decreased in the B_{12}-deficient rats. My unpublished data indicated that mRNA level of cystathionine β-synthase was significantly reduced in the B_{12}-deficient worms. These results suggest that abnormal accumulation of Hcy was attributable to the decreased enzyme activity of cystathionine β-synthase. Furthermore, cystathionine level was simultaneously increased in the B_{12}-deficient worm (**Table 8**). The MCM activity decreased by B_{12} deficiency would disrupt the normal catabolism of cystathionine to TCA cycle *via* propionyl-CoA pathway to increase cystathionine level.

Many studies have reported that a synergistic inhibition of respiratory chain and TCA cycle by propionyl-CoA and its alternative products, 2-methylcitrate (MCA) and malonate, as well as MMA [57]. α-Aminoadipic acid is the intermediate compound for degradation of lysine. Lysine and α-aminoadipic acid were significantly increased in the B_{12}-deficient worms, suggesting that lysine catabolism was disordered by TCA cycle inhibition caused by B_{12} deficiency.

Surprisingly, the B_{12}-deficient worms showed significant accumulation of ornithine, which is mainly formed from arginine in urea cycle [115] but may be synthesized from glutamate or derived from diet. *C. elegans* absolutely requires arginine as well as lysine, threonine, isoleucine, leucine, valine, methionine, phenylalamine, tryptophan, and histidine, as essential amino acids, and utilizes arginine as a phosphagen [116] instead of creatine. Although no homologous genes have been identified to indicate the existence of an intact urea cycle in *C. elegans* (www.Genome.jp/kegg), profiling the anaerobic response of worms using GC-MS showed the occurrence of urea, which is formed from arginine by arginase (EC.3.5.3.1) [117]. Wright has found an evidence for a functional urea cycle of low activity and excretion of urea in the free-living nematode *Panagrellus redivivus* [118]. Ornithine is precursors for polyamines that act as the modulators in neurotransmission [119] and for proline involved in collagen synthesis [120]. B_{12}-deficient worms showed the increase of hydroxyproline, which is a major component amino acid for the protein collagen. B_{12}-deficient worms showed a specific

morphological abnormality, similar to the short and plump ‘‘dumpy’’ mutant phenotype that is formed because of disordered cuticle collagen biosynthesis [65, 66]. This observation and my data indicate that the decreased level of hydroxyproline is one of the reasons of this impaired collagen biosynthesis.

Table 8. Free amino acids and vitamin B_{12}-related compounds in vitamin B_{12}-deficient *C.elegans*

	Control	B_{12}-deficient F5
	(μmol/g wet weight)	
Aspartic acid	1.29 ± 0.22^a	0.58 ± 0.52^b
Threonine	0.55 ± 0.04^a	0.80 ± 0.10^b
Serine	0.76 ± 0.07^a	0.93 ± 0.17^a
Asparagine	0.57 ± 0.07^a	0.41 ± 0.07^a
Glutamic acid	3.27 ± 0.38^a	3.41 ± 0.28^a
Glutamine	1.32 ± 0.22^a	1.28 ± 0.29^a
Glycine	0.73 ± 0.06^a	0.78 ± 0.05^a
Alanine	5.80 ± 0.66^a	6.05 ± 0.48^a
Valine	0.58 ± 0.06^a	1.03 ± 0.13^b
Cystathionine	0.57 ± 0.06^a	3.57 ± 0.31^b
Methionine	0.19 ± 0.03^a	0.12 ± 0.03^b
Isoleucine	0.37 ± 0.05^a	0.61 ± 0.08^b
Leucine	0.70 ± 0.09^a	1.07 ± 0.12^b
Tyrosine	0.22 ± 0.02^a	0.30 ± 0.02^a
Phenylalanine	0.35 ± 0.05^a	0.47 ± 0.10^a
Ornithine	0.21 ± 0.07^a	0.43 ± 0.05^b
Lysine	0.43 ± 0.04^a	0.71 ± 0.01^b
Histidine	0.34 ± 0.04^a	0.55 ± 0.12^a
Arginine	0.88 ± 0.10^a	1.14 ± 0.16^a
Hydroxyproline	0.03 ± 0.01^a	0.07 ± 0.06^a
Phosphoethanolamine	0.25 ± 0.05^a	0.58 ± 0.11^b
Aminoadipic acid	0.79 ± 0.09^a	1.44 ± 0.12^b

Data are presented as mean ± SD (n=5). Values with different superscript letters are significantly different ($p < 0.05$)

B_{12}-deficient worms showed the increased level of phosphoethanolamine (**Table 8**), which is a compound involved in phospholipid turnover, acting as a substrate for many

phospholipids of the cell membranes, especially phosphatidylcholine. Akesson *et al*. [121] have demonstrated that phosphatidylcholine was decreased in the liver of B_{12} deficient rats, which conversely increased phosphatidylethanolamine.

Effects of B_{12} deficiency on polyamines metabolism in C. elegans

Fig. 35 indicates the relationship between B_{12}-dependent Met synthetic pathway and polyamine metabolic pathway in mammals. Putrescine is the simplest polyamine and is synthesized from ornithine by ODC. Subsequent syntheses of spermidine and spermine absolutely require decarboxylated SAM, which is synthesized by the catalysis of SAM decarboxylase (SAMDC; EC 4.1.1.50). Pegg *et al*. [122] reported that some nematode worms including *C. elegans* have lost spermine synthase (SPMS; EC 2.5.1.22). To elucidate the mechanism of accumulation of ornithine in the B_{12}-deficient worms, putrescine and spermidine contents were assayed. Putrescine content did not change between B_{12}-deficient and control worms (**Fig. 36A**). On the other hand, spermidine content of the B_{12}-deficient worms was decreased to approximately 82% of the control worms (**Fig. 36B**). Bjelakovic *et al*. [123] have demonstrated that the supplementation of B_{12} alone or together with folic acid to rats increases hepatic spermidine levels, but not putrescine levels. These results suggest that spermidine is readily affected by cellular B_{12} levels.

As shown in **Fig. 37**, ODC activity was remarkably increased in the B_{12}-deficient worms relative to the controls. It is reported that ODC activity is significantly increased in murine L1210 leukaemia cells by the depletion of SAM [124] and in totally gastrectomized B_{12}-deficient rats [125]. These results suggest that the ODC activity increased in the B_{12}-deficient worms was attributable to the decreased SAM level, which further reduced the cellular spermidine level because decarboxylated SAM formed from SAM is essential for the synthesis of polyamine compounds.

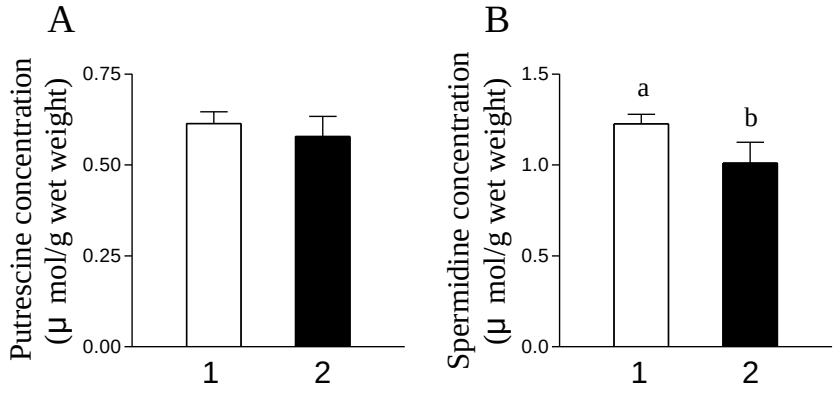

Fig. 36. Vitamin B_{12}-deficient worm causes polyamine metabolic disorder. (A) Putrescine and (B) spermidine concentration were measured in homogenates of worms grown under B_{12}-supplemented (1; white bar) and the B_{12}-deficient conditions (2; black bar) using HPLC. Data represent mean ± SD of three independent experiments; the different alphabets indicate values that are significantly different, $p < 0.05$.

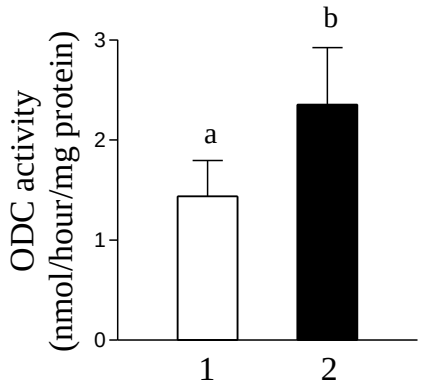

Fig. 37 . Effect of vitamin B_{12} deficiency on ornithine decarboxylase (ODC) activity in *C. elegans*. ODC activity was measured in homogenates of worms grown under B_{12}-supplemented (1; white bar) and B_{12}-deficient conditions (2; black bar) using HPLC. Data represent mean ± SD of three independent experiments; the different alphabets indicate values that are significantly different, $p < 0.05$.

The biosynthesis of polyamines is highly regulated by the activities of two key enzymes, ODC and SAMDC. To clarify the abnormal polyamine metabolism in the B_{12}-deficient worms, the gene expression of ODC (*odc-1*), SAMDC (*smd-1*), and SPDS (*spds-1*) was evaluated using the qPCR method. B_{12}-deficient worm showed a significant increase of ODC (*odc-1*) mRNA expression level (**Fig. 38A**), coinciding with the increased activity of ODC. Although the mRNA expression level of SPDS (*spds-1*) did not change among three experimental conditions (**Fig. 38B**), SAMDC

(*smd-1*) mRNA expression level was decreased to approximately 50% of the control worms (**Fig. 38C**). When B_{12}-deficient worms were transferred onto the B_{12}-supplemented medium and grown for one generation, the changed mRNA expression levels of *odc-1* and *smd-1* were recovered to each control level. These results indicate that ODC and SAMDC mRNA expression levels are readily affected by B_{12} deficiency.

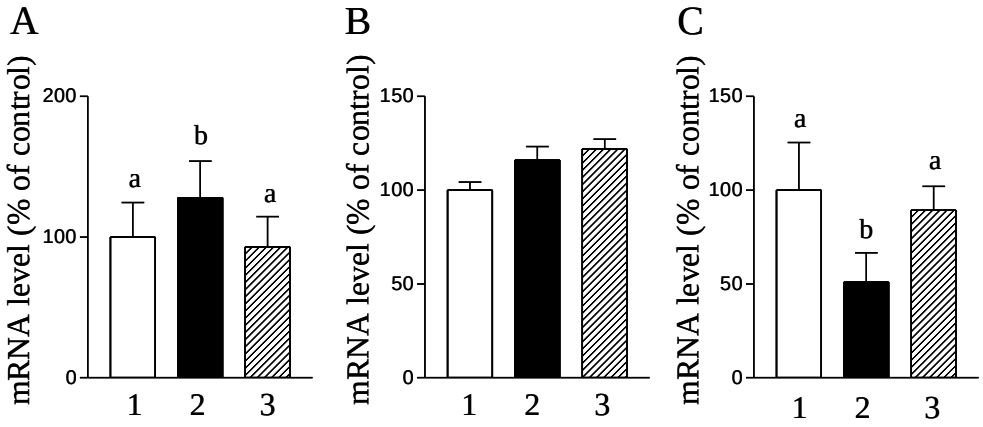

Fig. 38. The expression level of enzymes related to polyamine metabolism in B_{12}-deficient *C. elegans*. The mRNA expression of (A) ODC; ornithine decarboxylase (*odc-1*), (B) SPDS; spermidine synthase (*spds-1*), and (C) SAMDC; *S*-adenosylmethionine decarboxylase (*smd-1*) were determined in the worm grown under B_{12}-supplemented (1; white bar) or B_{12}-deficient (2; black bar) or recovered B_{12}-deficient conditions (3; shaded bar) by real-time PCR method. Data represent mean ± SD of three independent experiments; the different alphabets indicate values that are significantly different, $p < 0.01$.

SAM functions as an important methyl donor in all living organisms. The methyl group from SAM is transferred to certain acceptor to form SAH [126], which is a potent competitive inhibitor of transmethylation reactions. Thus, SAM/SAH ratio is used as an index of cellular transmethylation reactions [20] and was decreased in B_{12}- or folate-deficient mammals [127, 128]. As shown in **Fig. 39**, B_{12} deficiency significantly decreased SAM and SAM/SAH ratio, which is approximately 39% of the control worms. SAM/SAH ratio in B_{12}-deficient rats and humans was decreased to approximately 26% [129] and 62% [130] of the ratio in B_{12} sufficiency, respectively. These results indicate that B_{12} deficiency leads to reduction of various cellular methylation reactions such as DNA, RNA, proteins, and lipids.

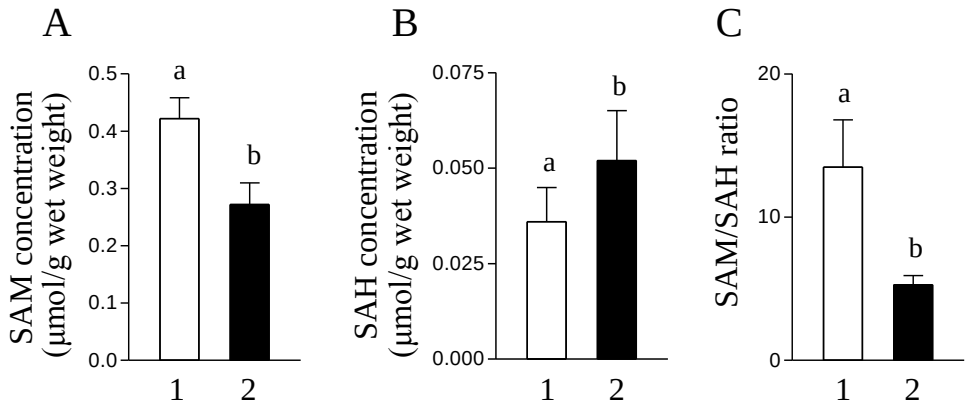

Fig. 39. Effects of vitamin B_{12} deficiency on *S*-adenosylmethionine (SAM) and *S*-adenosylhomocysteine (SAH) content in *C. elegans*. (A) SAM and (B) SAH contents were measured in homogenates of worms grown under B_{12}-supplemented (1; white bar) and B_{12}-deficient conditions (2; black bar) using HPLC. (C) SAM/SAH ratio calculated dividing (A) SAM value by (B) SAH value. Data represent mean ± SD of three independent experiments; the different alphabets indicate values that are significantly different, $p < 0.05$.

Polyamines have been reported to stimulate B_{12}-dependent MS so that the compounds appear to modulate MS activity [19]. To elucidate whether polyamines can stimulate *C. elegans* MS, effects of various concentrations of spermidine or putrescine on the activity of *C. elegans* holo-MS were studied (**Fig. 40**).

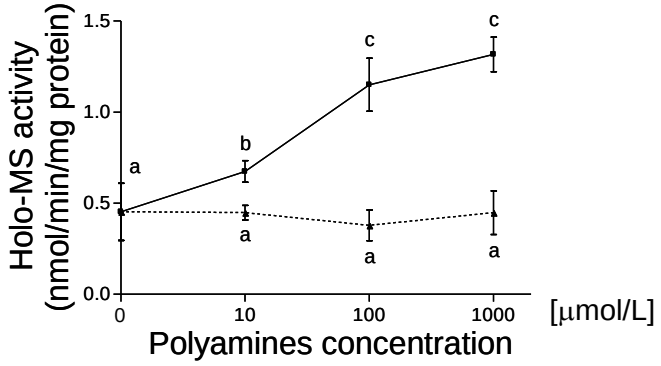

Fig. 40. Regulation of methionine synthase (MS) activity by polyamines. A cell homogenate of B_{12}-supplemented (control) worms used as a holo-MS enzyme preparation because most MS activity is derived from holoenzyme in *C. elegans*. Holo-MS activity was determined in the presence or absence of various concentrations (10, 100, and 1000 μmol/L) of putrescine (▲) or spermidine (■). Data represent mean ± SD of three independent experiments; the different alphabets indicate values that are significantly different, $p < 0.05$.

Holo-MS activity increased in a dose-dependent manner of spermidine and was approximately 2.5 times greater in the presence of 1 mmol/L spermidine. However, putrescine did not stimulate holo-MS. Thus, there is a possibility that MS is regulated by cellular spermidine level in *C. elegans*. These results suggest that MS is synergically inhibited due to the decreased spermidine in the B_{12}-deficient worms. It is reported that the depletion of polyamines leads to reductions of ovogenesis and egg-laying rates [131]. As shown in **Chapter II**, **Section 1**, B_{12}-deficient worms significantly decreased the egg-laying rates, probably due to the decreased spermidine.

Polyamines as well as Hcy activate NMDA receptor involved in the signal transmission between nerve cells [132, 133] and induce an excitotoxic neurodegenerative process [134]. Adachi *et al*. [135] have demonstrated polyamine concentration decreased in the cerebellum, brainstem and spinal cord of B_{12}-deficient rats. These observations and this study indicate that amino acid and polyamime metabolic disorders caused by B_{12} deficiency are closely related with neuropathy. **Fig. 41** summarizes the amino acid and polyamine metabolic disorders in the B_{12}-deficient *C. elegans*.

However, the detailed mechanism of B_{12}-deficient neuropathy including cognitive dysfunction remains to be completely elucidated. Since C. elegans is widely used as a model organism for studying the mechanisms of memory/learning [136], it becomes a suitable and powerful tool for the study of B_{12}-deficient neuropathy [137] and cognitive impairment [138] in humans.

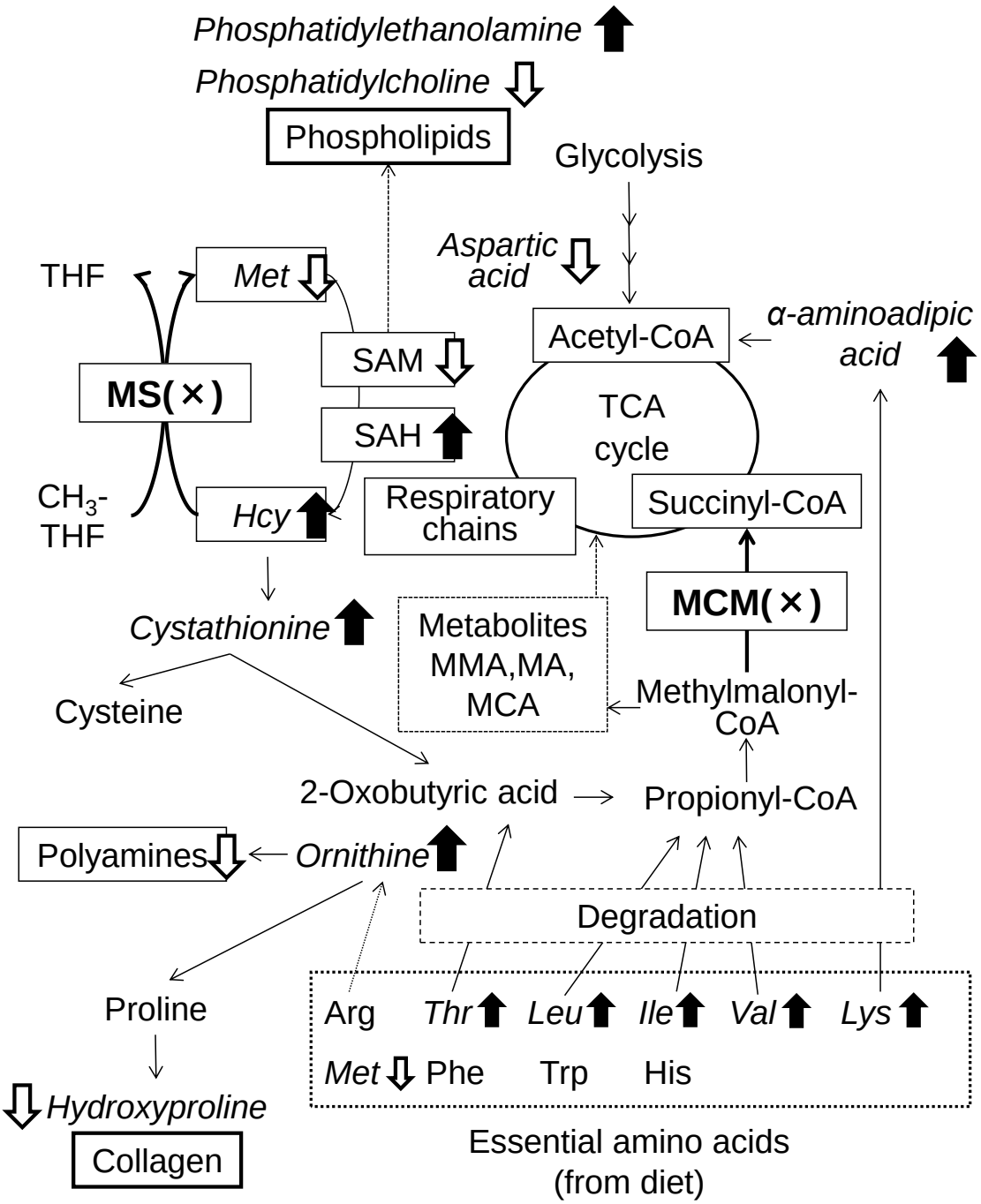

Fig. 41. Extent of the metabolic disorder in B_{12}-deficient *C. elegans*.

Summary

To evaluate whether B_{12} deficiency causes the metabolic disorders of these amino acids in *C. elegans*, free amino acid levels were analyzed in the B_{12}-deficient worms, compared with those of the control worms. Branched-chain amino acid (valine, leucine, and isoleucine) levels were significantly increased but methionine level was decreased in the B_{12}-deficient *C. elegans*, indicating that significant changes in these amino acid levels are directly attributable to the decreased MCM and MS activities caused by B_{12} deficiency. Surprisingly, the B_{12}-deficient worms showed significant accumulation of ornithine. Ornithine is a precursor of polyamines, which play multiple roles in cell growth and death including aging and diseases. Putrescine content did not change between B_{12}-deficient and control worms and spermidine content of B_{12}-deficient worms was decreased to approximately 82% of the control worms. These results indicate that amino acid and polyamine metabolic disorders are closely related with symptoms of B_{12} deficiency.

Chapter IV

Production of vitamin B_{12}-enriched food for preventing the deficiency among vegetarians and elderly subjects

B_{12} is synthesized only by certain bacteria and primarily concentrated in the bodies of higher predatory organisms in the natural food chain. Animal-derived foods such as meat, milk, egg, fish, and shellfish, but not plant-derived foods, are the major dietary sources of B_{12} [36]. Therefore, strict vegetarians are at a greater risk of developing B_{12} deficiency than nonvegetarians. The recommended dietary allowance (RDA) of B_{12} for adults is 2.4 μg/day in the United States (and Japan) [23, 139]. It is important to identify high B_{12}-containing plant-derived food to prevent vegetarians and elderly people from developing B_{12} deficiency. Some plant-derived foods such as edible algae or blue-green algae (cyanobacteria) contain large amounts of B_{12} [140]. However, inactive pseudo-B_{12} is reportedly predominant in various edible cyanobacteria [141, 142]. Thus, I develop a simple method for analyzing B_{12} compounds in various food samples using a miniaturized high-performance thin-layer chromatography (HPTLC) (**Section 1**). Moreover, I characterize B_{12} compounds in shiitake mushroom fruiting bodies as a plant-derived food (**Section 2**).

Mozafar [143] demonstrated that the addition of an organic fertilizer, cow manure, significantly increased the B_{12} content (17.8 ng/g dry weight) in spinach leaves. Using this value and assuming spinach leaves have a moisture content of 92.4% [144], the B_{12} content is approximately 0.14 μg/100 g fresh weight. Consumption of several hundred grams of fresh spinach would therefore be insufficient to meet the RDA of 2.4 μg/day for adult humans [23]. Furthermore, my unpublished works indicate that most organic fertilizers, particularly those made from animal manures, contain considerable amounts of inactive corrinoid compounds. These compounds have also been reported to be present in human feces and account for >98% of the total corrinoid content [145]. Thus, I characterize B_{12} compounds in biofertilizers containing purple photosynthetic bacteria that have the ability to synthesize B_{12} *de novo* (**Section 3**).

Some researchers have attempted to prepare certain B_{12}-enriched vegetables by treating them with a solution containing high levels of B_{12} [146, 147]. This resulted in a significant increase in the amount of B_{12} incorporated into the plants, suggesting that the B_{12}-enriched vegetables may be of special benefit to vegetarians. However, the B_{12} absorbed by the vegetables was not well characterized in these studies. Thus, I describe the production and characterization of B_{12}-enriched lettuce leaves cultivated using hydroponics (**Section 4**).

Section 1 Miniaturized high performance thin-layer chromatography of vitamin B_{12} compounds in foods

Introduction

Edible cyanobacteria (ex. *Spirulina* sp. and *Aphanizomenon flos-aquae*) contain a large amount of pseudo-B_{12}, which is inactive in humans [141, 142]. Human enterobacteria also can synthesize various corrinoid compounds with differences in the base moiety of the molecule [145]. Various high-quality precoated plates with low and uniform particle diameters are available for silica gel 60 TLC or high-performance TLC (HPTLC), which are suitable for analyzing water-soluble vitamins [148]. TLC (or HPTLC) has great advantages (simplicity, flexibility, speed, and relative inexpensiveness) for the separation and analysis of vitamins [148]. In general, TLC is used as a powerful separation and analytic tool, particularly in pharmaceutical preparations. The amount of B_{12} is very low in tissue, body fluids, and food products, and it can be specifically visualized using B_{12}-dependent *E. coli* 215-bioautography after being separated by TLC [149]. Although TLC bioautography is an excellent method for analyzing trace B_{12} samples, this technique requires skilled and time-consuming procedures [150]. To overcome this weakness of TLC in the analysis of B_{12} compounds, I used an immunoaffinity column for purifying and concentrating B_{12} compounds from samples and miniaturized TLC (or HPTLC) sheets for rapid identification. In this section, I describe a simple procedure for analyzing B_{12} compounds in various food samples using a miniaturized HPTLC.

Materials and Methods

Reagents and chemicals

CN-B_{12}, OH-B_{12}, CH_3-B_{12}, and AdoB_{12} were obtained from Sigma (St. Louis, MO, USA). Adeninyl cyanocobamide (pseudo-B_{12}) was prepared previously [151].

5-Hydroxybenzimidazolyl cyanocobamide (Factor III) and benzimidazolyl cyanocobamide (BIA) were provided by Dr. E. Stupperich (Ulm University, Ulm, Germany). Bovine livers and clams were obtained from a local market in Tottori-city, Japan. *S. platensis* and *A. flos-aquae* powders were obtained from MicroAlge Corporation (Gifu, Japan). Instrumentation Products for silica gel 60 F254 TLC, silica gel 60 RP-18F254s HPTLC, Lichrospher silica gel 60 F254s HPTLC, and silica gel 60 F254s HPTLC were obtained from Merck (Darmstadt, Germany). A TLC developing chamber (130 × 55 × 130 mm^3) was obtained from CAMAG (Muttenz, Switzerland). A TLC photograph device equipped with a Canon PowerShot G11 digital camera was obtained from LCScience Co. (Nara, Japan). Preparation of stock standard solutions of authentic B_{12} compounds (CN-B_{12}, OH-B_{12}, CH_3-B_{12}, and AdoB_{12}) and other corrinoids (pseudo-B_{12}, Factor III, and BIA) (**Fig. 42**) were dissolved in distilled water at final concentration of 100 μmol/L, and stored at 4°C until experimental use.

Extraction and purification of B_{12} compounds from food and biological materials

Dried edible algae (nori, *Porphyra* sp.), bovine livers, and clam meats (approximate 20 g) were homogenized using a mixer (TML160; Tescom & Co., Ltd, Tokyo, Japan). A portion (2 g) of the liver and clam homogenates and nori powder was used as the test sample. Total B_{12} compounds were extracted from each homogenate by boiling with 100 mL of 57 mmol/L acetate buffer (pH 4.5) containing 0.0004 % (w/v) KCN for 30 min to convert various B_{12} compound with different upper ligands (e.g., coenzyme forms of B_{12}) to CN-B_{12}. The extraction procedures were performed in a draught chamber (Dalton Co., Tokyo, Japan). The boiled suspension was centrifuged at 10,000 × *g* for 10 min. An aliquot (20 mL) of the supernatant was partially purified and concentrated using a Sep-Pak® Plus C18 cartridge (Waters Corp. Milford, USA) that had been washed with 5 mL of 75% (v/v) ethanol and equilibrated with 5 mL of distilled water. The C18 cartridge was washed with 5 mL of distilled water, and B_{12} compounds were eluted using 2 mL of 75% (v/v) ethanol. The eluate was evaporated in

a centrifugal concentrator (Integrated SpeedVac® System ISS110; Savant Instruments Inc., NY, USA). The residual fraction was dissolved in 2 mL of distilled water and centrifuged at 10,000 × *g* for 10 min to remove any insoluble material. The supernatant fraction was loaded onto an immunoaffinity column [EASIEXTRACT® B_{12} Immunoaffinity Column (P80) R-Biopharm AG, Darmstadt, Germany], and the column was washed with 10 mL of distilled water. After B_{12} compounds were eluted with 3 mL of methanol, the eluate was evaporated in a centrifugal concentrator (Integrated SpeedVac® System). The residual fraction was dissolved in 10 μL of distilled water and used as the purified B_{12} compounds. Corrinoid compounds present in the dried edible cyanobacteria (*S. platensis* and *A. flos-aquae*, each at 2 g) were extracted and purified under the same conditions described above.

TLC conditions

One microliter of B_{12} compounds purified from food and biological samples, authentic B_{12}, and other corrinoid compounds (100 μmol/L, each) were spotted onto Lichrospher silica gel 60 F254s HPTLC sheets (5.0 × 7.5 cm) and developed to a migration distance of 5 cm in the dark using 2-propanol/NH_4OH(28 %)/water (7:1:2 v/v/v) as solvent I and 1-butanol/2-propanol/water (10:7:10 v/v/v) as solvent II at room temperature (25°C).

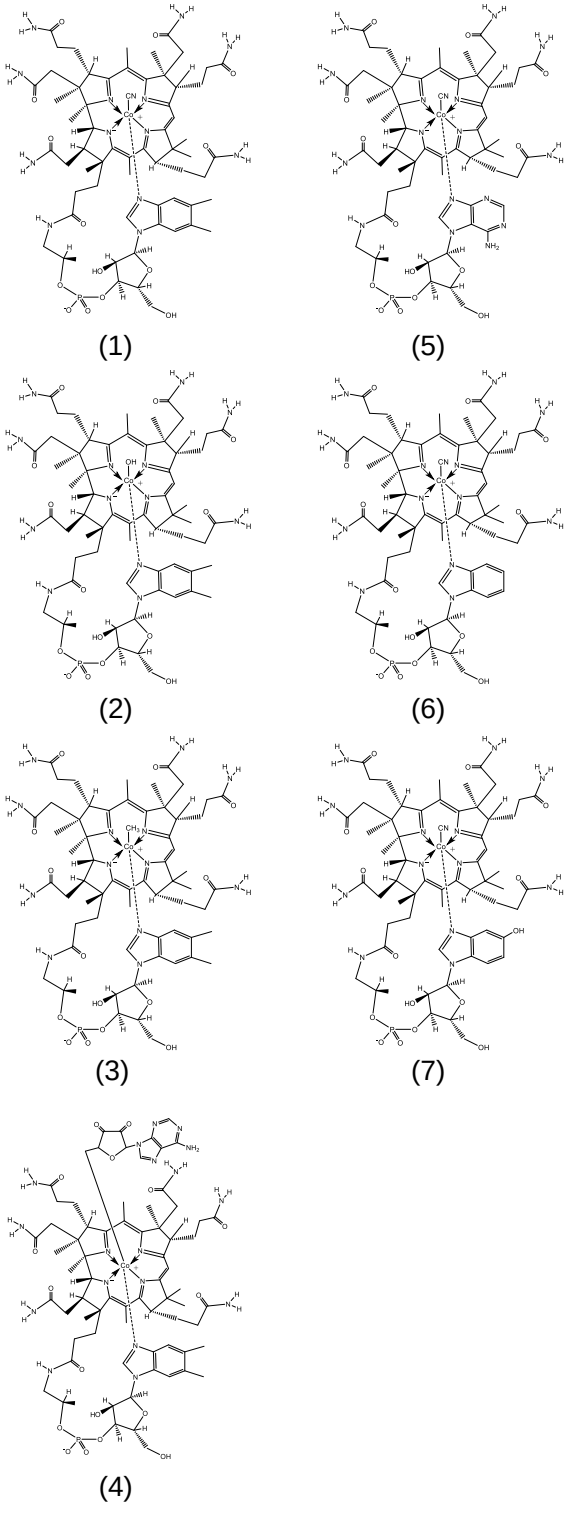

Fig. 42. Structural formula of vitamin B_{12} and its related compounds. (1) CN-B_{12}, (2) OH-B_{12}, (3) CH_3-B_{12}, (4) Ado-B_{12}, (5) Pseudo-B_{12}, (6) BIA, and (7) Factor III.

Results and Discussion

Selection of silica gel 60 TLC and HPTLC sheets

Using four types of silica gel-based TLC and HPTLC sheets, the separation (differences between the R_f value of each compound) and development time (time required for a migration distance of 5 cm) of authentic B_{12} compounds (CN-B_{12}, OH-B_{12}, CH_3-B_{12}, and AdoB_{12}) were evaluated in preliminary experiments. As shown in **Table 9**, silica gel 60 F254 TLC and Lichrospher silica gel 60 F254s HPTLC sheets showed shorter development times and higher separation efficiency.

Table 9. Selection of silica gel 60-based TLC and HPTLC sheets for analyzing vitamin B_{12} compounds

Time (min)	Separation (R_f values, solvent I/solvent II)	
TLC Silica gel 60 F254		
Solvent I (45)	CN-B_{12}	0.64/0.27
Solvent II (47)	CH_3-B_{12}	0.70/0.45
	OH-B_{12}	0.08/0.07
	AdoB_{12}	0.43/0.20
HPTLC Silica gel 60 RP-18 F254s		
Solvent I (97)	CN-B_{12}	1.00/0.60
Solvent II (96)	CH_3-B_{12}	0.97/0.40
	OH-B_{12}	0.98/0.02
	AdoB_{12}	0.95/0.06
HPTLC Lichrospher Silica gel 60 F254s		
Solvent I (43)	CN-B_{12}	0.68/0.27
Solvent II (42)	CH_3-B_{12}	0.72/0.45
	OH-B_{12}	0.05/0.00
	AdoB_{12}	0.44/0.20
HPTLC Silica gel 60 F254s		
Solvent I (71)	CN-B_{12}	0.76/0.23
Solvent II (68)	CH_3-B_{12}	0.80/0.33
	OH-B_{12}	0.04/0.03
	AdoB_{12}	0.08/0.17

Authentic CN-B_{12}, CH_3-B_{12}, OH-B_{12}, and Ado-B_{12} (1 μL of 100 μmol/L, each) were analyzed using TLC or HPTLC sheets (5 cm × 7.5 cm) in solvents I and II. The results were estimated with regard to time (development time for the migration distance of 5 cm) and separation (differences between R_f values)

When various concentrations of authentic CN-B_{12} were analyzed by Lichrospher silica gel 60 F254s HPTLC and silica gel 60 F254 TLC, spots were visually detected up to 25 and 50 pmol of CN-B_{12}, respectively, under ultraviolet (254 nm) irradiation (**Fig. 43**). These results indicated that the Lichrospher silica gel 60 F254s HPTLC sheet was the most suitable for the analysis of B_{12} compounds.

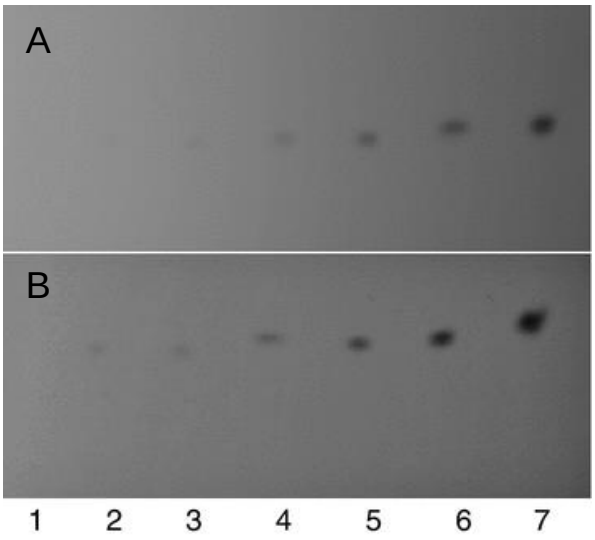

Fig. 43. Silica gel 60 F254 TLC and Lichrospher silica gel 60 F254s HPTLC chromatograms of various concentrations of authentic vitamin B_{12}. Various concentrations (1. 10 pmol, 2. 25 pmol, 3. 50 pmol, 4. 100 pmol, 5. 250 pmol, 6. 500 pmol, 7. 1,000 pmol) of authentic CN-B_{12} were analyzed by TLC (A) and HPTLC (B) in solvent I. Data represent the typical migration patterns of varied concentrations of authentic CN-B_{12} from three independent experiments.

Separation of various corrinoid compounds

Authentic CN-B_{12}, CH_3-B_{12}, OH-B_{12}, and AdoB_{12} (1 μL of 100 μmol/L, each) were analyzed using Lichrospher silica gel 60 F254s HPTLC. The R_f values of CN-B_{12}, CH_3-B_{12}, OH-B_{12}, and AdoB_{12} were 0.68 (0.27), 0.72 (0.45), 0.05 (0), and 0.44 (0.20) in solvent I (and II), respectively (**Fig. 44**). These HPTLC analyses required <45 min (a migration distance of 5 cm), which was significantly reduced compared with the time required for silica gel 60 TLC (2–3 h for a migration distance of 10 cm) [151]. Other corrinoid compounds that are inactive in humans (pseudo-B_{12}, Factor III, and BIA, at 1 μL of 100 μmol/L, each) with different base moieties (**Fig. 45**) were also separated with

R_f values of 0.52, 0.55, and 0.58, respectively, in solvent I (data not shown).

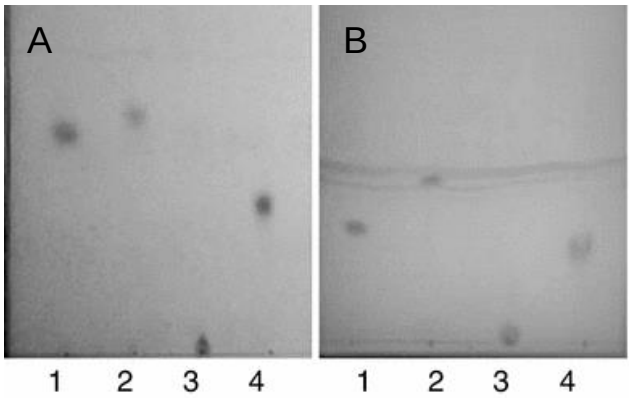

Fig. 44. Lichrospher silica gel 60 HPTLC F254s chromatograms of authentic vitamin B_{12} compounds. Authentic CN-B_{12} (1), CH_3-B_{12} (2), OH-B_{12} (3), and Ado-B_{12} (4) (1 µL of 100 µmol/L, each) were analyzed by HPTLC in solvents I (A) and II (B). Data represent the typical migration patterns of authentic B_{12} compounds from five independent experiments.

Identification of corrinoid compounds from various foods

To evaluate whether various B_{12}-rich foods including edible cyanobacteria contain ‘‘true’’ B_{12} or other corrinoid compounds using this miniaturized HPTLC technique, corrinoid compounds were extracted from bovine livers, clam meats, nori (*Porphyra* sp.), *S. platensis*, and *A. flosaquae* and purified using an immunoaffinity column, and they were identified by HPTLC (**Fig. 45**). Each compound purified from bovine livers, clam meats, and nori produced a clear single spot, the R_f value of which was identical to that of authentic B_{12}, but not to that of pseudo-B_{12}. Although the purified compounds from *S. platensis* were separated in two spots, the R_f values of which were identical to those of authentic B_{12} and pseudo-B_{12}, the compound from *A. flos-aquae* produced only a single spot with an identical R_f value to authentic pseudo-B_{12}. These results were identical with those of silica gel 60 TLC *E. coli* 215 bioautography, as described previously [141, 142, 152].

This study provides an alternative analysis method for B_{12} compounds in food without the use of expensive instruments, such as HPLC, and B_{12}-dependent

microorganisms (*E. coli* 215, etc.). The results of miniaturized Lichrospher HPTLC of authentic B_{12} compounds demonstrated the advantages of this technique as the short migration distances (5 cm) and the short development times (<45 min) in combination with high separation efficiency and sensitivity (>25 pmol at 254 nm).

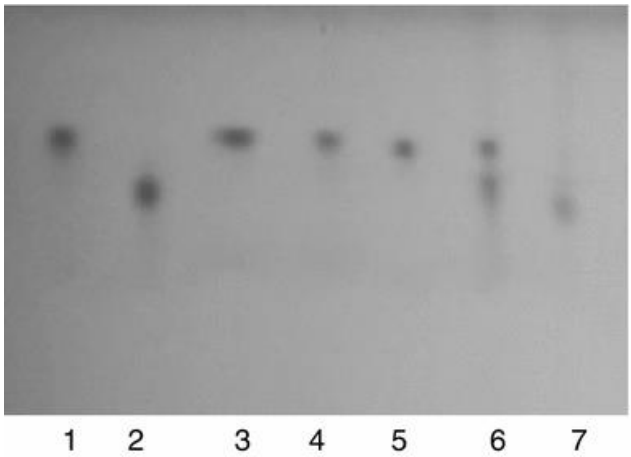

Fig. 45. Lichrospher silica gel 60 HPTLC F254s chromatograms of authentic vitamin B_{12}, pseudo-B_{12}, and corrinoid compounds purified from various foods and biological materials. One microliter each of authentic CN-B_{12} (1) and pseudo-B_{12} (2), and the corrinoid compounds purified from bovine livers (3), clam meats (4), nori (5), *Spirulina* sp. (6), and *A. flos-aquae* (7) were analyzed by HPTLC in solvent I. Data represent the typical migration patterns of corrinoid compounds from five independent experiments.

Summary

HPTLC is a separation technique commonly used to identify and quantify compounds in chemical mixtures. Preliminary experiments indicated that Lichrospher silica gel 60 F254s HPTLC sheets were the most suitable for analyzing B_{12} compounds. This study revealed the advantages of miniaturized Lichrospher HPTLC for analyzing authentic B_{12} compounds as short migration distances (5 cm) and short development times (<45 min) in combination with high separation efficiency and sensitivity (>25 pmol at 254 nm). The practicability of using miniaturized HPTLC was demonstrated by the separation and identification of B_{12} compounds purified from foods using an immunoaffinity column.

Section 2 Characterization of vitamin B_{12} compounds in the fruiting bodies of shiitake mushroom (*Lentinula edodes*)

Introduction

Among the wild edible mushroom fruiting bodies that are consumed by European vegetarians, black trumpet (*Craterellus cornucopioides*) and golden chanterelle (*Cantharellus cibarius*) mushroom fruiting bodies contain considerable levels (1.09-2.65 μg/100 g dry weight) of B_{12}, whereas the remaining mushroom fruiting bodies have zero or trace levels [153]. In my preliminary study, I found that Japanese edible wild (*Lactarius laeticolorus*, *Suillus spectabilis*, *Ramaria botrytis*, *Cortinarius pseudosalor*, *Boletopsis leucomelas,* and *Sarcodon aspratus*) and cultivated (*Pleurotus eryngii*, Grifola frondosa, and *Hypsizygus marmoreus*) mushroom fruiting bodies contained trace amounts (approximately 1.0 μg/100 g dry weight of B_{12}), whereas high levels of B_{12} were detected in commercially available dried fruiting bodies of shiitake mushroom (*Lentinula edodes*). Shiitake mushrooms are cultivated and consumed throughout the world. In particular, fresh and dried shiitake mushroom fruiting bodies are also used in various vegetarian dishes. Two types of high grade dried shiitake fruiting bodies are available in Japan: donko-type fruiting bodies with closed caps (early fruiting stage) and koushin-type fruiting bodies with open caps (late fruiting stage). However, little information is available on the B_{12} content in shiitake mushroom fruiting bodies, particularly whether the mushroom fruiting bodies contain "true" (authentic) B_{12} or an inactive corrinoid such as "pseudo-B_{12}" [154]. If shiitake mushroom fruiting bodies generally contain high levels of B_{12}, they would be good sources of B_{12} for vegetarians. In this section, I analyzed the B_{12} contents in various dried shiitake fruiting bodies that are commercially available in Japan and characterized the B_{12} compounds found in these fruiting bodies.

Materials and Methods

Materials

B_{12} was obtained from Sigma (St Louis, MO, USA). A B_{12} assay medium based on *Lactobacillus delbrueckii* subspecies *lactis* (formerly *L. leichmannii)* ATCC 7830 was obtained from Nissui (Tokyo, Japan). Silica gel 60 TLC aluminum sheets were obtained from Merck (Darmstadt, Germany). The raw and dried shiitake mushroom fruiting bodies were purchased in Japan. Raw mushrooms were lyophilized and then used in the experiments. Fruiting bodies of shiitake mushroom (cultivar Kinko-702) were cultivated on bed logs (one year-old bed logs of konara oak, Quercus serrata), harvested at the indicated stages 1-5, and dried at 50°C for 24 h. Bed logs (konara oak, *Quercus serrata*) after five times fruiting of shiitake mushroom (cultivar Kinko-702) were used for the experiments. *Lentinula edodes* TUFC 100154 and 100177 were obtained from Fungus/Mushroom Resource and Research Center, Tottori University, Japan. They were cultured in a malt medium (Bacto™ Malt Extract: Becton, Dickinson and Company, Sparks, MD, USA) for 3 weeks at 25 °C and each mycelium was collected, washed with distilled water, lyophilized, and used in the experiments.

Extraction and assay of B_{12} in shiitake mushrooms

Each dried fruiting body (approximately 10 g) was homogenized in a mixer (TML160; Tescom & Co., Ltd, Tokyo, Japan). A portion (5.0 g) of the homogenate was used as the test sample. The bed logs after fruiting of shiitake mushroom and uninoculated logs were chopped into small particles, homogenized in the mixer, and B_{12} compounds were extracted as described in **Chapter IV**, **Section 1**.

Bioautogram of B_{12} compounds using B_{12}-dependent Escherichia coli 215

A bioautogram of B_{12} compounds was produced using a published method [150].

The B_{12} extract (10 mL) prepared above was partially purified and concentrated using a Sep-Pak® Plus C18 cartridge (Waters Corp., Milford, MA, USA), which had been washed with 5 mL of 75% (v/v) ethanol and equilibrated with 5 mL of distilled water. The C18 cartridge was washed with 5 mL of distilled water and B_{12} compounds were eluted using 2 mL of 75% (v/v) ethanol. The eluate was evaporated in a centrifugal concentrator (Integrated Speed VacR System ISS110; Savant Instruments Inc., Hicksville, NY, USA). The residual fraction was dissolved in 1.0 mL of distilled water. The concentrated B_{12} extracts as well as authentic B_{12} and pseudo-B_{12}, were spotted onto the silica gel 60 TLC sheet and developed in the dark using 2-propanol/NH_4OH (28%)/water (7:1:2 v/v) at 25 °C. After drying the TLC sheet, it was overlaid with agar containing basal medium and precultured *E. coli* 215, and then incubated at 37°C for 20 h. The gel plate was then sprayed with a methanol solution containing 2,3,5-triphenyltetrazolium salt, and the B_{12} compounds were visualized as red, which indicated *E. coli* growth.

Identification of B_{12} compounds by LC/ESI-MS/MS

Dried shiitake fruiting bodies (donko-type sample a and koushin-type sample b) that contained high levels of B_{12} (50 g dry weight each) were homogenized in a mixer (TML160; Tescom & Co., Ltd) before being suspended in 500 mL of distilled water, 50 mL of 0.57 mol/L acetic buffer (pH 4.5) and 0.05 g KCN, and then boiled for 30 min to extract B_{12} compounds. The extraction procedures were performed in a draught chamber (Dalton Co., Tokyo, Japan). The boiled suspension was centrifuged at 10,000 × *g* for 10 min. An aliquot (approximately 200 mL) of the supernatant was placed in a Sep-Pak® Vac 20 cc (5 g) C18 cartridge (Waters Corp.), which had been washed with 75% (v/v) ethanol and equilibrated with distilled water. The C18 cartridges were washed with 30 mL of distilled water and B_{12} compounds were eluted using 30 mL of 75% (v/v) ethanol. The remaining supernatant was treated in the same way. The combined eluates were evaporated to dryness under reduced pressure. The residual fraction was dissolved in 5

mL of distilled water and centrifuged at 10,000 × *g* for 10 min to remove any insoluble material. The supernatant fraction was loaded onto an immunoaffinity column [EASI-EXTRACT® B_{12} Immunoaffinity Column (P80) R-Biopharm AG, Darmstadt, Germany], and B_{12} compounds were purified according to the manufacturer's recommended protocol. The purified mushroom B_{12} compounds and authentic B_{12} were dissolved in 0.1% (v/v) acetic acid and filtered using a Nanosep MF centrifuge device (0.4 μm; Pall Corp., Tokyo, Japan) to remove small particles. I analyzed an aliquot (2 μL) of the filtrate using an LCMS-IT-TOF system, which was coupled to an Ultra-Fast LC system (Shimadzu, Kyoto, Japan). Each purified corrinoid was injected into an InertSustain column (3 μm, 2.0 × 100 mm; GL Science, Tokyo, Japan) and equilibrated with 85% solvent A [0.1% (v/v) acetic acid] and 15% solvent B (100% methanol) at 40 °C. B_{12} compounds were eluted using a linear gradient of methanol (15% solvent B for 0-5 min, 15%-90% solvent B for 5-11 min, and 90%-15% solvent B for 11-15 min). The flow rate was 0.2 mL/min. The electrospray ion (ESI) conditions were determined by injecting authentic B_{12} into the MS detector to determine the optimum parameters for detecting the parent and daughter ions of B_{12} compounds. The ESI-MS was operated in the positive ion mode using argon as the collision gas. The identification of B_{12} (*m/z* 678.292) as $[M + 2H]^{2+}$ was confirmed by comparing the observed molecular ions and their retention times. For the bed logs after fruiting of shiitake mushrooms, the bed log sample b was chopped into small particles, homogenized in the mixer, and B_{12} compounds were extracted under the same conditions described above.

Preparation of B_{12}[c-lactone]

B_{12}[*c*-lactone] was synthesized by the method described previously [155]. The prepared compound was purified using a reversed-phase HPLC column (Wakosil-II 5C18RS, 4.6 × 150 mm; 5 μm particle size; Wako Pure Chemical Industries, Osaka, Japan).

Statistical analysis

The B_{12} contents in shiitake fruiting bodies and their bed logs were analyzed using a one-way ANOVA and post hoc analyses with Tukey's multicomparison test. These analyses were performed using GraphPad Prism® for Windows version 5.03 (GraphPad Software Inc., La Jolla, CA, USA). All the data are expressed as means and standard deviations, and differences were statistically significant at $p < 0.05$.

Results and discussion

B_{12} contents in commercially available fruiting bodies of shiitake mushrooms

The levels of B_{12} were assayed in various dried and raw shiitake mushroom fruiting bodies that are commercially available in Japan using a microbiological method based on *L. delbrueckii* ATCC 7830 (**Table 10**). The corrected B_{12} contents in the shiitake fruiting bodies varied significantly (1.28-12.71 μg/100 g dry weight), and high levels (4.43-21.56 μg as B_{12} equivalent/100 g dry weight) of alkali-resistant factor were found in all mushrooms. The B_{12} contents in dried donko-type fruiting bodies with closed caps (5.61 ± 3.90 μg/100 g dry weight) were not significantly different from those of dried koushin-type fruiting bodies with open caps (4.23 ± 2.42 μg/ 100 g dry weight). The B_{12} contents in raw shiitake fruiting bodies cultivated on sawdust substrate (3.95 ± 3.34 μg/100 g dry weight) were similar to those of dried shiitake fruiting bodies cultivated on bed logs. The results indicated that the B_{12} contents in shiitake fruiting bodies were twice (or more) than in European wild mushroom fruiting bodies, i.e., black trumpet and golden chanterelle mushrooms (1.09－2.65 μg/ 100 g dry weight).

E. coli 215 bioautogram analysis of the shiitake mushroom B_{12} compounds

The B_{12} compounds found in dried shiitake (donko- and koushin-types) fruiting

bodies were analyzed using an *E. coli* 215 bioautogram after separation by silica gel 60 TLC (**Fig. 46**). Each shiitake fruiting body extract produced a single clear spot, the R_f value of which was identical to that of authentic B_{12} but not to that of pseudo-B_{12} (inactive in humans).

Table 10. Vitamin B_{12} contents in commercially available shiitake mushroom fruiting bodies.

	Vitamin B_{12} content (μg/100g dry weight)		
	Apparent B_{12}	Alkali-resistant factor	Corrected B_{12}
Cultivated on bed log			
Dried Donko-type fruiting bodies			
a	34.27	21.56	12.71
b	14.93	11.34	3.59
c	17.82	13.55	4.27
d	12.71	11.01	1.70
e	23.50	19.28	4.22
f	18.84	11.67	7.17
Mean ± SD	20.35 ± 7.75	14.74 ± 4.55	$5.61 \pm 3.90^{g*}$
Dried Koushin-type fruiting bodies			
a	17.73	12.28	5.45
b	14.28	6.55	7.73
c	15.96	14.26	1.7
d	20.98	18.47	2.51
e	13.79	10.05	3.74
Mean ± SD	16.55 ± 2.92	12.32 ± 4.47	4.23 ± 2.42^{g}
Raw fruiting bodies			
a	13.48	9.54	3.94
b	8.24	4.43	3.81
c	11.35	10.07	1.28
d	17.73	8.28	9.45
e	13.46	12.18	1.28
Mean ± SD	12.85 ± 3.47	8.90 ± 2.87	3.95 ± 3.34^{g}

*Identical letter (g) indicates values that are not significantly different.

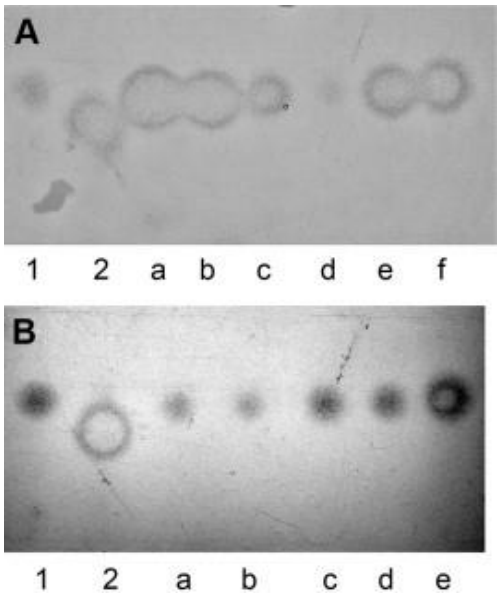

Fig. 46. *Escherichia coli* 215 bioautogram analysis of B_{12} compounds found in commercially available dried shiitake fruiting bodies. A: Dried donko-type shiitake fruiting bodies. 1, authentic B_{12}; 2, pseudo-B_{12}; aef, donko-type shiitake fruiting bodies. B: Dried koushin-type shiitake fruiting bodies. 1, authentic B_{12}; 2, pseudo B_{12}; a-e, oushin-type shiitake samples. The data show typical bioautograms from three independent experiments.

LC/ESI-MS/MS chromatograms of the shiitake mushroom B_{12} compounds

Corrinoids were purified from the donko-type fruiting body a extract using an immunoaffinity column and identified by LC/ESI-MS/MS. Watanabe *et al*. [153] demonstrated that authentic B_{12} eluted as a peak with a retention time of 7.4 min. The mass spectrum of authentic B_{12} primarily comprised a doubly-charged ion with an *m/z* of 678.2829 $[M + 2H]^{2+}$. The MS/MS spectra of B_{12} indicated that a monovalent ion with an *m/z* of 359.1008 predominated, which was largely attributable to the nucleotide moiety of B_{12}. The compounds purified from donko-type fruiting body were eluted to yield several total ion peaks, which indicated that impurities were still present (**Fig. 47A**). The mass spectrum of the main peak with an *m/z* value of 678.2914 had a retention time of 7.4 min in the purified sample, while the B_{12} doubly-charged ion had an *m/z* value of 678.2860 (**Fig. 47B**). The MS/MS spectrum of the purified compound containing the monovalent ion with an *m/z* value of 359.0984 was identical to that of authentic B_{12} (**Fig. 47C**). These results indicate that commercially available dried

shiitake fruiting bodies contained authentic B_{12} and not pseudo-B_{12}, which is inactive in humans.

Changes in B_{12} contents of the fruiting bodies during fruiting of shiitake mushroom (cultivar Kinko-702) on bed logs

Table 11 shows the changes in the B_{12} contents in fruiting bodies during fruiting of shiitake mushroom (cultivar Kinko-702) on bed logs. The fruiting stages of shiitake mushrooms were divided into five stages: stage 1, button-like forms; stage 2, closed caps; stage 3, half open caps; 4, 80% open caps; and stage 5, fully open caps. The B_{12} contents in shiitake fruiting bodies tended to increase from stage 1 (2.12 ± 0.46 μg/100 g dry weight) to stage 3 (4.73 ± 5.80 μg/100 g dry weight), after which they remained at constant levels. However, there were no significant differences in the B_{12} levels among the mushroom fruiting stages.

Biosynthesis of B_{12} in L. edodes

To clarify whether *Lentinula edodes* could synthesize B_{12} *de novo*, *L. edodes* TUFC 100154 and 100177 were axenically cultured in a malt medium. B_{12} was extracted from each mycelium and assayed using B_{12}-dependent *E. coli* 215. Each extract of *L. edodes* TUFC 100154 and 100177 did not produce spots with B_{12} activity (data not shown). Moreover, many genes (cobD, cobF, cobS, cobU, cobV, cbiB, cbiD, and cbiG) involved with B_{12} biosynthesis were absent from the *L. edodes* genome database (ForestGEN, Forestry and Forest Products Research Institute, Tsukuba, Japan). These results strongly suggest that the B_{12} compound found in dried shiitake mushrooms was not attributable to the *de novo* biosynthesis of B_{12}, so it was probably derived from B_{12} sources outside the mushrooms.

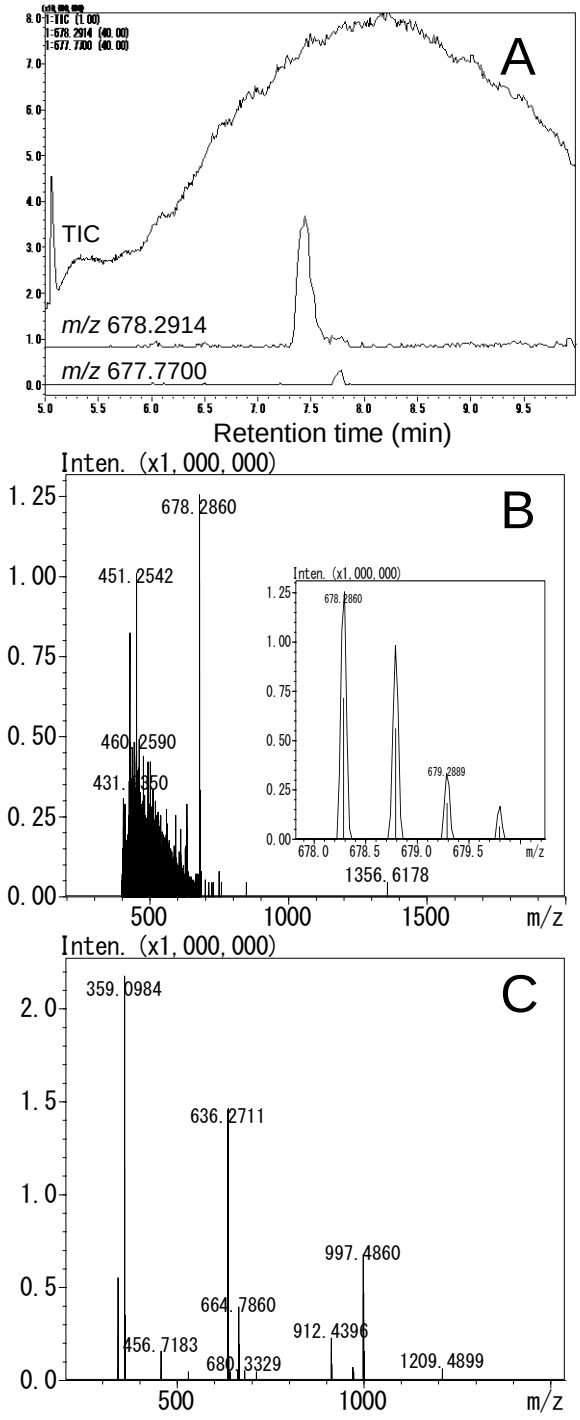

Fig. 47. LC/ESI-MS/MS chromatograms of the B_{12} compounds purified from a dried donko-type shiitake fruiting body sample a. A: Total ion chromatogram (TIC) and reconstructed chromatograms of the purified B_{12} compounds (m/z 678.2914) from dried donko-type shiitake sample a. B: Mass spectrum of the B_{12} compounds purified from the dried shiitake fruiting body at 7.4 min (the magnified spectrum ranging from m/z 678 to m/z 680 is shown as an inset in B). C: MS/MS spectrum for the m/z 678.2860 peak of the B_{12} compounds purified from the shiitake fruiting body a.

Table 11. Changes in vitamin B_{12} contents of fruiting bodies during fruiting of shiitake mushroom (cultivar Kinko-702) on bed logs.

Fruiting stages	Vitamin B_{12} content (μg/100g dry weight)		
	Apparent B_{12}	Alkali-resistant factor	Corrected B_{12}
Stage 1*	8.57 ± 5.00	6.45 ± 4.81	2.12 ± 0.46[a]**
Stage 2	7.82 ± 2.64	5.18 ± 3.55	2.64 ± 1.32[a]
Stage 3	10.35 ± 3.79	5.62 ± 3.90	4.73 ± 5.80[a]
Stage 4	12.01 ± 3.46	7.41 ± 3.24	4.60 ± 3.73[a]
Stage 5	11.69 ± 3.40	7.69 ± 3.54	3.99 ± 5.24[a]

*Fruiting stages of shiitake mushroom were divided into five stages (stage 1, button-like; stage 2, closed caps; stage 3, half open caps; stage 4, 80% open caps; and stage 5, fully open caps).
**Identical letter (a) indicates values that are not significantly different.

B_{12} contents in bed logs (Konara oak) after fruiting of shiitake mushroom (cultivar Kinko-702)

Table 12 shows the B_{12} contents in the bed logs after fruiting of shiitake mushroom (cultivar Kinko-702). High B_{12} levels were detected in the bed logs after fruiting of shiitake mushroom whereas uninoculated logs contained only traces of B_{12}. The bed logs after fruiting contained B_{12} levels that were similar to that in dried shiitake fruiting bodies. Corrinoids were purified from the bed log b extract with an immunoaffinity column and identified by LC/ESI-MS/MS (**Fig. 48**).

Table 12. Vitamin B_{12} contents in bed logs (Konara oak) after fruiting of shiitake mushroom (cultivar Kinko-702).

	Vitamin B_{12} content (μg/100g dry weight)		
	Apparent B_{12}	Alkali-resistant factor	Corrected B_{12}
Uninoculated logs	1.24 ± 0.88	0.87 ± 0.82	0.37 ± 0.18[d]*
Bed logs after fruiting			
a	5.39 ± 2.55	1.89 ± 0.15	3.51 ± 2.60[e]
b	9.82 ± 1.60	5.20 ± 2.60	4.68 ± 1.81[e]
c	7.96 ± 1.82	4.45 ± 1.58	3.51 ± 1.25[e]

*Different letters (d, e) indicates values that are significantly different.

The compounds purified from the bed log b were eluted as several total ion peaks, which indicated that impurities were still present (**Fig. 48A**). The mass spectrum of the main peak with an *m/z* value of 678.2914 had a retention time of 7.4 min in the purified sample, while the B_{12} doubly-charged ion had an *m/z* value of 678.2879 (**Fig. 48B**). The MS/MS spectrum of the purified sample containing the monovalent ion with an *m/z* value of 359.0976 was identical to that of authentic B_{12} (**Fig. 48C**). These results indicated that the bed logs after fruiting of shiitake mushroom contained authentic B_{12}, the level of which increased significantly during fruiting of shiitake mushroom. Given that *L. edodes* cannot synthesize B_{12} *de novo*, the B_{12} found in the bed logs may be attributable to B_{12}-synthesizing bacteria (e.g., *Pseudomonas* sp.), which can utilize certain wood degradation-by-products formed by *L. edodes* for their growth. However, we have no further detailed information on this process. Thus, biochemical and genetic studies are needed to determine why the bed logs after fruiting contained high levels of B_{12}.

Occurrence of the unnatural corrinoid B_{12}[c-lactone] in commercially available dried shiitake fruiting bodies

Chloramine-T, an antimicrobial agent, has widespread uses in medical, dental, veterinary, food processing, and agricultural fields because of its low cytotoxicity [156]. Bonnett [157] reported that chloramine-T is a source of electrophilic chlorine and it reacts with B_{12} to form B_{12}[*c*-lactone], which contains no halogen, at pH 4.0. To clarify whether the commercially available dried shiitake fruiting bodies contained B_{12}[*c*-lactone], I analyzed the purified shiitake extracts using LC/ESI-MS/MS. Authentic B_{12}[*c*-lactone] was eluted as a peak with a retention time of 7.7 min (**Fig. 49A**). The mass spectrum of B_{12}[*c*-lactone] primarily comprised a doubly-charged ion with an *m/z* of 677.7758 $[M + 2H]^{2+}$ (**Fig. 49B**). The MS/MS spectra of B_{12}[*c*-lactone] indicated that a monovalent ion with an *m/z* of 359.0993 predominated (the nucleotide moiety of B_{12}; **Fig. 49C**).

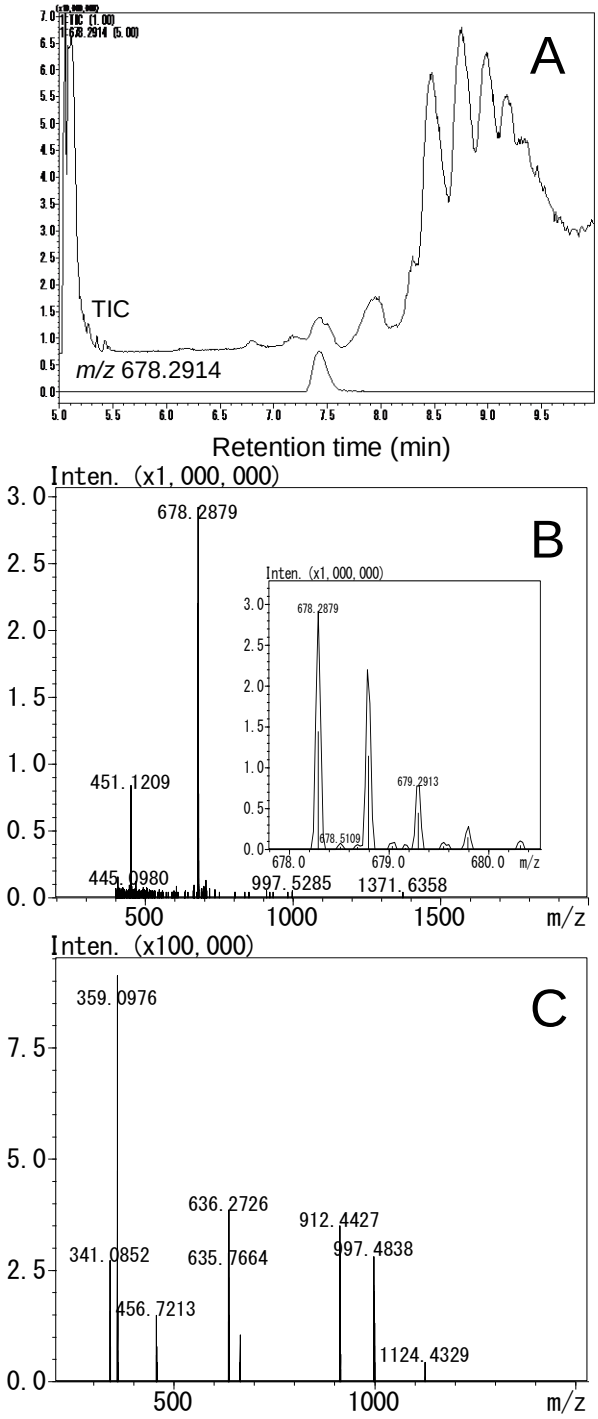

Fig. 48. LC/ESI-MS/MS chromatograms of the B_{12} compounds purified from the bed logs after fruiting of shiitake mushroom (cultivar Kinko-702). A: Total ion chromatogram (TIC) and reconstructed chromatograms of the B_{12} compounds (m/z 678.2914) purified from the bed log b. B: Mass spectrum of the B_{12} compounds purified from the bed log b at 7.4 min (the magnified spectrum ranging from m/z 678 to m/z 680 is shown as an inset in B). C: MS/MS spectrum of the m/z 678.2879 peak of the B_{12} compounds purified from the bed log b.

The compounds purified from the koushin-type fruiting body sample b were eluted as two ion peaks with *m/z* values of 678.2914 (**Fig. 49D**). The mass spectrum of the major peak had a doubly-charged ion with an *m/z* of 677.7737 $[M + 2H]^{2+}$ (**Fig. 49E**). The MS/MS spectrum of the major peak indicated that a monovalent ion with an *m/z* of 359.0988 (the nucleotide moiety of B_{12}) predominated (**Fig. 49F**). These data were completely identical to those of B_{12}[*c*-lactone]. The remaining ion peak with an *m/z* value of 678.2914 was eluted at 7.4 min, and its mass and MS/MS spectra were identical to those of authentic B_{12} (data not shown). These results indicated that the koushin-type dried fruiting body contained authentic B_{12} and B_{12}[*c*-lactone], which was not detected in the other commercially available dried shiitake fruiting bodies.

Shiitake fruiting bodies as a B_{12} source

Consumption of approximately 50 g of dried shiitake fruiting bodies could provide RDA for adults (2.4 μg/day) [23, 139], although ingestion of such large amounts of this mushroom fruiting body on a daily basis is not possible. However, dried shiitake fruiting bodies may be a plant-based source to prevent B_{12} deficiency in vegetarians.

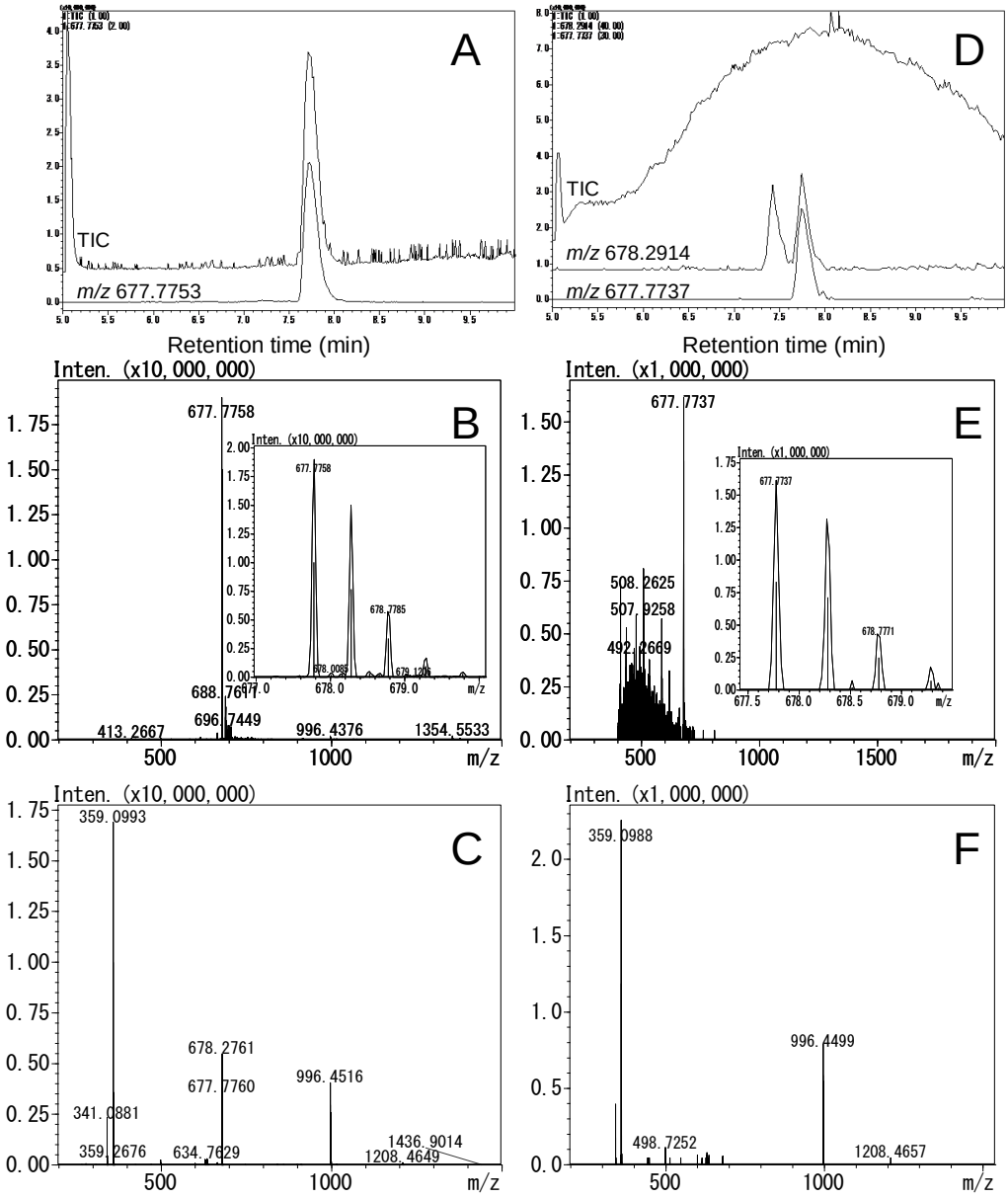

Fig. 49. LC/ESI-MS/MS chromatograms of B_{12} [*c*-lactone] and the B_{12} compounds purified from commercially available dried koushin-type shiitake sample b. A: Total ion chromatogram (TIC) and the reconstructed chromatogram (*m/z* 677.7753) of B_{12} [*c*-lactone]. B: Mass spectrum of prepared B_{12} [*c*-lactone] at 7.7 min (the magnified spectrum ranging from *m/z* 678 to *m/z* 680 is shown as an inset in B). C: MS/MS spectra for the m/z 677.7758 peak of prepared B_{12} [*c*-lactone]. D: TIC and reconstructed chromatograms of the purified B_{12} compounds (*m/z* 678.2914 and *m/z* 677.7737) from dried koushin-type shiitake fruiting body sample b. E: Mass spectrum of the B_{12} compounds purified from the shiitake sample b at 7.7 min (the magnified spectrum ranging from *m/z* 678 to *m/z* 680 is shown as an inset in E). F: MS/MS spectrum for the *m/z* 677.7737 peak of the B_{12} compounds purified from the shitake sample b.

Summary

This study determined the B_{12} content in commercially available dried fruiting bodies of shiitake mushroom, *L. edodes*. The B_{12} contents in dried donko-type fruiting bodies with closed caps (5.61 ± 3.90 μg/100 g dry weight), did not significantly differ from those of dried koushin-type fruiting bodies with open caps (4.23 ± 2.42 μg/100 g dry weight). The bed logs after fruiting of the mushroom also contained the B_{12} levels similar to that in the dried shiitake fruiting bodies. To determine whether the dried shiitake fruiting bodies and their bed logs contained B_{12} or other corrinoid compounds that are inactive in humans, I purified corrinoid compounds using an immunoaffinity column and identified B_{12} using B_{12}-dependent *E. coli* 215 bioautograms and LC/ESI-MS/MS chromatograms. Dried shiitake fruiting bodies rarely contained an unnatural corrinoid B_{12}[*c*-lactone] that is inactive in humans. Given that shiitake mushroom lacks the ability to synthesize B_{12} *de novo*, the B_{12} found in dried shiitake fruiting bodies must have been derived from the bed logs.

Section 3 Characterization of vitamin B_{12} compounds in organic fertilizers containing purple photosynthetic bacteria

Introduction

Mozafar [143] demonstrated that the addition of an organic fertilizer, cow manure, significantly increased the B_{12} content (17.8 ng/g dry weight) in spinach leaves. Biofertilizers are products containing living cells of beneficial microorganisms, which can accelerate and improve plant growth by providing nutritionally important elements (e.g., nitrogen and phosphorus) [158]. Although cyanobacteria are responsible for biological nitrogen (N_2) fixation in flooded rice fields [159], they contain large amounts of pseudo-B_{12} that is inactive in humans [36]. N_2-fixing purple photosynthetic bacteria were reported to have beneficial effects on plant growth [160] and the ability to synthesize B_{12} *de novo* [161]. If biofertilizers containing purple photosynthetic bacteria contain a substantial amount of "true B_{12}", these fertilizers would be useful for enriching B_{12} in plants. However, there is no information on the B_{12} content of biofertilizers containing purple photosynthetic bacteria or whether these biofertilizers contain "true B_{12}" or inactive corrinoid compounds (or both). In this section, I determined the B_{12} content of three biofertilizers containing purple photosynthetic bacteria and characterized the B_{12} compounds found in these biofertilizers using LC/ESI-MS/MS.

Materials and Methods

Materials

B_{12} was obtained from Sigma (St. Louis, MO, USA) and 5-hydroxybenzimdasolyl cyanocobamide (Factor III) was provided by Dr. stüpperich, Ulm University, Germany. The B_{12} assay medium for *L. delbrueckii* subspecies lactis (formerly *L. leichmannii*) ATCC 7830 was obtained form Nissui (Tokyo, Japan). Silica gel 60 TLC aluminum sheets were obtained from Merck (Darmstadt, Germany). A Shimadzu (Kyoto, Japan)

UV-visible spectrophotometer (UV-2550) was used to measure the turbidity of *L. delbrueckii* test cultures with the microbiological B_{12} assay method. Biofertilizers containing purple photosynthetic bacteria were purchased at local markets in Japan. All other reagents used were of the highest purity commercially available.

Extraction and assay of vitamin B_{12}

Each biofertilizer (1 L) was added to the same volume of 5 mmol/L acetate buffer (pH 4.5) containing 0.01% (w/v) potassium cyanide (KCN). B_{12} compounds were extracted as described in **Chapter IV**, **Section 1**.

Bioautography of vitamin B_{12} compounds with vitamin B_{12}-dependent Escherichia coli 215

Bioautography of the B_{12} compounds was done according to the method of Tanioka *et al*. [151].

LC/ESI-MS/MS analysis

B_{12} compounds were purified under the same conditions described above. The purified samples, authentic B_{12}, and Factor III were dissolved in 0.1% (v/v) acetic acid and filtered with a Nanosep MF centrifuge device (0.4 μm, Pall Corp., Tokyo, Japan) to remove small particles. An aliquot (2 μL) of the filtrate was then analyzed using LCMS-IT-TOF coupled with an Ultra-Fast LC system (Shimadzu, Kyoto, Japan). The purified sample was injected in an InterSustain column (3 μm, 2.0 × 100 mm, GL Science, Tokyo, Japan) and equilibrated with 85% solvent A [0.1% (v/v) acetic acid] and equilibrated with 85% solvent B (100% methanol) at 40°C. B_{12} compounds were eluted with a linear gradient of methanol (15% solvent B for 0-5 min, 15%-90% solvent B for 5-11 min, and 90%-15% solvent B for 11-15 min) at a flow rate of 0.2 mL/min. ESI conditions were determined by injecting authentic Factor III or B_{12} into the MS

detector to achieve optimum parameters to detect parent and daughter ions of the B_{12} compound. ESI-MS was operated in positive ion mode with argon as the collision gas. The identification of Factor III (*m/z* 672.272) and B_{12} (*m/z* 678.292) representing $[M+2H]^{2+}$ was confirmed by comparison of the observed molecular ions and the retention times.

Results and Discussion

The amount of B_{12} in three commercially available biofertilizers containing purple photosynthetic bacteria was determined using a microbiological method. No or traces of B_{12} were found in two of the biofertilizers (A and B) tested while the third (C) contained a considerable amount (53.5 μg/L) of the vitamin.

The B_{12} compounds found in biofertilizer C were analyzed with the *E. coli* 215 bioautogram after being separated with silica gel 60 TLC (**Fig. 50**). A concentrated extract of biofertilizer C was indentified as a clear single spot, with an R_f value identical to that of authentic B_{12} but not to that of pseudo-B_{12}, which is inactive in humans. For biofertilizers A and B, no or an indistinct spot was detected. B_{12} compounds were purified from the extracts of biofertilizer C with an immunoaffinity column and then identified by LC/ESI-MS/MS (**Fig. 51**). Hashimoto *et al*. [162] reported that authentic B_{12} ($C_{63}H_{88}CoN_{14}P$; monoisotopic mass 1354.5674) was eluted as a peak with a retention time of 7.30 min. MS results of authentic B_{12} indicated a major doubly-charged ion of *m/z* 678.2937 $[M+2H]^{2+}$, and isotope distribution data supported the determination that B_{12} predominantly formed a doubly-charged ion under the LC/ESI-MS conditions. MS/MS spectrum of B_{12} indicated that the ion of *m/z* 359.0981 was predominantly formed due to the nucleotide moiety of the molecule.

In the case of authentic Factor III ($C_{61}H_{84}CoN_{14}P$; monoisotopic mass 1342.5310), this corrinoid was eluted as a peak with a retention time of 7.14 min. MS of authentic Factor III had a major doubly-charged ion at *m/z* 672.2715 $[M+2H]^{2+}$ (**Fig. 51A and B**). MS/MS spectrum of Factor III indicated that the ion of *m/z* 347.0636 was

predominantly formed due to the nucleotide moiety (**Fig. 51C**).

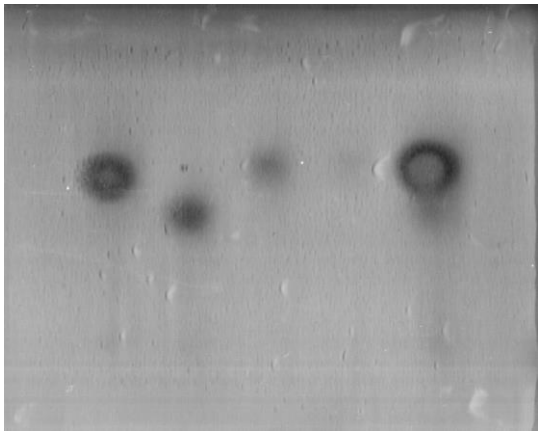

Fig. 50. *Escherichia coli* 215 bioautogram analysis of B_{12} compounds found in commercially available biofertilizers containing photosynthetic purple bacteria. 1) Authentic B_{12}, 2) authentic pseudo-B_{12}, 3) biofertilizer A concentrated extract (5 μL), 4) biofertilizer B concentrated extract (5 μL), and 5) biofertilizer C concentrated extract (2 μL). Data represent typical bioautograms of three independent experiments.

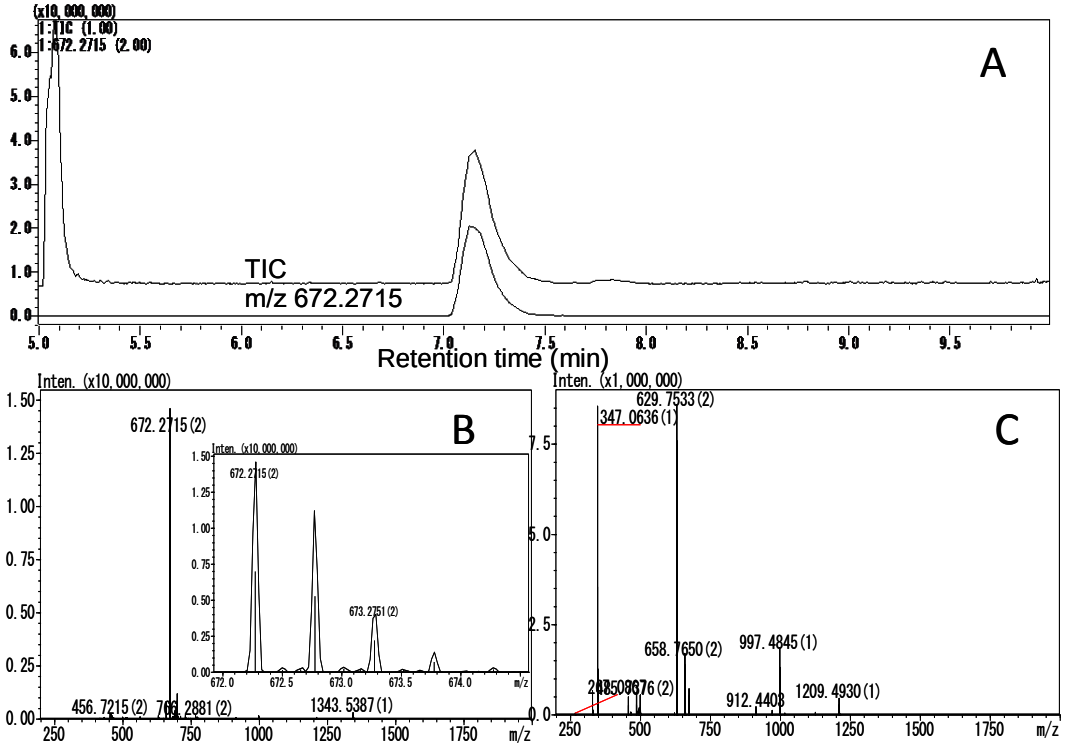

Fig. 51. Liquid chromatography/electrospray ionization mass spectrometry (LC/ESI-MS/MS) chromatograms of authentic Factor III. Factor III was analyzed with LCMS-IT-TOF (Shimadzu) as described in the text. The total ion chromatogram (TIC) of authentic Factor III is shown in panel A. The mass spectrum of authentic Factor III at 7.14 min is shown in panel B; the magnified spectrum from *m/z* 672 to 675 is inserted in the panel. The MS/MS spectrum for the peak of *m/z* 672.2715 from authentic Factor III is shown in panel C.

The purified sample was eluted as several total ion peaks, indicating that impurities still existed (**Fig. 52A**). The ion peaks of *m/z* 672.27 and 678.29 due to Factor III and B_{12}, respectively, were also found and their retention times were identical to those of authentic Factor III and B_{12}. MS at retention times of 7.14 and 7.35 min showed the formation of both Factor III and B_{12} doubly-charged ions of *m/z* 672.2715 (**Fig. 52B**) and 678.2996 (**Fig. 52C**), respectively. MS/MS spectrum of each ion peak was identical to that of authentic Factor III and B_{12} (**Fig. 52D** and **E**). These results indicated that biofertilizer C contained both B_{12} (main) and Factor III (minor). Since the N_2-fixing photosynthetic purple bacterium *Rhodobacter capsulatus*, used as a biofertilizer, has the ability to synthesize B_{12} *de novo* [161], Factor III may be derived from other concomitant bacteria in commercial biofertilizer C (**Fig. 53**).

Despite the detection of B_{12} in one of the biofertilizers tested, in my preliminary experiments, B_{12} was not detected in the lettuce leaves grown with and without biofertilizer C treatment of the soil and leaves once a week for three weeks according to the manufacturer's recommended protocol. These results indicated that commercially available biofertilizers containing purple photosynthetic bacteria are not suitable for B_{12}-enrichment of plants due to the low B_{12} content.

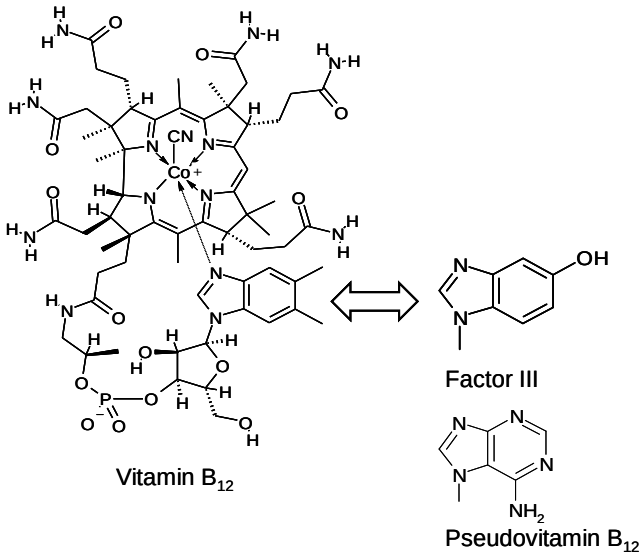

Fig. 52. LC/ESI-MS/MS chromatograms of purified B_{12} compounds from biofertilizer C. TIC and reconstructed chromatograms of *m/z* 678.29 and 672.27 of the purified B_{12} compound are shown in panel A. The mass spectra of the purified B_{12} compound at 7.14 and 7.30 min are shown in panels B and C, respectively; the magnified spectra from *m/z* 672 to 675 and *m/z* 678 to 681 are shown in panels D and E, respectively. The MS/MS spectra for the peak of *m/z* 672.27 and 678.29 from the purified B_{12} compound are shown in panels F and G, respectively.

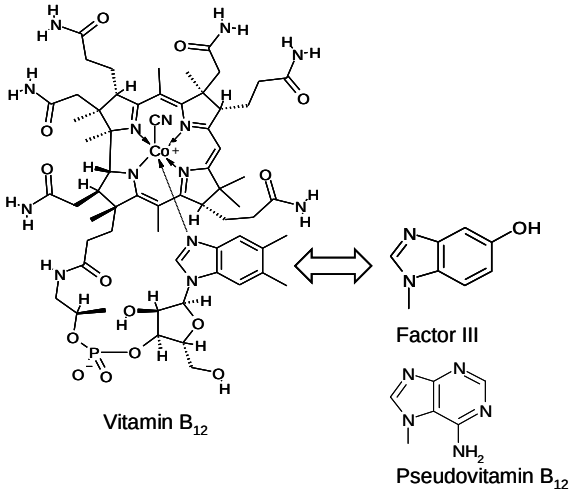

Fig. 53. Corrinoid compounds (vitamin B_{12} and Factor III) found in biofertilizer C containing purple photosynthetic bacteria. Partial structures of Factor III and pseudo-B_{12} showing only that portion of the molecule that differs from B_{12}.

Summary

There is currently no data available about the B_{12} content of biofertilizers containing purple photosynthetic bacteria or whether these biofertilizers contain "true B_{12}" or inactive corrinoid compounds (or both). Therefore, we determined the B_{12} content of three commercially available biofertilizers containing purple photosynthetic bacteria. No or traces of vitamin B_{12} were found in two of the biofertilizer (A and B) tested, while the third (C) contained a considerable amount (53.5 μg /L). To evaluate whether biofertilizer C actually contained B_{12} or other corrinoids inactive in humans, the extracted compounds were purified using an immunoaffinity column and then identified as B_{12} (main) and/or inactive corrinoids (minor, Factor III) using LC/ESI-MS/MS.

Section 4 Production and characterization of vitamin B_{12}-enriched lettuce (*Lactuca sativa* L) grown using hydroponics

Introduction

A large number of people have low serum B_{12} levels that result more commonly from malabsorption of protein-bound B_{12} (food-bound B_{12} malabsorption) rather than pernicious anemia [37]. Food-bound B_{12} malabsorption is found in people with certain gastric dysfunctions, particularly atrophic gastritis with low stomach acid secretion, which prevails in elderly people [38, 39]. As the bioavailability of crystalline (free) B_{12} is not altered in people with atrophic gastritis [163], the Institute of Medicine recommended that most of the RDA (2.4 μg/day) should be obtained by consuming foods fortified with B_{12} or supplements containing B_{12} [23].

Some researchers have attempted to prepare certain B_{12}-enriched vegetables by treating them with a solution containing high levels of B_{12} [146, 147]. This resulted in a significant increase in the amount of B_{12} incorporated into the plants, suggesting that the B_{12}-enriched vegetables may be of special benefit to vegetarians. However, the B_{12} absorbed by the vegetables was not well characterized in these studies.

Lettuce (*Lactuca sativa*) is an annual plant, which is most often grown as a leafy vegetable that is easily cultivated, is a popular vegetable, is commonly used in salads, soups, sandwiches, and wraps, and is a good source of β-carotene, potassium, vitamins, and nutrients [164]. Hydroponic cultivation is an emerging technology that allows better control of water and nutrient supply that improves plant productivity and reduces the use of pesticides [165]. If a sufficient amount of free B_{12} can be incorporated into lettuce leaves grown under hydroponic conditions, it would be an excellent source of free B_{12} for vegetarians and elderly people. In this section, I describe the production and characterization of B_{12}-enriched lettuce leaves cultivated using hydroponics.

Materials and methods

Materials

CN-B_{12} (crystalline N, average purity of 98.1%) prepared for human food supplementation was purchased from DSM Japan (Tokyo, Japan) and used for hydroponic cultivation. CN-B_{12} used as a standard in the bioassay was obtained from Sigma (St. Louis, MO, USA). Pseudo-B_{12} was prepared in our laboratory as described previously [145]. The B_{12} assay medium for *L. delbrueckii* subspecies *lactis* (formerly *L. leichmannii*) ATCC 7830 was obtained from Nissui (Tokyo, Japan), and silica gel 60 TLC aluminum sheets were obtained from Merck (Darmstadt, Germany). A Shimadzu ultraviolet (UV)-visible spectrophotometer (UV-2550; Kyoto, Japan) was used to measure the turbidity of the *L. delbrueckii* test cultures in the microbiological B_{12} assay. All other reagents were of the highest purity commercially available.

Growth conditions of the lettuce leaves

As shown in **Fig. 54**, the experiments were performed in a glasshouse from June to July 2011 (day length approximately 11 h, temperature range 18°C-32°C) at Tottori University, Japan (35° 52' N, 134° 17' E, 3 m above sea level). Seeds of a butter-type head lettuce (*L. sativa* L.) were purchased from Hohoku Seed Co. Ltd. (Tochigi, Japan) and germinated and grown for 24 days in black plastic pots containing sandy soil with an adequate supply of water. Uniform seedlings were then selected, carefully washed, and transferred into 3 L hydroponic lightproof pots (1 plant/pot) containing nutrient solutions (Otsuka House series no. 1 and 2, Otsuka AgriTechno Co., Ltd.) prepared according to the manufacturer’s protocol. The nutrient solutions in these pots were continuously aerated using an air pump, covered with styrene foam to protect against light exposure, and renewed every 5 days. The indicated amounts of CN-B_{12} were added to the nutrient solution 30 days after transplantation. The plants were left for 24 h under these conditions (not light shielded) and harvested. The edible portions of the plants

were weighed, slightly washed with tap water, and lyophilized using a freeze dryer (DC800, Yamato Scientific Co., Ltd., Tokyo, Japan). The dried leaves were stored at -80°C until analysis.

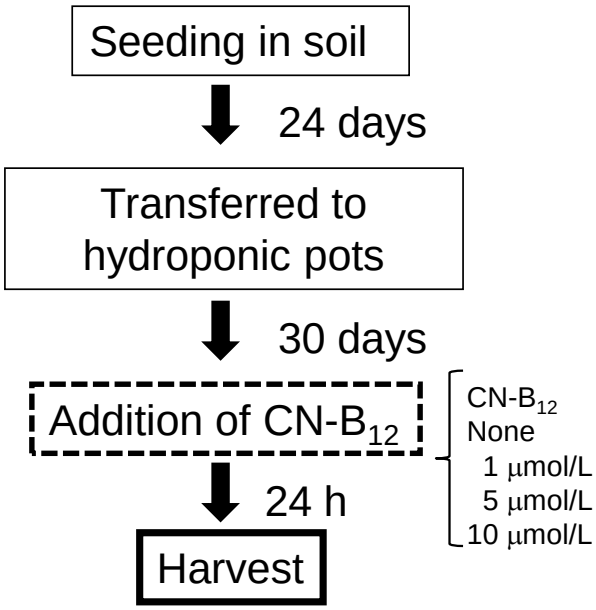

Fig. 54. Outline of the preparation of CN-B_{12}-enriched lettuces using hydroponic cultivation.

Extraction and assay of B_{12}

Two grams of each dried leaf of the various lettuces grown in the presence or absence of CN-B_{12} were used. B_{12} compounds were extracted as described in **Chapter IV**, **Section 1**.

For analysis of coenzyme forms of B_{12}, the compounds were extracted from 2 g of lyophilized powder of CN-B_{12}-enriched lettuce leaves (approximately164.6 ng of B_{12} per gram of fresh weight) as described in **Chapter II**, **Section 2**. All the procedures were performed in the dark.

Stability of CN-B_{12} in the hydroponic nutrient solution

CN-B_{12} was dissolved in the nutrient solution (pH 5.7) at a final concentration of 5 μmol/L. The solution was continuously aerated using an air pump under the same conditions described above and treated at 25°C for 24 h (12 h light/dark cycle; photon flux density 25.4±0.3 μmol/m^2/s) in a CLE-303 cultivation chamber (Tomy Seiko Co., Ltd., Tokyo, Japan). CN-B_{12} was also dissolved in 100 mmol/L KPB (pH 6.2), which had a pH value identical to that of the lettuce leaf homogenate, and then treated under the same conditions. The relative amounts of CN-B_{12} in the treated solutions were expressed as percentages of a CN-B_{12} solution (5 μmol/L) freshly prepared in distilled water.

To determine the stability of aqueous CN-B_{12} during 24 h incubation in a glasshouse, CN-B_{12} was dissolved in 100 mmol/L KPB (pH 6.2) and treated for 24 h in the glasshouse (sunlight; photon flux density 761.7±29.7 μmol/m^2/s). The CN-B_{12} solution was covered with aluminum foil to block sunlight exposure, and it represented the solution treated without sunlight exposure.

The UV-visible spectra of authentic CN-B_{12}, OH-B_{12}, and CN-B_{12} solutions (5 μmol/L each) with or without sunlight exposure were measured at room temperature using a Shimadzu spectrophotometer (UV 2550) and then analyzed by HPLC using a JASCO HPLC apparatus (PU-2080 Plus Pump, UV-2070 Plus Spectrophotometer, DG-2080-53 Degasser, CO-2065 column oven) and CDS ver.5 chromato-data processing system (LAsoft, Ltd. Chiba, Japan). A 20-μL aliquot of each sample was placed on a reversed-phase HPLC column (Wakosil-II 5C18RS, φ 4.6 x 150 mm; particle size 5 μm) and equilibrated at 40 °C with 20% (v/v) methanol containing 1% (v/v) acetic acid at a flow rate of 1.0 mL/min. The B_{12} compounds were isocratically eluted with the same solution and monitored by measuring the absorbance at 361 nm. The retention time of authentic OH-B_{12} and CN-B_{12} was 2.0 and 7.9 min, respectively.

Bioautography of B_{12} compounds with B_{12}-dependent Escherichia coli 215

Bioautography of B_{12} compounds was performed according to the method described by Tanioka *et al*. [151].

Identification of B_{12} compounds by LC/ESI-MS/MS

Samples were prepared under the same conditions described above. The purified B_{12} compounds and authentic CN-B_{12} were dissolved in 50 μL of 0.1% (v/v) acetic acid and filtered using a Nanosep MF centrifuge device (0.4 μm; Pall Corp., Tokyo, Japan) to remove small particles. A 10 μL aliquot of the filtrate was analyzed using an LCMS-IT-TOF system coupled to an Ultra-Fast LC system (Shimadzu, Kyoto, Japan). Each purified corrinoid was injected into an InertSustain column (3 μm, 2.0 × 100 mm; GL Science, Tokyo, Japan) and equilibrated with 85% solvent A [0.1% (v/v) acetic acid] and 15% solvent B (100% methanol) at 40°C. The B_{12} compounds were eluted using a linear gradient of methanol (15% solvent B for 0–5 min, 15%–90% solvent B for 5–11 min and 90%–15% solvent B for 11–15 min) at a flow rate of 0.2 mL/min. The electrospray ion (ESI) conditions were determined by injecting authentic CN-B_{12} into the MS detector to determine the optimum parameters for detecting parent and daughter ions of CN-B_{12}. The ESI-MS was operated in the positive ion mode using argon as the collision gas. The identification of CN-B_{12} (*m/z* 678.291) representing $[M + 2H]^{2+}$ was confirmed by comparison of the observed molecular ions and their retention times.

Sephadex G-50 gel filtration experiment

Free CN-B_{12} was separated from the CN-B_{12}-enriched lettuce leaves using a column (1.4 × 10 cm, econo-pack column, BioRad Laboratories, Hercules, CA, USA) of Sephadex G-50 fine (GE Healthcare UK Ltd., Amersham Place, Buckinghamshire, England) and then assayed. The lettuce leaves (1 g) were extracted in 10 mL of 100 mmol/L KPB (pH 7.0) at 4°C using a mortar and pestle and centrifuged at 10,000 × *g*

for 10 min at 4°C to remove the insoluble material. A 1 mL aliquot of the supernatant was applied to a column equilibrated with 100 mmol/L KPB (pH 7.0). The column was eluted with the same buffer at a flow rate of 1.0 mL/min, and 0.5 mL fractions were collected. Each fraction of the eluate was added to 100 μL of 0.57 mol/L acetate buffer (pH 4.5) and 40 μL of 0.5% (w/v) KCN, vigorously mixed, and boiled in the dark for 30 min. The treated fractions were then centrifuged at 10,000 × *g* for 10 min at 4°C to remove insoluble material, followed by assay of the CN-B_{12} content using the microbiological method. By measuring the absorbance at 280 nm, the macromolecular and free CN-B_{12} fractions were estimated using blue dextran and authentic CN-B_{12}, respectively.

Statistical analysis

Differences in the weight and B_{12} content of the lettuce leaves placed in the nutrient solutions with or without CN-B_{12} for 24 h were analyzed by one-way ANOVA and post-hoc analyses using Tukey's multicomparison test. Experimental data on the stability of CN-B_{12} in aqueous solution were also analyzed using the same tests. These analyses were performed using GraphPad Prism® for Windows version 5.03 (GraphPad Software Inc., La Jolla, CA 92037 USA). Data were expressed as means and standard deviations, with statistical significance defined as $p<0.05$.

Results and discussion

Stability of CN-B_{12} in hydroponic nutrient solution

To evaluate the stability of CN-B_{12} in a hydroponic nutrient solution, CN-B_{12} was dissolved in the nutrient solution (pH 5.9) and treated at 25°C for 24 h with or without 12 h light exposure (room fluorescent lighting; photon flux density 25.4 ± 0.3 μmol/m^2/s). No significant decrease in CN-B_{12} concentration was observed in both

solutions treated with or without light exposure (**Fig. 55**). The nutrient solutions were hardly exposed to light because hydroponic lightproof pots were covered with styrene foam.

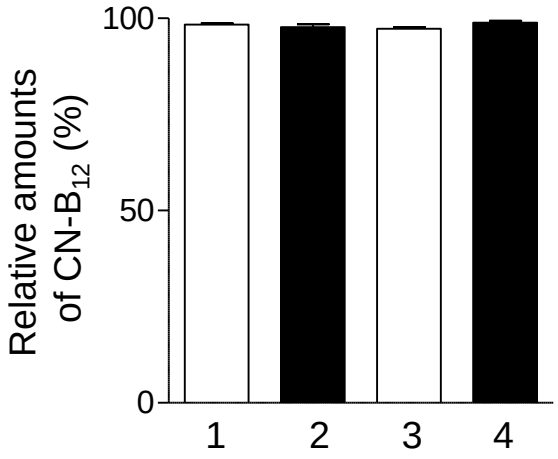

Fig. 55. Stability of CN-B_{12} in the hydroponic nutrient solution. CN-B_{12} was dissolved in the nutrient solution at a final concentration of 5 μmol/L. The solution was continuously aerated and treated with (1) or without (2) light exposure (12 h light/dark cycle) at 25 °C for 24 h. CN-B_{12} was also dissolved in 100 mmol/L KPB (pH 6.2), which had a pH value identical to that of the lettuce leaf homogenate, and was treated with (3) or without (4) light exposure (12 h light/dark cycle) under the same conditions. The CN-B_{12} solution was covered with aluminum foil to block light exposure and represented the solution treated without light exposure. The CN-B_{12} content of these samples (20 μL each) was analyzed using C18 reversed-phase HPLC. The relative amounts of CN-B_{12} in the treated solutions were expressed as percentages of the 5 μmol/L CN-B_{12} solution freshly prepared in distilled water. The data represent typical HPLC elution patterns from three independent experiments.

When CN-B_{12} was also dissolved in 100 mmol/L KPB (pH 6.2), which had a pH value identical to that of the lettuce leaf homogenate, and treated under the same conditions, CN-B_{12} was found to be stable in aqueous solution under the conditions. These results indicated that the procedures for preparation of CN-B_{12}-supplemented nutrient solution and subsequent transplantation of lettuce plants could be performed under fluorescent light.

However, when the CN-B_{12} solutions (pH 6.2) were treated for 24 h in the glasshouse (sunlight; photon flux density 761.7 ± 29.7 μmol/m^2/s), the color of these CN-B_{12} solutions slightly changed to that of the solution containing authentic CN-B_{12}

treated without sunlight exposure. However, the UV-visible spectrum of the sunlight-exposed CN-B_{12} (**Fig. 56A-4**) was not identical to that of authentic CN-B_{12} (absorption maxima at 361 and 550 nm) (**Fig. 56A-1**) but was similar to that of authentic OH-B_{12} (absorption maxima at 351 and 525 nm) (**Fig. 56A-2**). During reversed-phase HPLC, the sunlight-treated CN-B_{12} was eluted as two peaks [main (90.8 ± 0.4%) and minor (4.7 ± 0.7%) with retention times of 2.0 and 7.9 min, respectively]. These retention times were identical to those of authentic OH-B_{12} and CN-B_{12}, respectively (**Fig. 56B-1**, **2**, and **4**). The UV-visible spectrum and retention time of the CN-B_{12} solution treated without sunlight exposure remained unchanged (**Fig. 56A-3** and **B-3**). These results indicated that CN-B_{12} was converted to OH-B_{12} with CN^- of the corrin ring being replaced by H_2O owing to sunlight exposure. Ahmad *et al*. [166] demonstrated that CN-B_{12} was readily photolyzed in an aqueous solution to produce OH-B_{12} and that light-induced photolysis of CN-B_{12} occurred in a pH-dependent manner (i.e., a fast decrease at pH 4.5-6.5 and constant rate at pH 6.5-8.5). It has also been reported that OH-B_{12} is readily converted to coenzyme forms of B_{12} and is therefore more effective in B_{12} deficiency than in CN-B_{12} [167].

These results indicated that this CN-B_{12} reagent would be useful for the preparation of CN-B_{12}-enriched lettuce leaves cultivated using hydroponics.

B_{12} content of lettuce leaves 24 h after the plants were placed in nutrient solutions containing various concentrations of CN-B_{12}

Lettuces grown for 30 days in hydroponic culture were treated with the indicated amounts of CN-B_{12} for 24 h and then harvested (**Fig. 54**). The B_{12} concentration of the lettuce leaves significantly increased CN-B_{12} concentration up to 5 μmol/L (**Table 13**). No B_{12} was detected in lettuce leaves placed in a solution without CN-B_{12}. Although fresh weights (per plant stock) of lettuces appear to increase depending on CN-B_{12} concentrations, there is no significant difference in weights of the treated lettuces, except for control (no addition of CN-B_{12}) versus 10 μmol/L CN-B_{12}-supplemented

lettuces. These results indicated that although lettuce plants do not require B_{12} for growth, they can take up and concentrate B_{12} in their leaves. The B_{12} content of lettuce leaves may be controlled, to some extent, by changing the CN-B_{12} concentration in the nutrient solution. Because lettuce leaves treated with 1 μmol/L CN-B_{12} contained 1.3 ± 0.6 μg of B_{12} per total fresh weight (g) of plant stock, consumption of 2 stocks of these plants would supply the RDA for adults (2.4 μg/day). For lettuce leaves treated with 5 μmol/L CN-B_{12} (6.8 ± 3.4 μg of B_{12} per plant stock), consumption of only 2 or 3 leaves would be sufficient to meet the RDA.

These data showed that lettuce plants could take up only 0.03% of the CN-B_{12} contained in the 1 and 5 μmol/L solutions and that the CN-B_{12} uptake ratio was reduced to 0.02% in the 10 μmol/L CN-B_{12} solution. These results indicated that the CN-B_{12}-supplemented nutrient solution was reused several times during hydroponic cultivation.

Characterization of CN-B_{12} absorbed by lettuce leaves

To evaluate whether CN-B_{12} absorbed by the leaves was converted to other corrinoid compounds (i.e., pseudo-B_{12}, OH-B_{12}, coenzyme forms of B_{12}, and others), B_{12} in the leaves was extracted with or without KCN treatment that converts various B_{12} compounds with different upper ligands (e.g., OH-B_{12} and B_{12} coenzymes) to CN-B_{12} and then analyzed using a B_{12}-dependent *E. coli* 215 bioautogram after separation on silica gel 60 TLC. The KCN-treated extract of B_{12}-enriched leaves (approximately 164.6 ng of B_{12} per g of fresh weight) produced a single clear spot with an R_f value identical to that of the authentic CN-B_{12} but not pseudo-B_{12}, an inactive form in humans (**Fig. 57A**).An extract treated without KCN produced a single clear spot with a R_f value (0.63) identical to that of authentic CN-B_{12} (**Fig. 57B**) but not other B_{12} compounds [R_f values: OH-B_{12} (0.05), AdoB_{12} (0.53), and CH_3-B_{12} (0.67)].

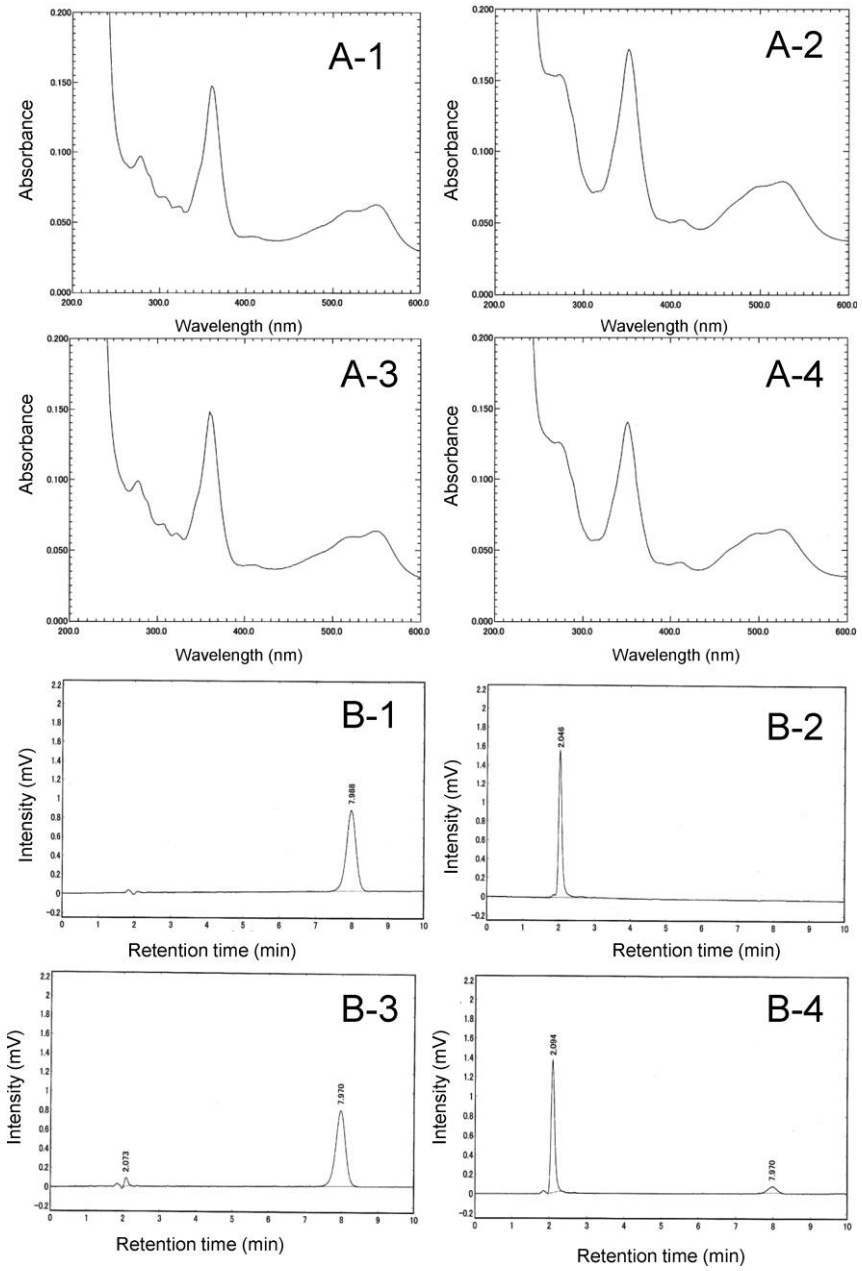

Fig. 56. Photolysis of CN-B_{12} in aqueous solution under glasshouse conditions. CN-B_{12} was dissolved in 100 mmol/L KPB (pH 6.2), which had a pH value identical to that of the lettuce leaf homogenate, and was treated with or without sunlight exposure under glasshouse conditions. The CN-B_{12} solution was covered with aluminum foil to block sunlight exposure and used as the solution treated without sunlight exposure. The UV–visible spectra of authentic CN-B_{12} (A-1), OH-B_{12} (A-2), and CN-B_{12} solutions treated with (A-4) or without (A-3) sunlight exposure (5 μmol/L each) were measured using a Shimadzu spectrophotometer. The authentic CN-B_{12} (B-1), OH-B_{12} (B-2), and CN-B_{12} solutions treated with (B-4) or without (B-3) sunlight exposure (20 μL each) were analyzed by HPLC and monitored by measuring the absorbance at 361 nm. The data represent typical ultraviolet–visible spectra and HPLC elution patterns from three independent experiments.

Table 13. Vitamin B_{12} content of leaves of lettuce plants placed for 24 h in nutrient solutions supplemented with different concentrations of CN-B_{12}[a]

		B_{12} content	
	fresh wt of plant stock* (g)	μg/total fresh wt of plant stock	ng/g fresh wt
none	28.8 ± 3.8[a]	ND	ND
addition of CN-B_{12}			
1.0 μmol/L	36.1 ± 8.5[ab]	1.3 ± 0.6[a]	38.6 ± 22.5[a]
5.0 μmol/L	40.3 ± 3.1[ab]	6.8 ± 3.4[b]	164.6 ± 74.7[b]
10.0 μmol/L	46.7 ± 3.2[b]	7.2 ± 0.8[b]	154.9 ± 26.7[b]

[a]The edible portions (leaves)* of the treated lettuces were weighed and lyophilized, followed by extraction of B_{12} and assay using the microbiological method. Values are expressed as the mean ± SD (n=3). The letters define statistically significant differences ($p < 0.05$). ND, undetectable.

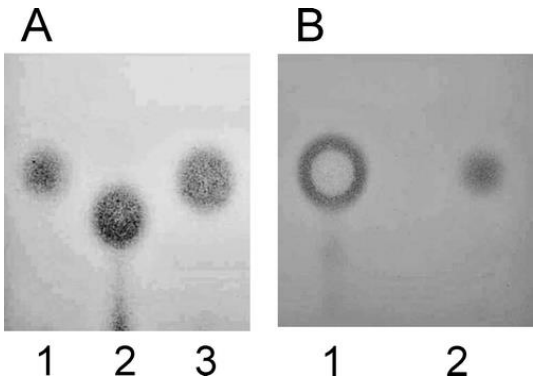

Fig 57. B_{12}-dependent *E. coli* 215 bioautogram after silica gel 60 TLC of B_{12} extracts of enriched leaves. The B_{12} compounds were extracted from the leaves in the presence (A) or absence (B) of KCN, separated on silica gel 60 TLC, and visualized using B_{12}-dependent *E. coli* 215. Lanes: (A) 1, authentic CN-B_{12}; 2, authentic pseudo CN-B_{12}; 3, lettuce leaf extract; (B) 1, authentic CN-B_{12}; 2, lettuce leaf extract. The data represent a typical bioautogram from three independent experiments.

These B_{12} extracts treated with or without KCN were further purified using a B_{12} immunoaffinity column and analyzed by LC/ESI-MS/MS. As shown in **Fig 58**, the mass spectra of authentic CN-B_{12} had a major doubly charged ion (precursor ions) with an *m/z* value of 678.2895 $[M+2H]^{2+}$ in the LC/ESI-MS conditions employed (**Fig. 58A** and **B**). MS/MS spectra analysis indicated that the ions with an *m/z* value of 359.1003 was attributable to the nucleotide moiety of authentic CN-B_{12}, whereas the ion with an

m/z value of 997.4858 was attributable to a corrin ring moiety that also formed in authentic CN-B_{12} (**Fig. 58C**).

As shown in the LC/ESI-MS/MS chromatograms of the KCN-treated extract, B_{12} compounds were eluted at a single ion peak with a retention time of 7.3 min (*m/z* 678.2914) (**Fig. 58D**). The retention time of the ion peak with an *m/z* value of 678.2914 was identical to that of authentic CN-B_{12}. The MS and MS/MS spectra of the ion peak were also identical to those of authentic CN-B_{12} (**Fig. 58E** and **F**). Moreover, LC/ESI-MS/MS chromatograms of the B_{12} extract without KCN were identical to those of authentic CN-B_{12} (**Fig. 58G**, **H**, and **I**). These results indicated that the CN-B_{12} absorbed by lettuce leaves was not changed to any other corrinoids, although CN-B_{12} was readily converted to OH-B_{12} in an aqueous solution under the same conditions (**Fig. 56A-4** and **B-4**). These findings suggested that lettuce plant tissues have the ability to block photolysis of aqueous CN-B_{12} from sunlight exposure. These results and the fact that higher plants have neither the ability to synthesize B_{12} *de novo* nor an absolute requirement for the vitamin to promote growth also indicates that the accumulation of CN-B_{12} by leaves has no effect on the physiological functions of lettuce plants.

To evaluate whether CN-B_{12}-enriched lettuce leaves contained "free CN-B_{12}" or "protein-bound CN-B_{12}," homogenates of selected leaves were analyzed using Sephadex G-50 gel filtration. The results demonstrated that the majority of CN-B_{12} present in the leaves (86%) was recovered in the free CN-B_{12} fractions (**Fig. 59B**). These results suggest that CN-B_{12}-enriched lettuce leaves are an excellent source of free CN-B_{12}.

Table 14 shows a comparison of B_{12} contents in CN-B_{12}-enriched lettuce and other vegetables treated with solutions containing high concentrations of CN-B_{12}. Mozafar and Oertli [147] reported that uptake of CN-B_{12} by soybean leaves did not reach saturation even at an extremely high concentration of B_{12} (3.2 μmol/L) in the nutrient solution. A previous study also showed that when soybean seedlings were placed in solution containing 10 μmol/L of CN-B_{12} for 24 h, the leaves contained a significantly higher level of B_{12} (9.8 μg/g fresh weight).

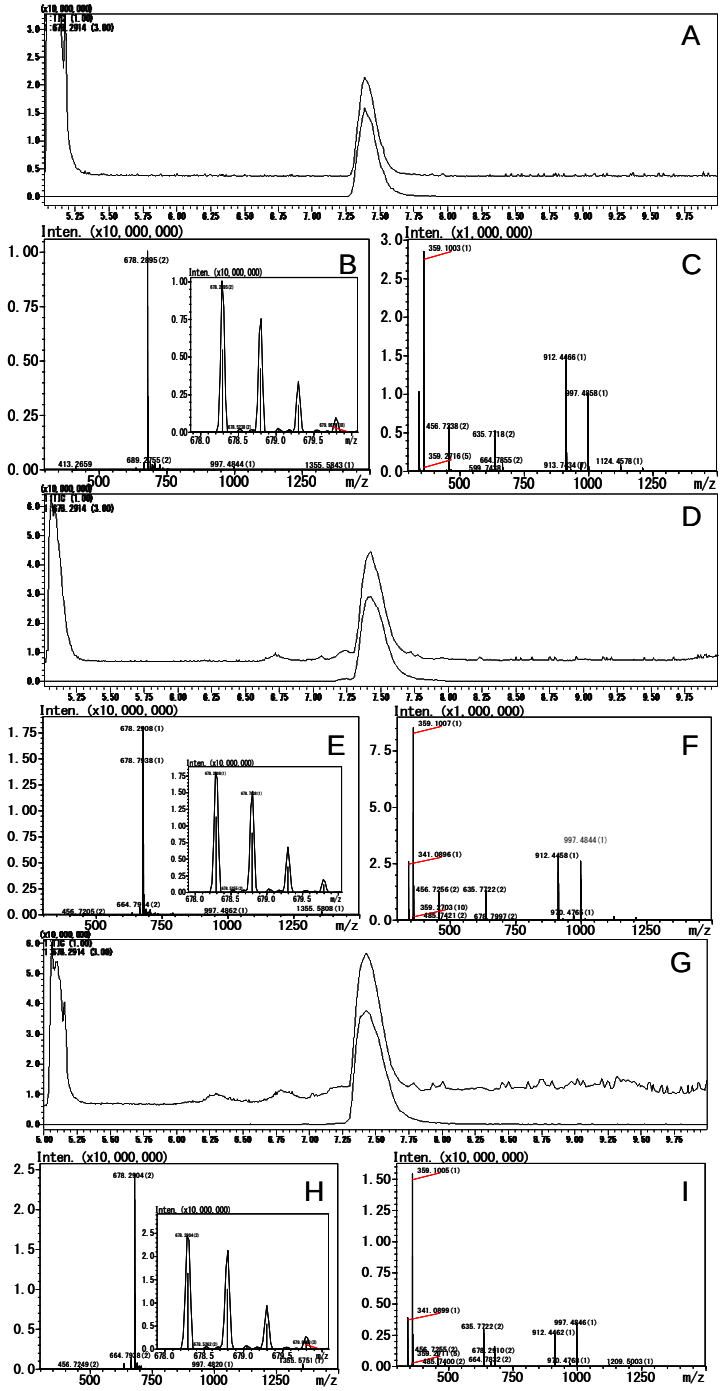

Fig. 58. LC/ESI-MS/MS chromatograms of authentic CN-B_{12} and leaf extracts treated with or without KCN. CN-B_{12} was analyzed using an LCMS-IT-TOF system (Shimadzu) as described under Materials and Methods. The total ion chromatogram (TIC) of authentic CN-B_{12} is shown in panel A. Panels D and G show the TICs and reconstructed chromatograms of the purified B_{12} compounds (*m*/*z* 678.2914) from the leaf extracts with and without KCN, respectively. The mass spectra of authentic CN-B_{12} and B_{12} compounds purified from the extracts treated with and without KCN at 7.30 min are shown in panels B, E, and H, respectively (the magnified spectrum ranging from *m*/*z* 678 to 680 is shown as an inset in each panel). The MS/MS spectra for the *m*/*z* 678.29 peak of authentic CN-B_{12} and B_{12} compounds purified from the extracts treated with and without KCN are shown in panels C, F, and I, respectively.

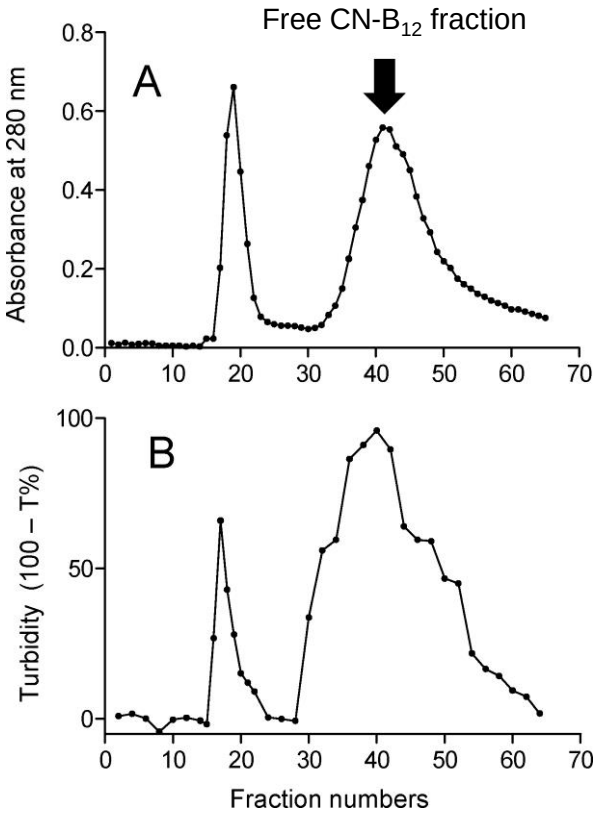

Fig. 59. Elution patterns of B_{12}-active compounds in leaves analyzed using Sephadex G-50 gel filtration: authentic blue dextran and CN-B_{12} mixture (A) and CN-B_{12}-enriched lettuce leaves (B). The macromolecular and free CN-B_{12} fractions were estimated by measuring the absorbance at 280 nm of blue dextran and authentic CN-B_{12}, respectively. The B_{12} content in the B_{12}-enriched lettuce leaves was assayed using the microbiological method. The data represent a typical elution pattern of the B_{12}-active compound of lettuce leaves from four independent experiments.

That study also showed that Japanese radish sprouts (kaiware daikon) had significant increases in B_{12} content (1.3 μg/g fresh weight) after their seeds were soaked for 6 h in a solution containing 200 μg/mL (147.6 μmol/L) of CN-B_{12} [148]. In the present study, I demonstrated that the B_{12} content in lettuce leaves (approximately 164.6 ng/g fresh weight) reached saturation at a CN-B_{12} concentration of 5 μmol/L. Because vegetables are generally a good source of dietary fibers, vitamins, and minerals [164], consumption of a large amount of vegetables enriched with a low level of CN-B_{12} would be better for human health than that of a small amount of a vegetable with a high

level of CN-B_{12}. Consumption of 62.2 g of CN-B_{12}-enriched lettuce leaves (approximately 38.6 ng/g fresh weight) grown in a low CN-B_{12} (1 μmol/L)-supplemented nutrient solution supplies the RDA for B_{12} of 2.4 μg/day. In addition, these leaves provide the daily intake of other nutrients, particularly folic acid and B_6, which are essential for normal homocysteine metabolism and for preventing disorders such as atherosclerosis and neuropathy [168]. The use of low levels of CN-B_{12} in nutrient solutions would also lower the production costs of the enriched plants. Indeed, the cost of CN-B_{12} for the preparation of 1 stock of B_{12}-enriched lettuce leaves grown in the low CN-B_{12} (1 μmol/L)-supplemented nutrient solution was calculated to be only approximately ¥ 6 (U.S. $0.06) under the experimental conditions used. If the nutrient solution is reused several times, this cost would be reduced significantly. Therefore, the cost for adding CN-B_{12} would not a major factor when preparing CN-B_{12}-enriched plants.

Table 14. Comparison of the B_{12} content in various B_{12}-enriched plants following treatment with CN-B_{12}-supplemented solution.

		B_{12} content			
		solution	(μg/g fresh wt)[a]		
plant	method	μmol/L	(ng/g fresh wt)[b]		ref
soybean leaves	hydroponic culture for 24 h	10.0	9.8[a]	(0.2 g)	150
radish sprout	seed soaking for 6 h	18.4	0.2[a]	(12.0 g)	151
		147.6	1.3[a]	(1.9 g)	
lettuce leaves	hydroponic culture for 24 h	1.0	38.6[b]	(62.2 g)	this study
		5.0	164.6[b]	(14.6 g)	
		10.0	154.9[b]	(15.5 g)	

The mean B_{12} values of soybean leaves and radish sprouts were calculated from the cited references. The amount of each enriched fresh plant that provides the adult RDA for B_{12} of 2.4 μg/day is shown in parentheses.

On the based on the fact that approximately 30% of people older than 50 years are estimated to have atrophic gastritis with low acid secretion in the stomach and decreased bioavailability of B_{12} from food (food-bound B_{12} malabsorption) [38, 39], the Institute of Medicine recommended that the majority of the RDA should be obtained

from foods fortified with B_{12} or supplements containing B_{12} [23]. The results of this study indicate that CN-B_{12}-enriched lettuce leaves would be an excellent source of free CN-B_{12}, particularly for vegetarians and elderly people.

Summary

When lettuces (*Lactuca sativa* L.) grown for 30 days in hydroponic culture were treated with various concentrations of CN-B_{12} for 24 h, its content in their leaves increased significantly from nondetectable to 164.6 ± 74.7 ng/g fresh weight. This finding indicated that consumption of only two or three of these fresh leaves is sufficient to meet the RDA for adults of 2.4 μg/day. Analyses using a B_{12}-dependent *E. coli* 215 bioautogram and LC/ESI-MS/MS demonstrated that the CN-B_{12} absorbed from the nutrient solutions by the leaves did not alter any other compounds such as coenzymes and inactive corrinoids. Gel filtration indicated that most (86%) of the CN-B_{12} in the leaves was recovered in the free CN-B_{12} fractions. These results indicated that CN-B_{12} enriched lettuce leaves would be an excellent source of free CN-B_{12}, particularly for strict vegetarians or elderly people with food-bound B_{12} malabsorption.

Chapter V
Conclusion

B_{12} is taken up by living cells and then converted into two coenzyme forms, $AdoB_{12}$ and CH_3-B_{12}, which function as the coenzymes for mitochondrial MCM and cytosolic MS, respectively. MCM catalyzes the coversion of (*R*)-methylmalonyl-CoA to succinyl-CoA, an intermediate of TCA cycle, and plays important roles in catabolic pathways of branched chain-amino acids (Val, Leu, Ile and Thr), odd-numbered fatty acids, cholesterol, and thymine. MS catalyzes the synthesis of Met from Hcy with CH_3-THF and plays important roles in sulfur amino acid, folate, polyamine, and SAM metabolisms. B_{12} deficiency results in growth retardation, metabolic disorders, and neuropathy in mammals. However, the underlying disease mechanisms are poorly understood; in particular, further research is required to elucidate the precise mechanisms of B_{12}-deficient neuropathy in elderly people and vegetarians, high risk populations. To investigate the precise mechanisms of these B_{12}-deficient symptoms, B_{12}-deficient rat have been used as a human model animal. However, they require for long periods to make them B_{12} deficiency. Therefore, the lack of robust B_{12}-deficient animal models such rats has limited investing animal models.

C. elegans has been widely used as a model organism for studying a variety of biological processes [34]. In addition, the enzymes involved in human methylmalonic aciduria caused by B_{12} deficiency have been studied in *C. elegans* [41, 42].

In **Chapter II, section 1,** I described the preparation and characterization of B_{12}-deficient *C. elegans* grown under B_{12}-deficient conditions. *C. elegans* absolutely required B_{12} for normal growth and B_{12} functioned as coenzymes of MCM and MS (**Fig. 8**). Under B_{12}-deficient conditions, the B_{12} content of the worms decreased gradually over four generations (**Fig. 7**). The B_{12} concentration in five generations (F5) worms was only 4% compared with that in the control worms. Worms grown under B_{12}-deficient conditions for five generations (15 days) showed the accumulation of MMA and Hcy as well as B_{12}-deficient mammals (**Fig. 8A** and **B**). Furthermore, MCM

and MS activities were significant decreased in worms grown under B_{12}-deficient conditions (**Fig. 8E** and **F**). Dietary B_{12} deprivation over five generations leads to a significantly decreased B_{12} status in *C. elegans*. B_{12}-deficient worms showed the decreased egg-laying capacity (infertility), the prolonged life cycle (growth retardation), and reduced lifespan. These phenotypes resemble the consequences of B_{12} deficiency in mammals (**Fig. 9**).

If development of animal models of B_{12} deficiency is facilitated by the use of a potent inhibitor of B_{12}-dependent enzymes, B_{12}-deficient animals would be prepared in a short time. The information that ribose-5'-carbamate alkylamine B_{12} derivatives show high-affinity binding of IF [45] and lack detectable biological activity in certain B_{12}-dependent microorganisms has caught my attention and I am developing a research for these compounds. Furthermore, B_{12} dodecylamine derivatives significantly decreased the levels of B_{12}-dependent enzymes in mammalian cells cultured *in vitro.*

As shown in **Chapter II**, **section 2**, CN-B_{12} dodecylamine derivative competitively inhibited the B_{12}-dependent enzymes MCM and MS of *C. elegans* (**Fig. 14**). The B_{12} concentration of worms grown in the presence of the CN-B_{12} derivative was only 35% compared with that of control worms (**Table 2**). In contrast, the CN-B_{12} dodecylamine derivative was absorbed and significantly accumulated by worms grown in the presence of the CN-B_{12} derivative (**Table 2**). These results suggest that the CN-B_{12} dodecylamine derivative did not inhibit the uptake of B_{12} in the intestine, but it was readily accumulated in worms and significantly decreased their B_{12} concentrations (**Table 2**). The CN-B_{12} dodecylamine derivative accumulated by worms was not converted to any other B_{12}-related compound, including its coenzyme forms (**Fig. 12**). When *C. elegans* was grown for 3 days in the presence of the CN-B_{12} dodecylamine derivative, MMA and Hcy levels were significantly increased compared with those of the control worms (**Fig. 13**). The increased MMA and Hcy levels were identical to those of B_{12}-deficient worms (**Fig. 13**). These results show that the worms developed severe B_{12} deficiency when they were treated with the CN-B_{12} dodecylamine derivative for only 3 days. These results indicate that B_{12}-deficient *C. elegans* was readily prepared by the feeding of

B_{12}-limited diet or CN-B_{12} dodecylamine derivative, a potent inhibitor of B_{12}-dependent enzymes.

B_{12}[*c*-lactam], a B_{12} analogue with a modification of side chain of C-ring, has been reported to antagonize B_{12} in the cultured HL 60 cells [43]. Subcutaneous administration of OH-B_{12}[*c*-lactam] to rats has indicated that the analogue has the ability to act as a potent inhibitor of the mammalian B_{12}-dependent enzymes to achieve B_{12} deficiency [44]. However, considerably high concentration of OH-B_{12}[*c*-lactam] must be administrated for several weeks with osmotic mini pumps in order to prepare B_{12}-deficient rats because IF hardly binds OH-B_{12}[*c*-lactam]. As described above, CN-B_{12} dodecylamime derivative exerted inhibitory effects against both B_{12}-dependent enzymes in *C. elegans*. The dodecylamine derivative-treated worms developed severe B_{12} deficiency in approximately 3 days. If the CN-B_{12} alkylamine derivatives act as potent inhibitors of mammalian B_{12}-dependent enzymes *in vivo*, B_{12}-deficient animals would be readily prepared by oral administration of the derivative.

When the mammalian cultured cells were treated with CN-B_{12} alkylamine derivatives in preliminary experiments, MCM and MS activities were not inhibited. Therefore, I prepared OH-B_{12} alkylamine derivatives and characterized the derivatives as potent inhibitors of the B_{12}-dependent enzymes in the mammalian cultured cells (**Chapter II**, **section 3**). Hexylamine, dodecylamine, and hexadecylamine derivatives of OH-B_{12} (1.0 μmol/L) were evaluated as B_{12}-dependent enzyme inhibitors in total and holo-MCM and -MS activities of the COS-7 cells grown in 0.1 mmol/L OH-B_{12}-supplemented medium (**Fig. 23**). All alkylamine derivatives did not affect the enzyme activity of total MCM (holo and apo-enzymes), but significantly inhibited the enzyme activity of the holo-MCM. While the addition of each alkylamine derivative showed the same degrees of inhibition in the enzyme activities of both total and holo-MS. The dodecylamine and hexadecylamine derivatives are stronger inhibitors in both holo-enzymes (about 30% and 45% activities of MCM and MS of the control cells, respectively) than the hexylamine derivative. McEwan *et al*. [45] have demonstrated that the dodecylamine derivative of B_{12} can bind IF considerably (36% of intact B_{12}),

but hexadecylamine derivative cannot. Therefore, OH-B_{12} dodecylamine derivative was selected for further experiments. One μmol/L OH-B_{12} dodecylamine derivative could inhibit significantly both total and holo-MS enzyme activities (about 47% and 45% activity of the control, respectively, in the presence of 1.0 μmol/L OH-B_{12}) (**Fig. 25**), but did not affect any holo-MCM activity (**Fig. 24**). The OH-B_{12} dodecylamine derivative could not inhibit the MS protein level, but inhibit MS enzyme activity (**Fig. 26**). These results indicate that the dodecylamine derivative of OH-B_{12} acts as a potent inhibitor of the B_{12}-dependent MS. Since the OH-B_{12} dodecylamine derivative is simply prepared over considerably high yield (~50%) relative to OH-B_{12}[*c*-lactam], the dodecylamine derivative would be a useful tool to prepare B_{12}-deficient mammalian cells and to elucidate the metabolic disorders caused by the reduced enzyme activity of MS which exerts an important influence on the cellular metabolisms. Moreover, B_{12} dodecylamine derivative shows high affinity binding of IF [45], suggesting that B_{12} deficiency in mammals may be readily induced by oral or intravenous administration of this compound.

As shown in **Chapter II**, **section 1**, B_{12} is essential for *C. elegans* growth and that prolonged B_{12} deficiency induces a number of phenotypes, including decreased egg-laying capacity (infertility), prolonged life cycle (growth retardation), and a reduced lifespan. Therefore, I propose that *C. elegans* is an ideal model organism for investigating the mechanisms driving such B_{12}-deficient phenotypes, as B_{12} deficiency can be induced in this animal in only 15 days. **Table 15** shows properties of B_{12}-deficient *C. elegans* and previously reported other B_{12}-deficient model animals. Mammals (i.e. rat) have considerably long lifespan and require for long periods to make them B_{12} deficiency. Thus, mammals are hard to use in studying the mechanisms of infertility, growth retardation, and lifespan. *C. elegans* is widely used as a model organism for studying the mechanisms of fertilization [68] and embryonic cell division [69]. Moreover, *C. elegans* is often used for understanding human brain and neuronal disorders [70] in addition to the effects of certain molecules on learning and memory [71]. The nervous system of *C. elegans* is composed of only 302 neurons and their

neural connections are extensively studied [96] and it is difficult to analyze the mechanisms of mammalian neurological functions because of their highly-integrated nervous systems composed of numerous and different nerve cells. However, bioinformatics analyses indicate that *C. elegans* does not have any orthologs of three B_{12}-transport proteins (HC, IF, and TC II) involved in human gastrointestinal absorption and subsequent blood circulation of B_{12}. Thus, *C. elegans* is not suitable for use as a model organism to study the mechanisms of some human B_{12}-deficient disease phenotypes, such as megaloblastic anemia, dysfunctions of intestinal absorption, and transport of B_{12}. These observations indicate *C. elegans* may become a suitable organism and a powerful new tool for the study of B_{12}-deficient human diseases such as infertility [58, 59, 61], fetal death [62, 72], neuropathy [73], and cognitive impairment [74].

Table 15. Characterization of *C. elegans* as a B_{12}-deficient animal model.

	Mammals	*C. elegans*
Preparation periods	△ [21] 100 days	○ [This study] 15 days
B_{12}-dependent enzymes	○ [21, 61] MCM,MS	○ [This study] MCM,MS
B_{12} absorption	○ [169]	× Lack of B_{12}-transport proteins
Infertility	△ [21] Long periods	○ [68] 15 days
Growth retardation	△ [21] Long periods	○ [52] 15 days
Lifespan	△ [170] 3 years	◎ [53] 20-30 days
Neurologic function	△ [171] Complex	◎ [71] Simple

During B_{12} deficiency, the failure of the B_{12}-dependent Met biosynthesis leads to accumulation of Hcy [84], which has pro-oxidant activity [84] and can activate NADPH oxidase to generate ROS [85]. NADPH oxidase is simultaneously stimulated by SAH accumulated by B_{12} deficiency [88]. On the other hand, one of RNS, NO, can inhibit both MCM and MS activities [89, 90]. These observations suggest that B_{12} deficiency disrupts cellular redox homeostasis to induce oxidative stress, which is implicated in various human diseases [88] including atherosclerosis and neurodegenerative diseases. Such diseases are major symptoms of B_{12} deficiency, although the underlying disease mechanisms are poorly understood. The nervous system of *C. elegans* is composed of 302 neurons, and their neural connections are studied extensively [96]. Worms sense various chemicals by sensory neurons and show several forms of plasticity. Worms subjected to prolonged exposure to attractive salt (NaCl) under starvation conditions show a dramatic reduction of chemotaxis to NaCl and eventually show a negative chemotaxis. Exposure to NaCl in the presence of food does not lead to a reduction of chemotaxis, suggesting that worms change their behavior by integrating two stimuli, NaCl and starvation [97]. Tomioka *et al*. [94] demonstrated that the insulin/PI 3-kinase pathway regulates this NaCl chmotaxis memory/learning in worms.

In **Chapter III**, **section 1**, I used this model animal to clarify how much oxidative stress is induced during B_{12} deficiency and then whether such oxidative stress leads to oxidative damages of cellular components.

H_2O_2 and NO contents increased approximately twice greater in the B_{12}-deficient worms than in the control worms (**Table 5**). The specific activities of NADPH oxidase and NOS in a worm cell homogenate were significantly increased during B_{12} deficiency. Both MDA (as a lipid peroxidation) and protein carbonyl (as a protein modification) levels were approximately twice greater in B_{12}-deficient worms than in the control worms. On the other hands, glutathione is an important antioxidant compound in all living cells, preventing cellular components from ROS. Control worms contained approximately 17.5 nmole of GSH per mg of worm proteins and no GSSG was detected (**Table 6**). However, the amount of GSH was significantly reduced in B_{12}-deficient

worms, which contained small amount of GSSG (approximately 0.6 nmol/mg protein). The result indicated that B_{12} deficiency induced significant reduction of GSH in worms. Furthermore, total SOD and Mn-SOD and Cat activities in B_{12}-deficient worms were decreased to approximately 50%, 60%, and 70% enzyme activities of the control worms, respectively (**Table 6**). These results indicated that both low molecular and enzymatic defense system against oxidative stress were significantly weakened during B_{12} deficiency. To evaluate the effects of B_{12} deficiency on the levels of mRNAs encoding proteins involved in cellular antioxidative systems, the level of mRNAs encoding SOD (*sod-1*, *sod-2*, *sod-3*, *sod-4*, and *sod-5*), GPx (F26E4.12), GST (*gst-10*), Cat (*ctl-1*, *ctl-2*, and *ctl-3*), and orthologous protein to human mitochondrial GSR (*gsr-1*), were measured by qPCR analysis. As shown in **Fig. 30**, B_{12} deficiency did not affect mRNA levels of most proteins involved in cellular antioxidative systems except for GST catalyzing the conjugation of GSH to xenobiotic substrates including peroxidized lipids [103]. Many studies [105-107] have demonstrated that SOD was potently inhibited by H_2O_2, which was accumulated during B_{12} deficiency. Cat as well as SOD is susceptible to oxidative inactivation by singlet oxygen [108].

To clarify effects of B_{12} deficiency on memory/learning function involved in insulin/PI-3 kinase signaling pathway in central nervous system, the *C. elegans* salt (NaCl) chemotaxis memory/learning assay system was used. Although B_{12} deficiency did not affect *C. elegans* chemotaxis to NaCl (not shown data), the C.I. value (index of the food-NaCl associative memory/learning) was significantly increased in B_{12}-deficient worms, compared with that of the controls (**Fig. 31**), indicating that B_{12} deficiency leads to sever memory/learning impairment in *C. elegans*. When B_{12}-deficient worms were grown under B_{12}-supplemented conditions during five generations, this memory/learning impairment was gradually improved with increased generations and completely recovered in B_{12}-deficient worms treated for five generations. To investigate the effects of antioxidants on memory/learning ability of the worms during B_{12} deficiency, worms were grown in five generations under the B_{12}-deficient medium with α-tocopherol (**Fig. 32A**) and GSH (**Fig. 32B**). When worms were grown under

B_{12}-deficient conditions for five generations, α-tocopherol was added in each generation stage (F1 – F5) of worms. The learning disability caused by B_{12} deficiency was improved up to approximately 50% of the control worm's ability in the worms treated with α-tocopherol during three to five generations. Remarkably the learning disability was recovered up to approximately 50% of the control worm's ability in the worms treated with GSH only during one generation. These results indicated that feeding of α-tocopherol or GSH for relatively long duration significantly prevented the memory/learning impairment caused by B_{12} deficiency in *C. elegans*.

As described above, B_{12} deficiency disrupts cellular redox homeostasis to induce oxidative stress, which leads to sever memory/learning impairment in *C. elegans*. Lipid peroxide induces further oxidative modification of cellular components [109]. Lipid peroxidation and protein oxidation were detected in mammalian tissues with Alzheimer disease [105-107] and develops various symptoms such as memory loss and cognitive impairments. **Fig. 60** shows the mechanisms of memory/learning dysfunction in B_{12}-deficient worm.

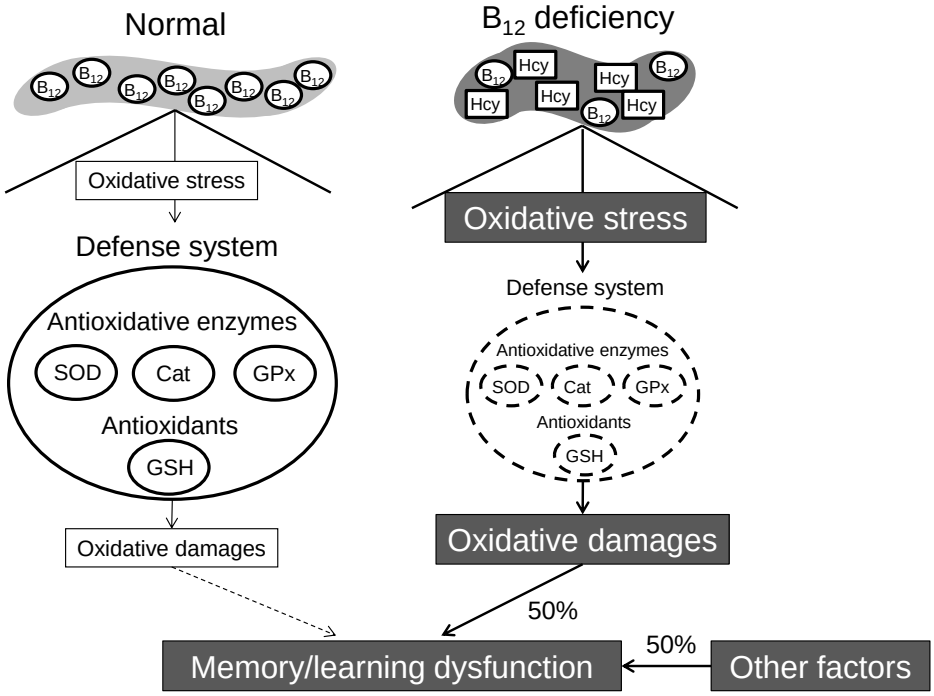

Fig. 60. The mechanisms of memory/learning dysfunction in B_{12}-deficient worm.

Both MCM and MS function as key-enzymes for the metabolisms of various amino acids, although Ebara *et al*. [22] demonstrated that B_{12} deficiency in rats caused serine and threonine metabolic disorders, which are attributable to impairment of the adenylyl cyclase system. Thus, B_{12} deficiency disrupts directly or indirectly various cellular metabolisms to lead the associated symptoms such as developmental disorders, infertility, and neuropathy. When I attempted to elucidate effects of B_{12} deficiency on amino acid metabolisms using *C. eleganns*, significant change of ornithine was detected (**Table 8**). Ornithine is an amino acid that is produced from arginine by the action of arginase in the urea cycle and is a precursor of polyamines which play multiple roles in cell growth and death including aging and diseases. As shown in **Chapter III**, **section 2**, I described that B_{12} deficiency causes various amino acid metabolisms, in particular occurrence of unusual accumulation of ornithine and leads to disruption of normal polyamine metabolism. As shown in **Table 8**, branched-chain amino acid (Val, Leu, and Ile) levels were significantly increased but methionine level was decreased in the B_{12}-deficient *C. elegans*, indicating that significant changes in these amino acid levels are directly attributable to the decreased MCM and MS activities caused by B_{12} deficiency. Ebara *et al*. [22, 33] reported that serine, threonine, and lysine levels significantly increased in plasma and urine of the B_{12}-deficient rats and that mRNA and protein levels of serine/threonine dehydratase (EC 4.3.1.19) that catalyzes the conversion of serine and threonine to pyruvate and 2-oxobutyrate, respectively, were significantly lowered by B_{12} deficiency. Similarly, significant increases of threonine and lysine were detected in the B_{12}-deficient worms (**Table 8**). Furthermore, cystathionine level was simultaneously increased in the B_{12}-deficient worm. The MCM activity decreased by B_{12} deficiency would disrupt the normal catabolism of cystathionine to TCA cycle *via* propionyl-CoA pathway to increase cystathionine level. Many studies have reported that a synergistic inhibition of respiratory chain and TCA cycle by propionyl-CoA and its alternative products, 2-methylcitrate and malonate, as well as MMA [57]. α-Aminoadipic acid is the intermediate compound for degradation of lysine. Lysine and α-aminoadipic acid were significantly increased in B_{12}-deficient worms,

suggesting that lysine catabolism was disordered by TCA cycle inhibition caused by B_{12} deficiency. B_{12}-deficient worms showed the increased level of phosphoethanolamine (**Table 8**), which is a compound involved in phospholipid turnover, acting as a substrate for many phospholipids of the cell membranes, especially phosphatidylcholine. Akesson *et al*. [121] have demonstrated that phosphatidylcholine was decreased in the liver of B_{12}-deficient rats, which conversely increased phosphatidylethanolamine.

Surprisingly, the B_{12}-deficient worms showed significant accumulation of ornithine, which is precursors for polyamines that act as the modulators in neurotransmission [122] and for proline involved in collagen synthesis [123]. B_{12}-deficient worms showed a significant increase of hydroxyproline, which is a major component amino acid for the protein collagen. B_{12}-deficient worms showed a specific morphological abnormality, similar to the short and plump ‘‘dumpy’’ mutant phenotype that is formed because of disordered cuticle collagen biosynthesis [65, 66]. These observations indicate that the increased level of hydroxyproline is one of the results of this impaired collagen biosynthesis.

To elucidate the mechanism of accumulation of ornithine in B_{12}-deficient worms, contents of putrescine and spermidine were assayed. Putrescine content did not change between B_{12}-deficient and control worms (**Fig. 36A**) but spermidine content of B_{12}-deficient worms was decreased to approximately 82% of the control worms (**Fig. 36B**). ODC catalyzes the decarboxylation of ornithine to form putrescine and regulates the synthesis of polyamines. As shown in **Fig. 37**, ODC activity was remarkably increased in B_{12}-deficient worms relative to the controls. It is reported that ODC activity is significantly increased in murine L1210 leukaemia cells by the depletion of SAM [124] and in totally gastrectomized B_{12}-deficient rats [125]. These results suggest that the ODC activity increased in B_{12}-deficient worms was attributable to the decreased SAM level, which further reduced the cellular spermidine level because decarboxylated SAM formed from SAM is essential for the synthesis of polyamine compounds. The gene expression of ODC (*odc-1*), SAMDC (*smd-1*), and SPDS (*spds-1*) was evaluated using the qPCR method to clarify the polyamine metabolic disorders in B_{12}-deficient

worms. B_{12}-deficient worm showed significant increase of ODC (*odc-1*) mRNA expression level (**Fig. 38A**), coinciding with the increased activity of ODC. Although the mRNA expression level of SPDS (*spds-1*) did not change among three experimental conditions (**Fig. 38B**), SAMDC (*smd-1*) mRNA expression level was decreased to approximately 50% of the control worms (**Fig. 38C**). These results indicate that ODC and SAMDC mRNA expression levels are readily affected by B_{12} deficiency.

SAM functions as an important methyl donor in all living organisms. The methyl group from SAM is transferred to certain acceptor to form SAH [126], which is a potent competitive inhibitor of transmethylation reactions. Thus, SAM/SAH ratio is used as an index of cellular transmethylation reactions [20]. As shown in **Fig. 39**, B_{12} deficiency significantly decreased SAM and SAM/SAH ratio, which is approximately 39% of the control worms. SAM/SAH ratio in B_{12}-deficient rats and humans was decreased to approximately 26% [129] and 62% [130] of the ratio in B_{12} sufficiency, respectively. These results indicate that B_{12} deficiency leads to reduction of various cellular methylation reactions such as DNA, RNA, proteins, and lipids.

Polyamines have been reported to stimulate B_{12}-dependent MS so that the compounds appear to modulate MS activity [19]. When effects of various concentrations of spermidine or putrescine on the activity of *C. elegans* holo-MS were studied (**Fig. 40)**, holo-MS activity increased in a dose-dependent manner of spermidine and was approximately 2.5 times greater in the presence of 1 mmol/L spermidine. However, putrescine did not stimulate holo-MS. These results suggest that MS is synergically inhibited due to decreased spermidine in B_{12}-deficient worms.

Polyamines as well as Hcy activate NMDA receptor involved in the signal transmission between nerve cells [132, 133] and induce an excitotoxic neurodegenerative process [134]. Adachi *et al*. [135] have demonstrated polyamine concentration decreased in the cerebellum, brainstem and spinal cord of B_{12}-deficient rats. These observations and this study indicate that amino acid/polyamine metabolic disorders caused by B_{12} deficiency are closely related with neuropathy. However, the detailed mechanism of B_{12}-deficient neuropathy including cognitive dysfunction

remains to be completely elucidated. Since *C. elegans* is widely used as a model organism for studying the mechanisms of memory/learning [136], it becomes a suitable and powerful tool for the study of B_{12}-deficient neuropathy [137] and cognitive impairment [138] in humans. **Fig. 61** shows the predicted mechanisms of B_{12}-deficient neuropathy.

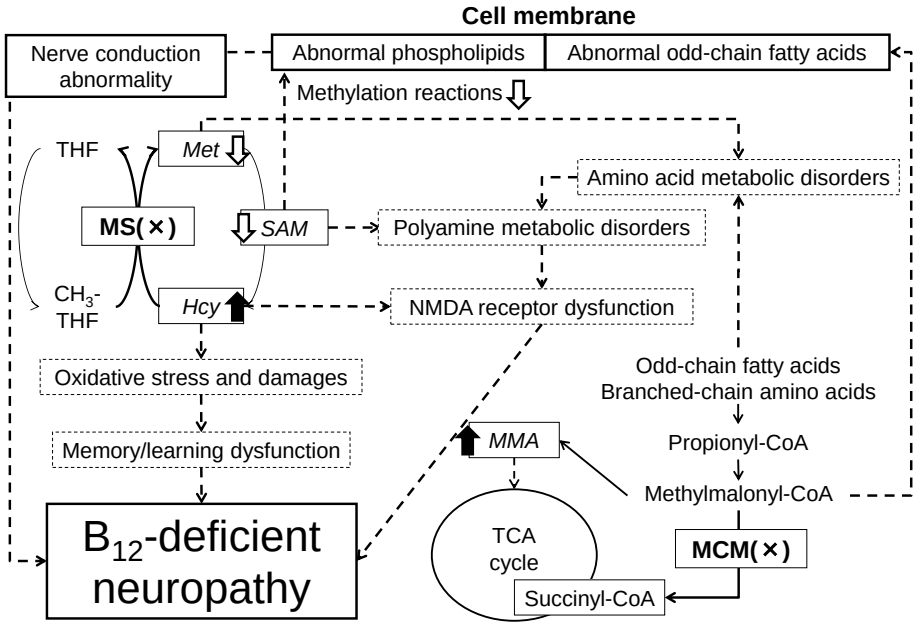

Fig. 61. Predicted mechanisms of B_{12}-deficient neuropathy.

B_{12} is synthesized only by certain bacteria and primarily concentrated in the bodies of higher predatory organisms in the natural food chain. Animal-derived foods such as meat, milk, egg, fish, and shellfish, but not plant-derived foods, are the major dietary sources of B_{12} [36]. Therefore, strict vegetarians are at a greater risk of developing B_{12} deficiency than nonvegetarians. A large number of people have low serum B_{12} levels that result more commonly from malabsorption of protein-bound B_{12} (food-bound B_{12} malabsorption) rather than pernicious anemia [37]. Food-bound B_{12} malabsorption is found in people with certain gastric dysfunctions, particularly atrophic gastritis with low stomach acid secretion, which prevails in elderly people [38, 39]. As the bioavailability of crystalline (free) B_{12} is not altered in people with atrophic gastritis [164], the Institute

of Medicine recommended that most of the RDA (2.4 μg/day) should be obtained by consuming foods fortified with B_{12} or supplements containing B_{12} [23]. It is important to identify high B_{12}-containing plant-derived food to prevent vegetarians and elderly people from developing B_{12} deficiency. Some plant-derived foods such as edible algae or blue-green algae (cyanobacteria) contain large amounts of B_{12} [140]. However, inactive pseudo-B_{12} is reportedly predominant in various edible cyanobacteria [141, 142].

Among the wild edible mushroom fruiting bodies that are consumed by European vegetarians, black trumpet (*Craterellus cornucopioides*) and golden chanterelle (*Cantharellus cibarius*) mushroom fruiting bodies contain considerable levels (1.09 - 2.65 μg/100 g dry weight) of B_{12}, whereas the remaining mushroom fruiting bodies have zero or trace levels [154]. However, preliminary experiments indicated that high levels of B_{12} were detected in commercially available dried fruiting bodies of shiitake mushroom (*Lentinula edodes*). Shiitake mushrooms are cultivated and consumed throughout the world. In particular, fresh and dried shiitake mushroom fruiting bodies are also used in various vegetarian dishes. In **Chapter IV**, **section 2**, I analyzed the B_{12} contents in various dried shiitake fruiting bodies that are commercially available in Japan and characterized the B_{12} compounds found in these fruiting bodies. As shown in **Table 10** , the corrected B_{12} contents in the shiitake fruiting bodies varied significantly (1.28 ― 12.71 μg/100 g dry weight), and high levels (4.43 ― 21.56 μg as B_{12} equivalent/100 g dry weight) of alkali-resistant factor were found in all mushrooms. The B_{12} contents in dried donko-type fruiting bodies with closed caps (5.61 ± 3.90 μg/100 g dry weight) were not significantly different from those of dried koushin-type fruiting bodies with open caps (4.23 ± 2.42 μg/ 100 g dry weight). The B_{12} contents in raw shiitake fruiting bodies cultivated on sawdust substrate (3.95 ± 3.34 μg/100 g dry weight) were similar to those of dried shiitake fruiting bodies cultivated on bed logs. The results indicated that the B_{12} contents in shiitake fruiting bodies were twice (or more) than in European wild mushroom fruiting bodies, i.e., black trumpet and golden chanterelle mushrooms. Corrinoids were purified from shiitake fruiting body an extracts

using an immunoaffinity column and identified by LC/ESI-MS/MS. As shown in **Fig. 46**, commercially available donko-type dried shiitake fruiting bodies contained authentic B_{12} and not pseudo-B_{12}, which is inactive in humans. However, one of koushin-type dried fruiting body contained authentic B_{12} and B_{12}[*c*-lactone] (**Fig. 49**), which was not detected in the other commercially available dried shiitake fruiting bodies. Bonnett [157] reported that chloramine-T an antimicrobial agent, which has widespread uses in medical, dental, veterinary, food processing, and agricultural fields [156], reacts with B_{12} to form B_{12}[*c*-lactone], a biologically inactive B_{12} analogue. Consumption of approximately 50 g of dried shiitake fruiting bodies could provide the RDA for adults (2.4 μg/day) [23, 139], although ingestion of such large amounts of this mushroom fruiting body on a daily basis is not possible.

Mozafar [143] demonstrated that the addition of an organic fertilizer, cow manure, significantly increased the B_{12} content (17.8 ng/g dry weight) in spinach leaves. Using this value and assuming spinach leaves have a moisture content of 92.4% [144], the B_{12} content is approximately 0.14 μg/100 g fresh weight. Consumption of several hundred grams of fresh spinach would therefore be insufficient to meet the RDA of 2.4 μg/day for adult humans [23]. Furthermore, my unpublished works indicate that most organic fertilizers, particularly those made from animal manures, contain considerable amounts of inactive corrinoid compounds. These compounds have also been reported to be present in human feces and account for >98% of the total corrinoid content [145]. Biofertilizers are products containing living cells of beneficial microorganisms, which can accelerate and improve plant growth by providing nutritionally important elements (e.g., nitrogen and phosphorus) [158]. Although cyanobacteria are responsible for biological nitrogen (N_2) fixation in flooded rice fields [159], they contain large amounts of pseudo-B_{12} that is inactive in humans [36]. N_2-fixing purple photosynthetic bacteria were reported to have beneficial effects on plant growth [160] and the ability to synthesize B_{12} *de novo* [161]. If biofertilizers containing purple photosynthetic bacteria contain a substantial amount of "true B_{12}", these fertilizers would be useful for enriching B_{12} in plants. As described in **Chapter IV**, **section 3**, no or traces of B_{12} were found in

two of the biofertilizers (A and B) tested while the third (C) contained a considerable amount (53.5 μg/L) of the vitamin. However, biofertilizer C contained both B_{12} (main) and Factor III (minor) (**Fig. 51** and **52**). Since the N_2-fixing photosynthetic purple bacterium *Rhodobacter capsulatus*, used as a biofertilizer, has the ability to synthesize B_{12} *de novo* [161], Factor III may be derived from other concomitant bacteria in commercial biofertilizer C. In preliminary experiments, B_{12} was not detected in the lettuce leaves grown with and without biofertilizer C treatment of the soil and leaves once a week for three weeks according to the manufacturer's recommended protocol. These results indicated that commercially available biofertilizers containing purple photosynthetic bacteria are not suitable for B_{12}-enrichment of plants due to the low B_{12} content.

Some researchers have attempted to prepare certain B_{12}-enriched vegetables by treating them with a solution containing high levels of B_{12} [146, 147]. This resulted in a significant increase in the amount of B_{12} incorporated into the plants, suggesting that the B_{12}-enriched vegetables may be of special benefit to vegetarians. However, the B_{12} absorbed by the vegetables was not well characterized in these studies. Hydroponic cultivation is an emerging technology that allows better control of water and nutrient supply that improves plant productivity and reduces the use of pesticides [165]. If a sufficient amount of free B_{12} can be incorporated into lettuce leaves grown under hydroponic conditions, it would be an excellent source of free B_{12} for vegetarians and elderly people. Thus, I produced and characterized B_{12}-enriched lettuce leaves cultivated using hydroponics (**Chapter IV, Section 4**).

Lettuces grown for 30 days in hydroponic culture were treated with the indicated amounts of CN-B_{12} for 24 h and then harvested. The B_{12} concentration of the lettuce leaves significantly increased CN-B_{12} concentration up to 5 μmol/L (**Table 13**). No B_{12} was detected in lettuce leaves placed in a solution without CN-B_{12}. The B_{12} content of lettuce leaves may be controlled, to some extent, by changing the CN-B_{12} concentration in the nutrient solution. Because lettuce leaves treated with 1 μmol/L CN-B_{12} contained 1.3 ± 0.6 μg of B_{12} per total fresh weight (g) of plant stock, consumption of 2 stocks of

these plants would supply the RDA for adults (2.4 μg/day). For lettuce leaves treated with 5 μmol/L CN-B_{12} (6.8 ± 3.4 μg of B_{12} per plant stock), consumption of only 2 or 3 leaves would be sufficient to meet the RDA. The CN-B_{12} absorbed by lettuce leaves was not changed to any other corrinoids (**Fig. 57**), although CN-B_{12} was readily converted to OH-B_{12} in an aqueous solution under the same conditions **(Fig. 56A-4** and **B-4**). These findings suggested that lettuce plant tissues have the ability to block photolysis of aqueous CN-B_{12} from sunlight exposure. The majority of CN-B_{12} present in the leaves (86%) was recovered in the free CN-B_{12} fractions (**Fig. 59B**), suggesting that CN-B_{12}-enriched lettuce leaves are an excellent source of free CN-B_{12}.

Because vegetables are generally a good source of dietary fibers, vitamins, and minerals [164], consumption of a large amount of vegetables enriched with a low level of CN-B_{12} would be better for human health than that of a small amount of vegetables with a high level of CN-B_{12}. Consumption of 62.2 g of CN-B_{12}-enriched lettuce leaves (approximately 38.6 ng/g fresh weight) grown in a low CN-B_{12} (1 μmol/L)-supplemented nutrient solution supplies the RDA for B_{12} of 2.4 μg/day. In addition, these leaves provide the daily intake of other nutrients, particularly folic acid and B_6, which are essential for normal Hcy metabolism and for preventing disorders such as atherosclerosis and neuropathy [168]. The use of low levels of CN-B_{12} in nutrient solutions would also lower the production costs of the enriched plants. Indeed, the cost of CN-B_{12} for the preparation of 1 stock of B_{12}-enriched lettuce leaves grown in the low CN-B_{12} (1 μmol/L)-supplemented nutrient solution was calculated to be only approximately ¥ 6 (U.S. $0.06) under the experimental conditions used. If the nutrient solution is reused several times, this cost would be reduced significantly. Therefore, the cost for adding CN-B_{12} would not a major factor when preparing CN-B_{12}-enriched plants.

B_{12} contents of various plant-derived foods summarizes in **Table 16**. Dried green and purple lavers (nori) contain substantial amounts of B_{12} (approximately 130 μg/100 g dry weight), although other edible algae contained none or only traces of B_{12}.

Table 16. B_{12} content of animal- and plant-derived foods.

		B_{12} content (μg/100 g edible portion)	Corrinoid compounds	*Ref*
Animal-derived foods	Meat	9.4	B_{12}	36
	Milk	0.4	B_{12}	36
	Eggs	1.3	B_{12}	36
	Fish	8.9	B_{12}	36
Plant-derived foods	**Mushrooms**	(μg/100 g dry weight)		
	Shiitake	5.6 ± 3.9	B_{12}, B_{12}[*c*-lactone]	This study
	Black trumpet	2.2 ± 0.4	B_{12}	153
	Golden chanterelle	1.5 ± 0.4	B_{12}	153
	Lion's mane mushroom	0.4 ± 0.3	B_{12}, B_{12}[*c*-lactone]	172
	Cyanobacteria			
	Spirulina tablets	127–244	Pseudo-B_{12}	141
	Algae			
	Chlorella tablets	201−286	B_{12}	173
	Dried purple laver	133.8	B_{12}	154
	Vegetables			
	B_{12}-enriched spanish leaves	1.8	B_{12} ?	143
	B_{12}-enriched lettuce (Hydroponic cultivation; 1 μmol/L)	55.3	B_{12} (free)	This study

In the case of unicellular alga and cyanobacteria available for human supplements, *chlorella* tablets contain substantial amounts of B_{12} (approximately 200 - 290 μg/100g dry weight) but *spilurina* tablets contain a large amount of pseudo-B_{12} (approximately 130 - 240 μg/100g dry weight). Most of the edible cyanobacteria used for human

supplements predominately contain pseudo-B_{12} [141]. Wild and cultured edible mushroom fruiting bodies (black trumpet, golden chanterelle, lion's mane mushroom, and shiitake mushroom) contain extremely low B_{12} (< 10 μg/100 g dry weight) comparing with these edible algae. The edible eukaryotic algae (nori and *chlorella*) are excellent B_{12} sources for vegetarians. However, most of B_{12} found in these algae appear to be the protein-bound B_{12}. Food (or protein)-bound B_{12} malabsorption prevails in elderly people [38, 39]. Thus, B_{12}-enriched lettuce would be an excellent source of free B_{12} for elderly people. **Fig. 62** showed the summary of production of B_{12}-enriched food for preventing the B_{12} deficiency.

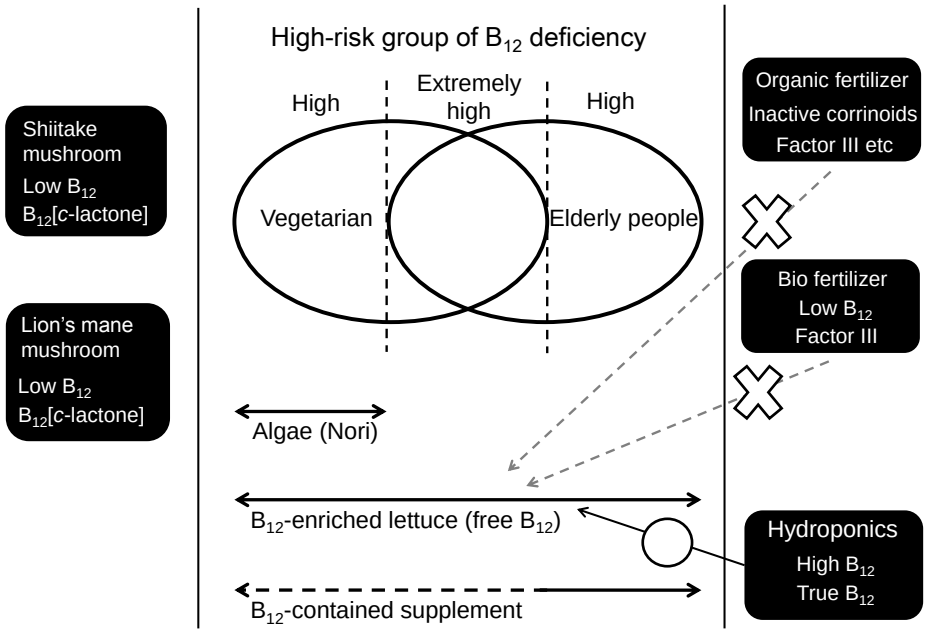

Fig. 62. Summary of production of B_{12}-enriched food for preventing the B_{12} deficiency.

In **Chapter IV**, **section 1**, I also developed a simple method for analyzing B_{12} compounds in various food samples using a miniaturized HPTLC.

References

[1] Perlman D and Umbreit WW (Ed). (1959) Microbial synthesis of cobamides. Advances in Applied Microbiology, 1, pp.87-122. Academic Press, NY.

[2] Froese DS, Healy S, McDonald M, Kochan G, Oppermann U, Niesen FH and Gravel RA. (2010**)** Thermolability of mutant MMACHC protein in the vitamin B_{12}-responsive cblC disorder. *Mol Genet Metab*, **100**, 29–36.

[3] Alpers DH, Russell-Jones GI and Banerjee R (Ed). (1999) *Intrinsic factor, haptocorrin, and their receptors. In Chemistry and Biochemistry of Vitamin B_{12}* (Banerjee R. ed.), pp. 411-439. John Wiley & Sons, NY.

[4] Rothenberg SP, Quadros EV and Regec A (1999) *Transcobalamin II. In Chemistry and Biochemistry of Vitamin B_{12}* (Banerjee R. ed.), pp. 441-473. John Wiley & Sons, NY.

[5] Fowler B. (1998) Genetic defects of folate and cobalamin metabolism. *Eur J Pediatr*, **157**, 60–66.

[6] Fyfe JC, Madsen M, Hojrup P, Christensen EI, Tanner SM, de la Chapelle A, He Q and Moestrup SK. (2004) The functional cobalamin (vitamin B_{12})-intrinsic factor receptor is a novel complex of cubilin and amnionless. *Blood*, **103**, 1573–1579

[7] Moestrup SK, Kozyraki R, Kristiansen M, Kaysen JH, Rasmussen HH, Brault D, Pontillon F, Goda FO, Christensen EI, Hammond TG and Verroust PJ. (1998) The intrinsic factor-vitamin B_{12} receptor and target of teratogenic antibodies is a megalin-binding peripheral membrane protein with homology to developmental proteins. *J Biol Chem*, **273**, 5235–5242,

[8] Miousse IR, Watkins D and Rosenblatt DS. (2011) Novel splice site mutations and a large deletion in three patients with the *cblF* inborn error of vitamin B_{12} metabolism. *Mol Genet Metab*, **102**, 505–507.

[9] Rutsch F, Gailus S, Miousse IR, Suormala T, Sagne C, Toliat MR, Nurnberg G, Wittkampf T, Buers I, Sharifi A, Stucki M, Becker C, Baumgarthner M, Robenek H, Marquardt T, Höhne W, Gasnier B, Rosenblatt DS, Fowler B and Nürnberg P.

(2009) Identification of a putative lysosomal cobalamin exporter altered in the *cblF* defect of vitamin B_{12} metabolism. *Nat Genet*, **41**, 234–239.

[10] Quadros EV and Sequeira JM. (2013) Cellular uptake of cobalamin: Transcobalamin and the TCblR/CD320 receptor. *Biochimie*, **95**, 1008–1018

[11] Youngdahl-Turner P, Rosenberg LE and Allen RH. (1978) Binding and uptake of transcobalamin II by human fibroblasts. *J Clin Investig*, **61**, 133–141.

[12] Fenton W, Hack A, Willard H, Gertler A and Rosenberg L. (1982) Purification and properties of methylmalonyl coenzyme A mutase from human liver. *Arch Biochem*, **214**, 815–823.

[13] Chen Z, Crippen K, Gulati S and Banerjee R. (1994) Purification and kinetic mechanism of a mammalian methionine synthase from pig liver. *J Biol Chem*, **269**, 27193–27197.

[14] Dobson CM, Wai T, Leclerc D, Kadir H, Narang M, Lerner-Ellis JP, Hudson TJ, Rosenblatt DS and Gravel RA. (2002) Identification of the gene responsible for the *cblB* complementation group of vitamin B_{12}-dependent methylmalonic aciduria. *Hum Mol Genet*, **11**, 3361–3369.

[15] Leal NA, Park SD, Kima PE and Bobik TA. (2003) Identification of the human and bovine ATP:Cob(I)alamin adenosyltransferase cDNAs based on complementation of a bacterial mutant. *J Biol Chem*, **278**, 9227–9234.

[16] Takahashi-Iniguez T, Garcia-Arellano H, Trujillo-Roldan MA and Flores ME. (2011) Protection and reactivation of human methylmalonyl-CoA mutase by MMAA protein. *Biochem Biophys Res Commun*, **404**, 443–447.

[17] Takahashi-Iniguez T, Garcia-Hernandez E, Arreguin-Espinosa R and Flores ME. (2012) Role of vitamin B_{12} on methylmalonyl-CoA mutase activity. *J Zhejiang Univ Sci B*, **13**, 423–437.

[18] Banerjee R. (2001) Radical peregrinations catalyzed by coenzyme B_{12}-dependent enzymes. *Biochemistry*, **40**, 6191-6198.

[19] Kenyon SH, Nicolaou A, Ast T and Gibbons WA. (1996) Stimulation in vitro of vitamin B_{12}-dependent methionine synthase by polyamines. *Biochem J*, **316**,

661-665.

[20] Lu SC. (2000) S-Adenosylmethionine. *Int J Biochem Cell Biol*, **32**, 391-395.

[21] Toyoshima S, Watanabe F, Saido H, Pezacka EH, Jacobsen DW, Miyatake K and Nakano Y. (1996) Accumulation of methylmalonic acid caused by vitamin B_{12}-deficiency disrups normal cellular metabolism in rat liver. *Br J Nutr*, **75**, 929-938.

[22] Ebara S, Toyoshime S, Matsumura T, Adachi S, Takenaka S, Yamaji R, Watanabe F, Miyatake K, Inui H and Nakano Y. (2001) Cobalamin deficiency results in severe metabolic disorder of serine and threonine in rats. *Biochim Biophys Acta*, **1568**, 111-117.

[23] Institute of Medicine (1998) Vitamin B12. Dietary Reference Intakes for Thiamin, Riboflavin, Niacin, Vitamin B6, Folate, Vitamin B12, Pantothenic Acid, Biotin, and Choline. Washington, DC: Institute of Medicine, National Academy Press, pp.306–356.

[24] Pepper MR and Black MM. (2011) B_{12} in fetal development. *Semin Cell Dev Biol*, **22**, 619-623.

[25] Clarke R, Smith AD, Jobst KA, Refsum H, Sutton L and Ueland PM. (1998) Folate, vitamin B_{12}, serum total homocysteine levels in confirmed Alzheimer's disease. *Arch Neurol*, **55**, 1449–1455.

[26] McIlroy SP, Dynan KB, Lawson JT, Patterson CC and Passmore AP.(2002) Moderately elevated plasma homocysteine, methylentetrahydrofolate reductase genotype, and risk for stroke, vascular dementia and Alzheimer Disease in Northern Ireland. *Stroke*, **33**, 2351–2356.

[27] Ravaglia G, Forti P, Maioli F, Martelli M, Servadei L, Brunetti N, Porcellini E and Licastro F. (2005) Homocysteine and folate as risk factors for dementia and Alzheimer disease. *Am J Clin Nutr*, **82**, 636–643.

[28] Faraci FM and Lentz SR. (2004) Hyperhomocysteinemia, oxidative stress and cerebral vascular dysfunction. *Stroke*, **35**, 345–348.

[29] Dwyer BE, Raina AK, Perry G and Smith MA. (2004) Homocysteine and

Alzheimer's disease: a modifiable risk? *Free Radic Biol Med*, **36**, 1471–1475.

[30] McCaddon A, Regland B, Hudson P and Davies G. (2002) Functional vitamin B_{12} deficiency and Alzheimer disease. *Neurology*, **58**, 1395-1399.

[31] Pegg EA. (1986) Recent advances in the biochemistry of polyamines in eukaryotes. *Biochem J*, **234**, 249-262.

[32] Rebecca E, Gordon KW. and Romola SB. (2000) Vitamin B_{12} deficiency in dementia and cognttive impairment: the effects of treatment on neuropsychological function. *Int J Geriatr Psych*, **15**, 226-233.

[33] Ebara S, Nakao M, TomodaM, Yamaji R, Watanabe F, Inui H and Nakano Y. (2008) Vitamin B_{12} deficiency results in the abnormal regulation of serine dehydratase and tyrosine aminotransferase activities correlated with impairment of the adenylyl cyclase system in rat liver. *Br J Nutr*, **99**, 503–510.

[34] Susana GM, Ana M, Laura D, Simone P, Felipe SL, Montserrat D and Celestino SB. (2012) Oxidative status of stressed *Caenorhabditis elegans* treated with Epicatechin. *J Agric Food Chem*, **60**, 8911-8916.

[35] Culetto E and Sattelle DB. (2000) A role for *Caenorhabditis elegans* in understanding the function and interactions of human disease genes. *Hum Mol Genet*, **9**, 869–877.

[36] Watanabe F. (2007) Vitamin B_{12} sources and bioavailability. *Exp Biol Med*, **232**, 1266–1274.

[37] Baik HW and Russell RW. (1999) Vitamin B_{12} deficiency in the elderly. *Annu Rev Nutr*, **19**, 357-377.

[38] van Asselt DZ, van den Brok WJ, Lamers CB, Corstens FH and Hoefnagels WH. (1996) Free and protein-bound cobalamin absorption in healthy middle-aged and older subjects. *J Am Geriatr Soc*, **44**, 949-953.

[39] Krasinski SD, Russell RW, Samloff IM, Jacob RA, Dallal GE, McGrandy RB and Hartz SC. (1986) Fundic atrophic gastritis in an elderly population: effect on hemoglobin and several serum nutritional indicators. *J Am Geriatr Soc*, **34**, 800-806.

[40] Watanabe F, Tanioka Y, Miyamoto E, Fujita T, Takenaka H and Nakano Y. (2007) Purification and characterization of corrinoid-compounds from the dried powder of edible cyanobacterium, *Nostoc commune* (Ishikurage). *J Nutr Sci Vitaminol*, **53**, 183-186.

[41] Chandler RJ and Venditti CP. (2005) Genetic and genomic systems to study methylmalonic academia. *Mol Genet Metabol*, **86**, 34-43.

[42] Chandler RJ, Aswani V, Tsai MS, Falk M, Wehrli N, Stabler S, Allen R, Sedensky M, Kazazian HH and Venditti CP. (2006) Propionyl-CoA and adenosylcobalamin metabolism in *C. elegan*s: Evidence for a role methylmalonyl-CoA epimerase in intermediary metabolism. *Mol Genet Metabol*, **89**, 64-73.

[43] Matthews JH (1997) Cyanocobalamin [*c*-lactam] inhibits vitamin B_{12} and causes cytotoxicity in HL60 cells: methionine protects cells completely. *Blood*, **89**, 4600-4607.

[44] Stabler SP, Brass EP, Marcell PD and Allen RH (1991) Inhibition of cobalamin-dependent enzymes by cobalamin analogs in rats. *J Clin Invest*, **87**, 1422-1430.

[45] McEwan JF, Veitch HS and Russell-Jones GJ (1999) Synthesis and biological activity of ribose-5'-carbamate derivatives of vitamin B_{12}. *Bioconjugate Chem*, **10**, 1131-1136.

[46] Brenner S. (1974) The genetics of *Caenorhabditis elegans*. *Genetics*, **77**, 71–94.

[47] Al-Dirbashi OY, Jacob M, Al-Hassnan Z, Chabayta RW, El-Badaoui F and Rashed MS. (2006) Determination of methylmalonic acid in urine by HPLC with intramolecular excimer-forming fluorescence derivatization. *Biomed Chromatogr*, **20**, 54–60.

[48] Febriani AD, Sakamoto A, Ono H, Sakura N, Ueda K, Yoshii C, Kubota M and Yanagawa J. (2004) Determination of total homocysteine in dried blood spots using high performance liquid chromatography for homocystinuria newborn screening. *Pediatr Int*, **46**, 5–9.

[49] Miyamoto E, Tanioka Y, Nishizawa-Yokoi A, Yabuta Y, Ohnishi K, Misono H,

Shigeoka S, Nakano Y and Watanabe F. (2010) Characterization of methylmalonyl-CoA mutase involved in the propionate photoassimilation of *Euglena gracilis* Z. *Arch Microbiol*, **192**, 437–446.

[50] Tanioka Y, Yabuta Y, Yamaji R, Shigeoka S, Nakano Y, Watanabe F and Inui H. (2009) Occurrence of pseudovitamin B_{12} and its possible function as the cofactor of cobalamin-dependent methionine synthase in a cyanobacterium *synechocystis* sp. PCC6803. *J Nutr Sci Vitaminol*, **55**, 518–521.

[51] Huang L, Zhang J, Hayakawa T and Tsuge H. (2001) Assays of methylenetetrahydrofolate reductase and methionine synthase activities by monitoring 5-methyltetrahydrofolate and tetrahydrofolate using high-performance liquid chromatography with fluorescence detection. *Anal Biochem*, **299**, 253–259.

[52] Byerly L, Cassada RC and Russell RL. (1976) The life cycle of the nematode *Caenorhabditis elegans*. I. Wild-type growth and reproduction. *Dev Biol*, **51**, 23-33.

[53] Johnson T and Wood W. (1982) Genetic analysis of life-span in *Caenorhabditis elegans*. *Proc Natl Acad Sci USA*, **79**, 6603-6607.

[54] Bradford MM. (1976) A rapid and sensitive method for the quantitation of microgram quantities of protein utilizing the principle of protein-dye binding. *Anal Biochem*, **72**, 248-254.

[55] Yamada K, Kawata T, Wada M, Isshiki T, Onoda J, Kawanishi T, Kunou A, Tadokoro T, Tobimatsu T, Maekawa A and Toraya. (2000) Extremely low activity of methionine synthase in vitamin B_{12}-deficient rats may be related to effects on coenzyme stabilization rather than to changes in coenzyme induction. *J Nutr*, **130**, 1894–1900.

[56] Nakao M, Hironaka S, Harada N, Adachi T, Bito T, Yabuta Y, Watanabe F, Miura T, Yamaji R, Inui H and Nakano Y. (2009) Cobalamin deficiency results in an abnormal increase in L-methylmalonyl-coenzyme-A mutase expression in rat liver and COS-7 cells. *Br J Nutr*, **101**, 492-498.

[57] Toyoshima S, Watanabe F, Saido H, Miyatake K and Nakano Y. (1995) Methylmalonic acid inhibits respiration in rat liver mitochondria. *J Nutr*, **125**,

2846-2850.

[58] Blair JH, Stearns HE and Simpson GM. (1968) Vitamin B_{12} and fertility. *Lancet*, **1**, 49-50.

[59] Jackson IMD, Doig WB and McDonald G.. (1967) Pernicious anemia as a cause of infertility. *Lancet*, **2**, 1159-1160.

[60] Shane B and Stokstad ELR. (1985) Vitamin B_{12}-folate interrelationships. *Ann Rev Nutr*, **5**, 115-141.

[61] Yamada K, Kawata T, Wada M, Mori K, Tamai H, Tanaka N, Tadokoro T, Tobimatu T, Toraya T and Maekawa A. (2007) Testicular injury to rats fed on soybean protein-based vitamin B_{12}-deficient diet can be reduced by methionine supplementation. *J Nutr Sci Vitaminol*, **53**, 95-101.

[62] Bennett M. (2001) Vitamin B_{12} deficiency, infertility and recurrent fetal loss. *J Reprod Med*, **46**, 209-212.

[63] Halsted CH and Medici V. (2011) Vitamin-dependent methionine metabolism and alcoholic liver sisease. *Adv Nutr*, **2**, 421-427.

[64] Stabler SP. (2000) B_{12} and nutrition, in: R. Banerjee (Ed.), Chemistry and Biochemistry of B_{12}, John Wiley & Sons, Inc., New York, pp. 343-365.

[65] Meredith K and Edgar RS. (1986) Genetic studies of unusual loci that affect body shape of the nematode *Caenorhabditis elegans* and may code for cuticle structural proteins. *Genetics*, **113**, 621-639.

[66] Iain LJ. (1994) The cuticle of the nematode *Caenorhabditis elegans*: a complex collagen structure. *BioEssays*, **16**, 171-177.

[67] Thaler R, Agsten M, Spitzer S, Paschalis EP, Karlic H and Klaushofer K. (2011) Homocysteine suppresses the expression of the collagen cross-linker lysyl oxidase involving IL-6, Fli 1, and epigenetic DNA methylation. *J Biol Chem*, **286**, 5578-5588.

[68] Geldziler BD, Marcello MR, Shakes DC and Singson A. (2011) The genetics and cell biology of fertilization. *Methods Cell Biol*, **106**, 343-375.

[69] Platzer U and Meinzer HP. (2004) Genetic networks in the early development of

Caenorhabditis elegans. *Int Rev Cytol*, **234**, 47-100.

[70] Calahoro F and Ruiz-Rubio M. (2011) *Caenorhabditis elegans* as an experimental tool for the study of complex neurological diseases: Parkinson's disease, Alzheimer's disease and autism spectrum disorder. *Invert Neurosci*, **11**, 73-83.

[71] Ardiel EL and Rankin CH. (2012) An elegant mind: learning and memory in *Caenorhabditis elegans*. *Learn Mem*, **17**, 191-201.

[72] Candio M, Magnaldo S, Bayle J, Dor JF, Gillet Y, Bongain A and Van Obberghen E. (2003) Clinical B_{12} deficiency in one case of recurrent spontaneous pregnancy loss. *Clin Chem Lab Med*, **41**, 1026-1027.

[73] Metz J. (1992) Cobalamin deficiency and the pathogenesis of nervous system disease. *Ann Rev Nutr*, **12**, 59-79.

[74] Lindballe DL, Fedosov S, Sherliker P, Hin H, Clarke R and Nexo E. (2011) Association of cognitive impairment with combinations of vitamin B_{12}-related parameters. *Clin Chem*, **57**, 1436-1443.

[75] Resources Council, Science and technology Agency. (1995) Standard Tables of Food Composition in Japan-Vitamin K, B6, and B12. Science and Technology Agency, Tokyo, Japan, pp. 16-56.

[76] Miyamoto E, Yabuta Y, Y Chung SK, Enomoto T and Watanabe F (2009) Characterization of vitamin B_{12} compounds from Korean purple laver (*Porphyra* sp.) products. *J Agric Food Chem*, **57**, 2793-2796.

[77] Dixon M (1972) The graphical determination of K_m and K_i. *Biochem J*, **129**, 197-202.

[78] Abramoff MD, Magalhaes PJ and Ram SJ (2004) "Image Processing with ImageJ". Biophotonics International, volume 11, issue 7, pp. 36-42.

[79] Sponne IE, Gaire D, Stabler SP, Droesch S, Barbe FM, Allen RH, Lambert DA & Nicolas JP (2000) Inhibition of vitamin B_{12} metabolism by OH-cobalamin c-lactam in rat oligodendrocytes in culture: a model for studying neuropathy due to vitamin B_{12} deficiency. *Neurosci Lett*, **288**, 191-194.

[80] Brass EP, Tahiliani AG, Allen RH and Stabler SP (1990) Coenzyme A metabolism

in vitamin B_{12}-deficient rats. *J Nutr*, **120**, 290-297.

[81] Saido H, Watanabe F, Tamura Y, Nanai Y, and Nakano Y. (1993) Effects of vitamin B_{12} analogues with alternation in side chains of the corrin ring on urinary methylmalonate excreation in vitamin B_{12}-deficient rats. *Biosci Biotechnol Biochem*, **57**, 607-610.

[82] Chen Z, Chakraborty S and Banerjee B. (1995) Demonstration that mammalian methionine synthases are predominantly cobalamin-loaded. *J Biol Chem*, **270**, 19246-19249.

[83] Waly W, Olteanu H, Banerjee R, Choi SW, Mason JB, Parker BS, Sukumar S, Shim S, Sharma A, Benzecry JM, Power-Charnitsky VA and Deth RC. (2004) Activation of methionine synthase by insulin-like growth factor-1 and dopamine: A target for neurodevelopmental toxins and thimerosal. *Mol Psychiatry*, **9**, 358-370.

[84] Andrzej JO and Kilmer SM. (1993) Homocysteine metabolism and the oxidative modification of proteins and lipids. *Free Radic Biol Med*, **14**, 683-693.

[85] Yaw LS, Kathy KWA, Connie WHW and Karmin O. (2006) Homocysteine stimulates phosphorylation of NADPH oxidase p47phox and p67phox subunits in monocytes via protein kinase Cβ activation. *Biochem J*, **398**, 73-82.

[86] Rhea M, Liana D and Peter JOB (2011) Rescuing hepatocytes from iron-catalyzed oxidative stress using vitamins B_1 and B_6. *Toxicology in Vitro*, **25**, 1114-1122.

[87] Ward NE, Jones J and Maurice DV. (1988) Essential role of adenosylcobalamin in leucine synthesis from L-leucine in the domestic chicken. *J Nutr*, **118**, 159-164.

[88] Jessica AS, Nynke EH, Henk JB, Sinead ML, Coen DAS, Jan AR, Paul AJK., Victor WMH and Hans WMN. (2012) S-Adenosylhomocysteine induces apoptosis and phosphatidylserine exposure in endothelial cells independent of homocysteine. *Atherosclerosis*, **221**, 48-54.

[89] Amanpreet K, Vijay SS, Darren EC, Virgil LW, Renate BP and Gerry RB. (2005) Nitric oxide inhibits mammalian methylmalonyl-CoA mutase. *J Biol Chem*, **280**, 10073-10082.

[90] Idrees OD, Tanima G., Yongchang C, Vladimir G.K, Vijay SS and Gerry RB.

(2001) Nitric oxide inhibits methionine synthase activity *in vivo* and disrupts carbon flow through the folate pathway. *J Biol Chem*, **276**, 27296-27303.

[91] Wozniak M, Rydzewski B, Baker SP and Raizada MK (1993) The cellular and physiological actions of insulin in the central nervous system. *Neurochem Int*, **22**, 1–10.

[92] Coker GT, Studelska D, Harmon S, Burke W, O'Malley KL. (1990) Analysis of tyrosine hydroxylase and insulin transcripts in human neuroendocrine tissues. *Brain Res Mol Brain Res*, **8**, 93-98.

[93] Abbott MA, Wells DG and Fallon JR. The lnsulin receptor tyrosine kinase substrate p58/53 and the insulin receptor are components of CNS synapses. *J Neurosci*, **19**, 7300-7308.

[94] Tomioka M, Adachi T, Suzuki H, Kunitomo H, William RS and Iino Y. (2006) The insulin/PI 3-Kinase pathway regulates salt chemotaxis learning in *Caenorhabditis elegans*. *Neuron*, **51**, 613-625.

[95] Zhao WQ, Chen H, Quon MJ and Alkon DL. (2004). Insulin and the insulin receptor in experimental models of learning andmemory. *Eur J Pharmacol*, **490**, 71–81.

[96] White JG., Southgate E, Thomson JN. and Brenner S. (1986) The structure of the nervous system of *Caenorhabditis elegans*. *Philos Trans R Soc Lond B Biol Sci*, **314**, 1–340.

[97] Saeki S, Yamamoto M and Iino Y. (2001) Plasticity of chemotaxis revealed by paired presentation of a chemoattractant and starvation in the nematode *Caenorhabditis elegans*. *J Exp Biol*, **204**, 1757–1764.

[98] Zafari AM, Ushio-Fukai M, Marjorie A, Qiqin Y, Aalok S, David G.H, Taylor WR and Kathy KG. (1998) Role of NADH/NADPH oxidase-derived H_2O_2 in angiotensin II-induced vascular hypertrophy. *American Heart Association*, **32**, 488-495.

[99] Jiang YG. and Patrice P. (2005) Raw material enzymatic activity determination: A specific case for validation and comparison of analytical methods-The example of

superoxide dismutase (SOD). *J Pharm Biomed*, **40**, 1143-1148.

[100] Rosemary SA, Lesley CW, Tania CS and Julianne TD. (2006) Lipid rafts in *Cryptococcus neoformans* concentrate the virulence determinants phospholipase B_1 and Cu/Zn superoxide dismutase. *Eukaryotic Cell*, **5**, 488-498.

[101] Nakamura A and Goto S. (1995) Analysis of protein carbonyls with 2,4-dinitrophenyl hydrazine and its antibodies by immunoblot in two-dimensional gel electrophoresis. *J Biochem*, **119**, 768-774.

[102] Ishihara T, Iino Y, Mohri A, Mori I, Gengyo-Ando K, Mitani S and Katsura I. (2002) HEN-1, a secretory protein with an LDL receptor motif, regulates sensory integration and learning in *Caenorhabditis elegans*. *Cell*, **109**, 639-649.

[103] William PW, Tony M. and Bernard TG. (2004) A new role for glutathione: protection of vitamin B_{12} from depletion by xenobiotics. *Chem Res Toxicol*, **17**, 1562-1567.

[104] Gusarov I, Gautier L, Smolentseva O, Shamovsky I, Eremina S, Mironov A and Nudler E. (2013) Bacterial nitric oxide extends the lifespan of *C. elegans*. *Cell*, **152**, 818-830.

[105] Allan BD, Alessandra C, Christopher ML and Jennifer D. (2002) Evidence that amyloid beta-peptide-induced lipid peroxidation and its sequelae in Alzheimer's disease brain contribute to neuronal death. *Neurobiol Aging*, **23**, 655-664.

[106] Allan BD and Christopher ML. (2002) Lipid peroxidation and protein oxidation in Alzheimer's disease brain: potential causes and consequences involving amyloid β-peptide-associated free radical oxidative stress. *Free Radic Biol Med*, **32**, 1050-1060.

[107] Jia MZ and Domenico P. (2010) Acceleration of brain amyloidosis in an Alzheimer's disease mouse model by a folate, vitamin B_6 and B_{12}-deficient diet. *Exp Gerontol*, **45**, 195-201.

[108] Escobar JA, Rubio MA and Lissi EA. (1996) SOD and catalase inactivation by singlet oxygen and peroxyl radicals. *Free Radic Biol Med*, **20**, 285-290.

[109] Barry H. and Susanna C. (1993) Lipid peroxidation: its mechanism, measurement,

and significance. *Am J Clinical Nutrition*, **57**, 715-725.

[110] Wang, W., Kramer, P.M., Yang, S., Pereira, M.A., and Tao, L. (2001) Reversed-phase high-performance liquid chromatography procedure for the simultaneous determination of S-adenosyl-L-methionine and S-adenosyl-L-homocysteine in mouse liver and the effect of methionine on their concentrations. *J Chromatogr B*, **762**, 59-65.

[111] Yamamoto, A., Shim, I.S., Fujihara, S., Yonezawa, T., and Utsui, K. (2004) Effect of difference in nitrogen media on salt-stress response and contents of nitrogen compounds in rice seeding. *Soil Sci Plant Nutr*, **50**, 85-93.

[112] Kvannes, J and Flatmark, T. (1987) Rapid and sensitive assay of ornithine decarboxylase activity by high-performance liquid chromatography of the o-phthalaldehyde derivative of putrescine. *J Chromatogr*, **419**, 291-295.

[113] Venza, M., Visalli, M., Cicciu, D., and Teti, D. (2001) Determination of polyamines in human saliva by high-performance liquid chromatography with fluorescence detection. *J Chromatogr B*, **757**, 111-117.

[114] Kawata T, Tadano N, Iijima T and Maekawa A. (1989) Effect of vitamin B_{12}-deficiency on activity of hepatic cystathionine beta-synthase in rats. *J Nutr Sci Vitaminol*, **35**, 101-110.

[115] Guoyao WO, Sidney M and Morris Jr. (1998) Arginine metabolism: nitric oxide and beyond. *Biochem J*, **336**, 1-17.

[116] Hualing L, Changhong R, Jinping S, Xingyi H, Feilong Z, Yan G, Yonghong W, Langlai X, Changsheng C and Chenggang Z. (2010) A proteomic view of *Caenorhabditis elegans* caused by short-term hypoxic stress. *Proteome Sci*, **8**, 49-62.

[117] Jeffrey AB, Robert JM, Alex FB, Kevin WH, Susan TW and Shane LR. (2012) Profiling the anaerobic response of *C. elegans* using GC-MS. *Plos one*, **7**, e46140.

[118] Wright DJ. (1975) Elimination of nitrogenous compounds by *Panagrellus redivivus*. Studies on nitrogen catabolism in *Panagrellus redivivus*. *Comp Biochem Physiol*, **52**, 247-253.

[119] Morgan, DML. (1987) Polyamines. *Essays in Biochem*, **23**, 82-115.

[120] William D, Lan L, Sylvia VR, Kelly JP, and Rew IS. (2000) Physiological cyclic stretch directs L-arginine transport and metabolism to collagen synthesis in vascular smooth muscle. *FASEB J*, **14**, 1775-1783.

[121] Akesson B, Fehling C and Jagerstad M. (1978) Effect of vitamin B_{12} deficiency on phosphatidylethanolamine methylation in rat liver. Br. J. Nutr. 40, 521-527.

[122] Pegg EA and Michael AJ. (2010) Spermine synthase. *Cell Mol Life Sci*, **67**, 113-121.

[123] Bjelakovic G, Pavlovic D, Jevtovic T, Stojanovic I, Sokolovic D, Bjelakovic GB, Nikolic J and Bašic J. (2006) Vitamin B_{12} and Folic Acid Effects on Polyamine Metabolism in Rat Liver. *Pteridines*, **17**, 90-94.

[124] Kramer DL, Sufrin JR and Porter CW. (1987) Relative effects of S-adenosylmethionine depletion on nucleic acid methylation and polyamine biosynthesis. *Biochem J*, **247**, 259-265.

[125] Scalabrino G., Monzio-Compagnoni B, Ferioli ME, Lorenzini EC, Chiodini E and Candiani R. (1990) Subacute combined degeneration and induction of ornithine decarboxylase in spinal cords of totally gestrectomized rats. *Lab Invest*, **62**, 297-304.

[126] Zong-Zhi H, Jose MM, Gary K and Shelly CL. (1999) Differential effect of thioacetamide on hepatic methionine adenosyltransferase expression in the rat. *Hepatology*, **29**, 1471-1478.

[127] Donald GW and John MS. (1995) 3. The biochemical basis of the neuropathy in cobalamin deficiency. *Baillieres Clin Haematol*, **3**, 479-497.

[128] Sandra HMD, Ana MR, Carlos GB, Maria PD, Laura L, Gladys B, Miguel L, Angelica AM, Francisca S and Daniel B. (2008) Methylation status in healthy subjects with normal and serum folate concentration. *Nutrition*, **24**, 1103-1109.

[129] Taban-Shomal O, Kilter H, Wagner A, Schorr H, Umanskaya N, Hübner U, Böhm, M, Herrmann W and Herrmann M. (2009) The cardiac effects of prolonged vitamin B_{12} and folate deficiency in rats. *Cardiovasc Toxicol*, **9**, 95-102.

[130] Guerra-Shinohara EM, Morita OE, Pagliusi RA, Blaia-d'Avila VL, Allen RH and Stabler SP. (2007) Elevated serum S-adenosylhomocysteine in cobalamin-deficient megaloblastic anemia. *Metabolism*, **56**, 339-347.

[131] MacRae M, Kramaer DL and Coffino P. (1998) Developmental effect of polyamine depletion in *Caenorhabditis elegans*. *Biochem J*, **333**, 309-315.

[132] Donevan, S.D and Rogawski, M.A. (1995) Intracellular polyamines mediate inward rectification of Ca (2^{+})-permeable alpha-amino-3-hydroxy-5-methyl-4-isoxazole propionic acid receptors. *Proc Natl Acad Sci USA*, **92**, 9298-9302.

[133] Mori H and Mishina M. (1995) Structure and function of the NMDA receptor channel. *Neuropharmacology*, **34**, 1219-1237.

[134] Mattoson MP and Shea TB. (2003) Folate and homocysteine metabolism in neural plasticity and neurodegenerative disorders. *Trends Neurosci*, **26**, 137-146.

[135] Adachi K, Izumi M, Osano Y, Miura N, Takatu S, Terao S and Mitsuma T. (2003) Polyamine concentrations in the brain of vitamin B_{12}-deficient rats. *Exp Biol Med*, **228**, 1069-1071.

[136] Ardiel EL and Rankin CH. (2012) An elegant mind: learning and memory in *Caenorhabditis elegans*. *Learn Mem*, **17**, 191-201.

[137] Metz J. (1992) Cobalamin deficiency and the pathogenesis of nervous system disease. *Ann Rev Nutr*, **12**, 59-79.

[138] Lindballe DL, Fedosov S, Sherliker P, Hin H, Clarke R and Nexo E. (2011) Association of cognitive impairment with combinations of vitamin B_{12}-related paramenters. *Clin Chem*, **57**, 1436-1443.

[139] Shibata K, Fukuwatari T, Imai E, Hayakawa H, Watanabe F, Takimoto H, Watanabe T, Umegaki K. (2013) Dietary reference intakes for Japanese 2010: Water-soluble vitamins. *J Nutr Sci Vitaminol*, **59**, 67-82.

[140] Watanabe F, Takenaka S, Katsura H, Masumder SA, Abe K, Tamura Y and Nakano Y. (1999) Dried green and purple lavers (nori) contain substantial amounts of biologically active vitamin B_{12} but less of dietary iodine relative to

other edible seaweeds. *J Agric Food Chem*, **47**, 2341-2343.

[141] Watanabe F, Katsura H, Takenaka S, Fujita T, Abe K, Tamura Y, Nakatsuka T and Nakano Y. (1999) Psedovitamin B_{12} is the predominant cobamide of an algal health food, Spirulina tablets. *J Agric Food Chem*, **47**, 4736-4741.

[142] Miyamoto E, Tanioka Y, Nakao T, Barla F, Inui H, Fujita T, Watanabe F and Nakano Y. (2006) Purification and characterization of a corrinoid-compound in an edible cyanobacterium *Aphanizomenon flos-aquae* as a nutritional supplementary food. *J Agric Food Chem*, **54**, 9604-9607.

[143] Mozafar A. (1994) Enrichment of some B-vitamins in plants with application of organic fertilizers. *Plant and Soil*, **167**, 305-311.

[144] *Standard Tables of Food Composition in Japan-2010*, The Council for Science and Technology, Ministry of Education, Culture, Sports, Science and Technology, JAPAN, Ed.; Official Gazette Co-operation of Japan: Tokyo, Japan, 2010.

[145] Allen RH and Stabler SP. (2008) Identification and quantitation of cobalamin and cobalamin analogues in human feces. *Am J Clin Nutr*, **87**, 1324−1335.

[146] Mozafar A and Oertli JJ. (1992) Uptake of a microbially-produced vitamin (B_{12}) by soybean roots. *Plant Soil*, **139**, 23-30.

[147] Sato K, Kudo Y and Muramatsu K. (2004) Incorporation of a high level of vitamin B_{12} into a vegetable, kaiware daikon (Japanese radish sprout), by the absorption from its seeds. *Biochim Biophys Acta*, **1672**, 135−137.

[148] Watanabe F and miyamoto E. (2003) Hydrophilic vitamins. In: Sherma J, Fried B (eds) Handbook of thin-layer chromatography, 3rd edn. Marcel Dekker, Inc. New York, pp 589-605 (revised and expanded).

[149] Watanabe F and yabuta Y. (2011) Microbiological detection of vitamin B_{12} and other vitamins. In: Rychlik M (ed) Fortified foods with vitamins－analytical concepts to assure better and safer products. Wiley & Sons Inc, Hoboken, pp 165-171.

[150] Tanioka Y, Yabuta Y, Miyamoto E, Inui h and Watanabe F. (2008) Analysis of vitamin B_{12} in food by silica gel 60 TLC and bioautography with vitamin

B_{12}-dependent *Escherichia coli* 215. *J Liq Chrom Rel Technol*, **31**, 1977-1985.

[151] Tanioka Y, Miyamoto E, yabuta Y, Onishi K, Fujita T, Yamaji R, Misono H, Shigeoka S, Nakano Y, Inui H and Watanabe F. (2010) Methyladeninylcobamide functions as the cofactor of methionine synthase in a cyanobacterium, *Spirulina plantensis* NIES-39. *FEBS Lett*, **584**, 3223-3226.

[152] Watanabe F, Takenaka S, Katsura H, Miyamoto E, Abe K, Tamura Y, Nakatsuka T and Nakano Y. (2000) Characterization of vitamin B_{12} compound in edible purple laver, Porphyrayezoensis. *Bioci Biotechnol Biochem*, **64**, 2712-2715.

[153] Watanabe F, Schwarz J, Takenaka S, Miyamoto E, Ohnishi N, Nelle E, Hochstrasser R and Yabuta Y. (2012) Characterization of vitamin B_{12} compounds in the wild edible mushrooms black trumpet (*Craterellus cornucopioides*) and golden chanterelle (*Cantharellus cibarius*). *J Nutr Sci Vitaminol*, **58**, 438-441.

[154] Watanabe F, Yabuta Y, Tanioka Y and Bito T. (2013) Biologically active vitamin B_{12} compounds in foods for preventing deficiency among vegetarians and elderly subjects. *J Agric Food Chem*, **61**, 6769-6775.

[155] Pathare PM, Wilbur DS, Heusser S, Quadros EV, McLoughlin P and Morgan AC. (1996) Synthesis of cobalamin-biotin conjugates that vary in the position of cobalamin coupling. Evaluation of cobalamin derivative binding to transcobalamin II. *Bioconjugate Chemistry*, **7**, 217-232.

[156] Steverink ATG and Steunenberg H. (1979) Determination of chloramine-T in foodstuffs. *J Agric Food Chem*, **27**, 932-934.

[157] Bonnett R. (1963) The chemistry of the vitamin B_{12} group. *Chem Rev*, 63, 573-605.

[158] Mohammadi K and Sohrabi Y. (2012) Bacterial biofertilizers for sustainable crop production: A review. *J Agric Biol Sci*, **7**, 307-316.

[159] Choudhury AT and Kennedy IR. (2004) Prospects and potentials for systems of biological nitrogen fixation in sustainable rice production. *Biol Fertil Soils*, **39**, 219-227.

[160] Gamal-Eldin H and Elbanna K. (2011) Field evidence for the potential of

Rhodobacter capsulatus as biofertilizer for flooded rice. *Curr Microbiol*, **62**, 391-395.

[161] Zappa S, Li K and Bauer C. (2010) The tetrapyrrole biosynthetic pathway and its regulation in *Rhodobacter capsulatus*. *Adv Exp Med Biol*, **675**, 229-250.

[162] Hashimoto E, Yabuta Y, Takenaka S, Yamaguchi Y, Takenaka H and Watanabe F. (2012) Characterization of corrinoid compounds from edible cyanobacterium *Nostochopsis* sp. *J Nutr Sci Vitaminol*, **58**, 50.

[163] McEvoy AW, Fenwick JD, Boddy K and James OF. (1982) Vitamin B_{12} absorption from the gut does not decline with age in normal elderly humans. *Age Ageing*, **11**, 180−183.

[164] Report of the subdivision on resources In Standard Tables of Food Composition in Japan−2010; The Council for Science and Technology, Ministry of Education, Culture, Sports, Science and Technology: Tokyo, Japan, 2010; pp 106−107.

[165] Palermo M, Paradiso R, De Pascale S and Fogliano V. (2012) Hydroponic cultivation improves the nutritional quality of soybean and its products. *J Agric Food Chem*, **60**, 250−255.

[166] Ahmad I, Hussain W and Fareed AA. (1992) Photolysis of cyanocobalamin in aqueous solution. *J Pharm Biomed Anal*, **10**, 9−15.

[167] Andersson HC and Shapira E. (1998) Biochemical and clinical response to hydroxocobalamin versus cyanocobalamin treatment in patients with mehylmalonic acidemia and homocystinuria (cblC). *J Pediatr*, **132**, 121-124.

[168] Scalabrino G. (2009) The multi-faced basis of vitamin B_{12} (cobalamin) neurotrophism in adult central nervous system: Lessons learned from its deficiency. *Prog Neurobiol*, **88**, 203-220.

[169] Cooper BA and Castle WB. (1960) Sequential mechanisms in the enhanced absorption of vitamin B_{12} by intrinsic factor in the rat. *J Clin Invest*, **39**, 199-214.

[170] Joseph K. (1988) The striatal dopamine dependency of life span in male rats. Longevity study with (-) deprenyl. *Mech Aging Dev*, **46**, 237-262.

[171] Graziadei PPC and Graziadei GAM. (1979) Neurogenesis and neuron

regeneration in the olfactory system of mammals. I. Morphological aspects of differentiation and structural organization of the olfactory sensory neurons. *J Neurocytol*, **8**, 1-18.

[172] Teng F, Bito T, Takenaka S, Yabuta Y and Watanabe F. (2014) Vitamin B_{12}[*c*-lactone], a biologically inactive corrinoid compound, occurs in cultured and dried lion's mane mushroom (*Hericium erinaceus*) fruiting bodies. *J Agric Food Chem*, **62**, 1726-1732.

[173] Kittaka-Katsura H, Fujita T, Watanabe F and Nakano Y. (2002) Purification and characterization of a corrinoid compound from *Chlorella* tablets as an algal health food. *J Agric Food Chem*, **50**, 4994-4997.

Acknowledgements

The author wishes to express his sincere thanks and gratitude to his adviser, Dr. Fumio Watanabe, Professor of Division of Applied Bioresources Chemistry, The United Graduate School of Agricultural Sciences, and School of Agricultural Biological and Environmental Sciences, Tottori University, for his kind guidance and encouragement throughout the course of this study.

The author expresses his deep gratitude to Dr. Tsuyoshi Kawano, Professor of Division of Applied Bioresources Chemistry, The United Graduate School of Agricultural Sciences, and School of Agricultural Biological and Environmental Sciences, Tottori University and Dr. Takahiro Ishikawa, The United Graduate School of Agricultural Sciences, Tottori University and Department of Life Sciences and Biotechnology, Faculty of Life and Environmental Sciences, Shimane University, for their valuable advices.

The author is grateful to Dr. Yukinori Yabuta, Associate Professor of The United Graduate School of Agricultural Sciences, and School of Agricultural Biological and Environmental Sciences, Tottori University, for his helpful, stimulating advice and discussion.

Special thanks are also due to Dr. Yohei Matsunaga, Department of Pathology, Emory University, for his technical assistances and discussions.

Finally, the author wishes to express his sincere thanks to members of Food Science Laboratory and Nutritional Science Laboratory, for their encouragement throughout the course of this study.

Summary

B_{12} deficiency results in growth retardation, metabolic disorders, and neuropathy in mammals. However, the underlying disease mechanisms are poorly understood; in particular, further research is required to elucidate the precise mechanisms of B_{12}-deficient neuropathy in elderly people and vegetarians, high risk populations. To investigate the precise mechanisms of these B_{12}-deficient symptoms, B_{12}-deficient rat have been used as a human model animal. However, they require for long periods to make them B_{12} deficiency. Therefore, the lack of robust B_{12}-deficient animal models such rats has limited investing animal models.

C. elegans grown under B_{12}-deficient conditions for five generations develop severe B_{12} deficiency associated with various phenotypes that include decreased egg-laying capacity (infertility), prolonged life cycle (growth retardation), and reduced lifespan (**Chapter II**, **Section 1**). These phenotypes resemble the consequences of B_{12} deficiency in mammals, and can be induced in *C. elegans* in only 15 days. Thus, *C. elegans* is a suitable animal model for studying the biological processes induced by vitamin deficiency.

I evaluated whether the dodecylamine derivative of B_{12} acts as a potent inhibitor of B_{12}-dependent enzymes in *C. elegans* and COS-7 (**Chapter II**, **Section 2 and 3**). The levels of MMA and Hcy, which serve as indicators of B_{12} deficiency, were significantly increased in *C. elegans* treated with the dodecylamine derivative, indicating severe B_{12} deficiency. Kinetic studies show that the affinity of the CN-B_{12} dodecylamine derivative was greater for two B_{12}-dependent enzymes, MCM and MS, compared with their respective coenzymes, suggesting that the dodecylamine derivative inactivated these enzymes. When OH-B_{12} dodecylamine derivative did not show any cytotoxicity in the cultured cells, the derivative could not affect holo-MCM activity, but significantly

inhibit holo-MS activity in the cell homogenates of COS-7 grown in OH-B_{12}-supplemented medium. These results indicate that the B_{12} dodecylamine derivative acts as a potent inhibitor of B_{12}-dependent enzymes and induces severe B_{12} deficiency in *C. elegans* and COS-7.

Oxidative stress is implicated in several human diseases including atherosclerosis and neurodegenerative diseases. Such diseases are major symptoms of B_{12} deficiency, although the underlying disease mechanisms are poorly understood. **Chapter II**, **Section 1** indicates that *C. elegans* grown under conditions of B_{12} deficiency develops severe B_{12} deficiency. In this study, I described the effects of B_{12} deficiency on various oxidative stress markers in worms to elucidate whether the reduced MS reaction is associated with oxidative stress and with neurological dysfunction (**Chapter III**, **Section 1**). NADPH oxidase and NO synthase activities were significantly increased in B_{12} deficient worms. Therefore, H_2O_2 and NO were increased in B_{12}-deficient worms. MDA and carbonyl proteins contents were significantly increased in B_{12}-deficient worms. Whereas, GSH content, SOD and Cat activities were significantly decreased during B_{12} deficiency. These results indicate that B_{12} deficiency causes severe oxidative stress in worms. Moreover, B_{12}-deficient worms showed a significant memory/learning impairment, which could be considerably prevented by the addition of GSH or vitamin E. These results indicated that B_{12} deficiency in *C. elegans* results in severe oxidative stress, which is one of the causes of the memory/learning impairment.

To evaluate whether B_{12} deficiency causes the metabolic disorders of these amino acids in *C. elegans* (**Chapter III**, **Section 2**), free amino acid levels were analyzed in the B_{12}-deficient worms, compared with those of the control worms. Branched-chain amino acid (valine, leucine, and isoleucine) levels were significantly increased but methionine level was decreased in the B_{12}-deficient *C. elegans*, indicating that

significant changes in these amino acid levels are directly attributable to the decreased MCM and MS activities caused by B_{12} deficiency. Surprisingly, the B_{12}-deficient worms showed significant accumulation of ornithine. Ornithine is a precursor of polyamines, which play multiple roles in cell growth and death including aging and diseases. Putrescine content did not change between B_{12}-deficient and control worms and spermidine content of B_{12}-deficient worms was decreased to approximately 82% of the control worms. These results indicate that amino acid and polyamine metabolic disorders are closely related with symptoms of B_{12} deficiency.

Some researchers have attempted to prepare certain B_{12}-enriched vegetables by treating them with a solution containing high levels of B_{12}. This resulted in a significant increase in the amount of B_{12} incorporated into the plants, suggesting that the B_{12}-enriched vegetables may be of special benefit to vegetarians. However, the B_{12} absorbed by the vegetables was not well characterized in these studies. Hydroponic cultivation is an emerging technology that allows better control of water and nutrient supply that improves plant productivity and reduces the use of pesticides. If a sufficient amount of free B_{12} can be incorporated into lettuce leaves grown under hydroponic conditions, it would be an excellent source of free B_{12} for vegetarians and elderly people.

When lettuces (*Lactuca sativa* L.) grown for 30 days in hydroponic culture were treated with various concentrations of CN-B_{12} for 24 h, its content in their leaves increased significantly from nondetectable to 164.6 ± 74.7 ng/g fresh weight (**Chapter IV**, **Section 4**). This finding indicated that consumption of only two or three of these fresh leaves is sufficient to meet the RDA for adults of 2.4 μg/day. Analyses using a B_{12}-dependent *E. coli* 215 bioautogram and LC/ESI-MS/MS demonstrated that the CN-B_{12} absorbed from the nutrient solutions by the leaves did not alter any other

compounds such as coenzymes and inactive corrinoids. Gel filtration indicated that most (86%) of the CN-B_{12} in the leaves was recovered in the free CN-B_{12} fractions. These results indicated that CN-B_{12} enriched lettuce leaves would be an excellent source of free CN-B_{12}, particularly for strict vegetarians or elderly people with food-bound B_{12} malabsorption.

摘要

本研究は、ビタミン B_{12}(B_{12})欠乏症、特に神経障害の発症メカニズムを解明するために、ヒトのモデル生物である線虫(*Caenorhabditis elegans*)を用いてB_{12}欠乏症モデルの調製を行った。線虫をB_{12}欠乏条件下で 5 世代(15 日間)生育させた時、体内B_{12}含量が低下すると共にB_{12}依存性酵素メチルマロニル-CoA ムターゼ活性ならびにメチオニンシンターゼ活性が著しく減少し、B_{12}欠乏症の指標であるメチルマロン酸とホモシテイン(Hcy)が顕著に蓄積したことから、線虫がB_{12}欠乏状態であることが明らかになった。B_{12}欠乏線虫は著しい産卵数の減少と世代交代時間の増加を示し、B_{12} 欠乏哺乳動物で報告されている不妊症や成長遅延と一致する結果を示した。また、新規なB_{12}酵素阻害剤(B_{12} ドデシルアミン誘導体)を開発し、線虫を極めて短期間(3 日間)に B_{12}欠乏状態へ誘導させることにも成功した。以上の結果から、線虫が新規なB_{12}欠乏症モデルとして基礎医学の分野で哺乳動物の代替生物として活用できることを明かにした。

B_{12}欠乏線虫は著しく Hcy を体内に蓄積していたが、Hcy はジスルフィド結合を形成する過程で H_2O_2 やスーパーオキシドアニオンラジカルなどの活性酸素種を発生させることが知られている。そこで、酸化ストレス関連のバイオマーカーを検討したところ、B_{12} 欠乏線虫では活性酸素種や活性窒素種の生成に関与する NADPH 酸化酵素と一酸化窒素合成酵素の活性が著しく上昇し、H_2O_2や一酸化窒素化合物の顕著な蓄積が示された。一方、還元型グルタチオンなどの抗酸化物質やスーパーオキシドディスムターゼなどの抗酸化酵素の活性が著しく減少していた。また、B_{12} 欠乏線虫では酸化ストレス障害の指標である過酸化脂質やカルボニル化タンパク質が顕著に増加していた。以上の結果から、B_{12}欠乏による Hcy の蓄積が生体内のレドックス制御の破綻を誘発させ、極めて著しい酸化ストレス障害を引き起こすことをはじめて明らかにした。

B_{12}欠乏性神経障害の発症メカニズムを解明するために、線虫の連合学習アッセイ法を用いてB_{12}欠乏線虫の記憶・学習能を評価した。その結果、B_{12}欠乏線虫は著しく記憶・学習能が低下していた。また、B_{12}欠乏線虫をB_{12}添加条件下で生育させた時、低下した記憶・学習

能が完全に回復したことから、記憶・学習能の低下が B_{12} の欠乏に起因することが明らかとなった。また、B_{12} 欠乏線虫が著しい酸化ストレス障害を呈していたことから、酸化ストレス障害が記憶・学習能に及ぼす影響を検討するために、抗酸化物質(ビタミンＥと還元型グルタチオン)を添加した条件下で B_{12} 欠乏線虫を調製した。その結果、抗酸化物質の添加により B_{12} 欠乏線虫の記憶・学習能の低下が約 50%に抑制された。以上の結果から、B_{12} 欠乏線虫の記憶・学習能の低下は、酸化ストレスとそれ以外の要因で引き起こされることをはじめて明らかにした。本研究結果は、ヒトにおいて抗酸化物質の積極的な摂取が B_{12} 欠乏性神経障害の症状を顕著に軽減させる可能性を示唆している。

B_{12} 欠乏性神経障害の酸化ストレス以外の発症要因を特定するために、B_{12} 依存性酵素が関与するアミノ酸代謝に着目した。B_{12} 欠乏ラット等で報告されている分岐鎖アミノ酸やメチオニンの代謝異常以外に、B_{12} 欠乏線虫においてオルニチンの顕著な蓄積が新規に観察された。オルニチンは神経伝達関連物質ポリアミンの前駆体であることから、線虫体内のポリアミン量を測定したところ、B_{12} 欠乏線虫ではスペルミジンが著しく減少していた。B_{12} 欠乏線虫では、生体内のメチル化反応の基質であり、ポリアミン合成に必須である *S*-アデノシルメチオニンが顕著に減少しており、これがスペルミジンの低下の原因であることを突き止めた。

これらの結果より、B_{12} 欠乏性神経障害の発症要因は生体内のレドックス制御の破綻のみならず、生体内メチル化反応の低下が神経細胞膜のリン脂質組成を変化させることによる神経伝達異常、また Hcy およびポリアミン代謝異常が記憶保存に関与する受容体の活性調節機構を攪乱することで学習機能を低下させるなど、複合的な要因が関与することを明らかにした。

本研究では B_{12} 欠乏症の高い発症率を示す菜食主義者と高齢者に焦点をあて、B_{12} 欠乏症の発症を予防するために B_{12} 強化野菜の開発を検討した。予備実験から、家畜の糞などを主原料とした有機肥料にはヒトで不活性なコリノイド化合物が含まれていたことから、B_{12} 産生能を有する紅色光合成細菌を主原料とする肥料でサラダ菜を栽培することで B_{12} 強化野菜の作

成を検討した。その結果、使用した紅色光合成細菌の肥料においてもヒトで不活性なコリノイド化合物が含まれており、紅色光合成細菌を土壌ならびに葉面に施肥したサラダ菜からは B_{12} を検出することはできなかった。そこで、効率的に B_{12} 強化野菜を調製するために植物工場で採用されている水耕栽培技術を用いて検討した。水耕栽培で生育したサラダ菜を収穫前 24 時間、種々な濃度の B_{12} を添加した養液に曝露した時、養液中の B_{12} 濃度に応じてサラダ菜の B_{12} 含量は増加したが、養液中の B_{12} 濃度が 5μmol/L の時サラダ菜の B_{12} 含量は飽和した。また、サラダ菜に含まれる B_{12} の約 86%が遊離型の B_{12} として存在していることが明らかになった。これらの結果より、B_{12} 強化サラダ菜は菜食主義者や高齢者において吸収されやすい遊離型 B_{12} の供給源になることが示唆され、低濃度に B_{12} が強化されたサラダ菜においては、1 日に 60 g 程度を摂取することで、B_{12} の推奨量(2.4 μg/日)を満たすと共に他のビタミンやミネラルならびに食物繊維質の補完にも機能すると考えられた。

学位論文の基礎となる学会誌公表論文のリスト

1. Tomohiro Bito, Yohei Matsunaga, Yukinori Yabuta, Tsuyoshi Kawano, Fumio Watanabe (2013) Vitamin B_{12} deficiency in *Caenorhabditis elegans* results in loss of fertility, extended life cycle, and reduced lifespan. *FEBS Open Bio*, **3**, 112-117. (**Chapter II**, **Section 1**)

2. Tomohiro Bito, Noriharu Ohishi, Yuka Hatanaka, Shigeo Takenaka, Eiji Nishihara, Yukinori Yabuta, and Fumio Watanabe (2013) Production and Characterization of Cyanocobalamin-Enriched Lettuce (*Lactuca sativa* L.) Grown Using Hydroponics. *JOURNAL OF AGRICULTURAL AND FOOD CHEMISTRY*, **61**, 3852-3858. (**Chapter IV**, **Section 4**)

3. Tomohiro Bito・Yukinori Yabuta・Fumio Watanabe (2013) Miniaturized HPTLC of Vitamin B_{12} Compounds in Foods. *Chromatographia*, **76**, 1333-1337. (**Chapter IV**, **Section 1**)

4. Tomohiro Bito, Yukinori Yabuta, Tsuyoshi Ichiyanagi, Tsuyoshi Kawano, Fumio Watanabe (2014) A dodecylamine derivative of cyanocobalamin potently inhibits the activities of cobalamin-dependent methylmalonyl-CoA mutase and methionine synthase of *Caenorhabditis elegans*. *FEBS Open Bio*, **4**, 722-729. (**Chapter II**, **Section 2**)

5. Tomohiro Bito, Mariko Yasui, Toshio Iwaki, Yukinori Yabuta, Tsuyoshi Ichiyanagi, Ryoichi Yamaji, Yoshihisa Nakano, Hiroshi Inui, Fumio Watanabe (2014) Dodecylamine Derivative of Hydroxocobalamin Acts as a Potent Inhibitor of Cobalamin-Dependent Methionine Synthase in Mammalian Cultured COS-7 Cells. *Food and Nutrition Sciences*, **5**, 1318-1325. (**Chapter II**, **Section 3**)

6. Tomohiro Bito, Fei Teng, Noriharu Ohishi, Shigeo Takenaka, Emi Miyamoto, Emi Sakuno, Kazuhisa Terashima, Yukinori Yabuta, Fumio Watanabe (2014) Characterization of vitamin B_{12} compounds in the fruiting bodies of shiitake mushroom (*Lentinula edodes*) and bed logs after fruiting of the mushroom. *MYCOSCIENCE*, **55**, 462-468. (**Chapter IV**, **Section 2**)